

Identifying the source of the Gerhard Minnebron aquifer

AJ Louw

 **orcid.org/0000-0002-8210-0253**

Dissertation accepted in fulfilment of the requirements for the degree *Master of Science in Environmental Sciences with Hydrology and Geohydrology* at the North-West University

Supervisor: Dr TC de Klerk

Graduation July 2022

27041387

ACKNOWLEDGEMENTS

I firstly want to thank my Heavenly Father, without Him nothing would have been possible. He gave me the strength and determination to finish my paper. He also provided me with insight and knowledge in times when I needed it most. I will be eternally grateful for His grace and unending love.

I want to thank numerous people who supported me throughout this journey:

- My wife Chanté, thank you for always being there, helping me with everything and for always supporting and encouraging me. I will always be grateful for your support and love. This paper is as much mine as yours. Thank you for loving and assisting me during this time and all the difficult times.
- My Parents, you were always asking about the research and how I was progressing. Thank you for your time and effort and thank you for giving me the opportunity & support to complete my master's degree.
- Dr Theuns De Klerk my supervisor, thank you for your feedback and expertise, without your help and knowledge I could not have done this.
- My fellow MSc. Students, thank you for always seeing the humour in our trials and tribulations and always being willing to help when I asked.
- To Vic and Amanda Fitzmaurice, thank you for your support, encouragement and for always being there for me.
- I also want to thank the Centre for Water Sciences and Management for making this opportunity possible as well as the North-West University.
- Lastly, I want to thank Dr Rainier Dennis & Prof. Ingrid Dennis, you two encouraged and inspired me to pursue a career in Hydrogeology & Hydrology. Thank you for always being able to assist and advise.

ABSTRACT

Fresh drinkable groundwater is a very valuable resource, one that needs to be used, developed, managed and conserved. The Gerhard Minnebron (GMB) is such a resource, it is an important resource for the communities and agriculture downstream. The GMB has experienced development and usage without the conservation or protection of the resource. Protecting the GMB from any further pollution and contamination is crucial for the future of the resource. To achieve this the extent of the GMB's water source should be determined. This study aimed to determine the origins of the water in the Gerhard Minnebron aquifer.

One efficient tool to determine surface and groundwater flow is Tracers. There are many different types of tracers, they can be added artificially, or they could occur naturally. Artificial tracers are organic compounds, salts, and fluorescent dyes. Natural tracers are either isotopes or natural gas species. This research made use of a natural tracer namely stable isotopes of Oxygen and Hydrogen. The stable isotopes Deuterium (2H) and Oxygen -18 (^{18}O) were chosen because they cause no contamination, they're inexpensive, already present in the water cycle, and easy to analyse and detect. Making use of the stable isotopes the source of the GMB's water would be determined. Basic chemical anions and cations analysis were conducted to provide any additional links or aid in determining the source of the GMB's water.

For this study, stable isotope samples were collected at 42 different locations all over the WFS. The samples were collected from different bodies of water, such as groundwater, stream water, dam water and mine water through pipelines and canals. The isotope samples were collected in HDPE bottles and stored out of any direct sunlight preventing evaporation. The samples were analysed with a Picarro L2130-i Isotope and Gas Concentration Analyser. Stable isotopes with chemical analysis of the collected samples were successful in determining the aim of this study in identifying the source of the GMB's water. The chemical analysis was done on 36 collected samples using ion chromatography. Relevant graphs were created from the chemical and isotope results to identify trends and correlations used to determine the source of the GMB's water.

The isotope analysis revealed three distinct groups. Group one was dominated by groundwater samples displaying very little isotope enrichment and plotted on or close to the local meteoric water line (LMWL). The second group displayed some isotope enrichment and plotted slightly below the LMWL the second group was a mixture of different sources. The third and final group was dominated by surface water samples and plotted well below the LMWL displaying the most isotope enrichment.

The chemical concentrations varied with each sample, but high concentrations of bicarbonate and Sulphate was present in most of the samples. Overall groundwater samples displayed low concentrations of all elements. The GMB displayed high concentrations of sulphate and bicarbonate. The chemical signatures in the GMB also correlated with the signatures from surface waters and groundwater samples to the south of the WFS.

The stable isotopes Deuterium (^2H) Oxygen -18 (^{18}O), and the chemistry data provided sufficient evidence to identify the source of the Gerhard Minnebron's aquifer. The data revealed that the source of the aquifer is the dolomites to the North-East of the GMB with inflows coming from surface water's, rainwater and groundwater from adjacent aquifers and compartments.

To identify the source more accurately, tracers such as CFC's, additional isotopes, chemical tracers, and physical tracers like dyes are recommended. The area is hydrogeologically very complex and additional research into the aquifer interactions would be very valuable, additional samples collected over a larger sampling area and annual sampling is recommended for future studies.

Key terms: Gerhard Minnebron, Tracers, Stable Isotopes, Deuterium, Oxygen-18, Dolomite, Wonderfonteinspruit

ACRONYMS AND ABBREVIATIONS

AMD	Acid Mine Drainage
GMB	Gerhard Minnebron
DWAF	Department of Water and Forestry
WFS	Wonderfonteinspruit
SMOW	Standard Mean Ocean Water
VSMOW	Vienna Standard Mean Ocean Water
D	Deuterium
LMWL	Local Meteoric Water Line
MWL	Meteoric Water Line
GMWL	Global Meteoric Water Line
RMWL	Regional Meteoric Water Line
Ca	Calcium
Mg	Magnesium
Mamsl	Meters Above Mean Sea Level
Mbgl	Metres Below Ground Level
HDPE	High Density Polyethylene
CRDS	Cavity Ring Down Spectroscopy
MCM	Micro-Combustion Module
GW	Groundwater
SP	Spring water
SW	Surface water
PL	Pipeline

TABLE OF CONTENTS

ABSTRACT	II
ACRONYMS AND ABBREVIATIONS	IV
TABLE OF CONTENTS.....	V
LIST OF EQUATIONS	IX
LIST OF TABLES	X
LIST OF FIGURES.....	X
CHAPTER 1: INTRODUCTION.....	1
1.1 Introduction:	1
1.2 Problem Statement:.....	2
1.4 Research Question and Objectives:.....	3
1.5 Research Layout:	4
1.6 Research design and limitations:.....	5
CHAPTER 2: STUDY AREA.....	6
2.1 Location and history:	6
2.2 Physical Characteristics:	8
2.3 Hydrology:	9
2.4 Geology:	11
2.5 Hydrogeology:	20

2.7 Impacts of mining on the Hydrology and hydrogeology:	24
2.8 Land cover:	28
2.9 Water quality:	32
CHAPTER 3: LITERATURE REVIEW.	34
3.1 Introduction to Isotopes:	34
3.2 Factors that influence Isotope fractions:	46
3.2.1 <i>Temperature effect:</i>	46
3.2.2 <i>Seasonal effect:</i>	47
3.2.3 <i>Altitude effect:</i>	47
3.2.4 <i>Continental effect:</i>	48
3.2.5 <i>Latitude effect:</i>	49
3.2.6 <i>Amount effect:</i>	50
3.3 Hydrologic Cycle:	50
3.3.1 <i>Concept of Hydrologic Cycle:</i>	51
3.3.2 <i>Components of the Hydrologic Cycle:</i>	51
3.4 Hydrologic cycle in karst environments:	55
3.5 Isotopes in Hydrology:	56
3.5.1 <i>Stable isotopes in rainfall:</i>	56
3.5.2 <i>Evaporation:</i>	57
3.5.3 <i>Stable isotopes in soil:</i>	59
3.5.4 <i>Stable isotopes in surface & groundwater:</i>	60
3.5.4.1 <i>Surface water:</i>	61

3.5.4.2 Groundwater:.....	62
3.5.5 Sources & Mechanisms of recharge:	63
3.6 Isotopes in Karst environments:	64
3.7 Applications of Stable Isotopes:	65
3.8 Land use impacts on isotopes:	66
3.9 Case Studies:.....	66
3.9.1 Case study 1:	66
3.9.2 Case study 2:	68
3.9.3 Case study 3:	74
3.9.4 Case study 4:	79
3.9.5 Case study 5:	83
3.9.6 Case study 6:	86
3.9.7 Case study 7:	89
CHAPTER 4: METHODOLOGY.....	94
4.1 Introduction:	94
4.2 Sampling of Stable isotopes:.....	94
4.3 Sampling locations:	94
4.4 Sampling method:	99
4.5 Analyser operation and components:.....	102
4.5.1 Analyser:	103
4.5.2 Application:.....	105

CHAPTER 5: RESULTS & DISCUSSION.....	108
5.1 Stable Isotope data.....	108
5.1.1 <i>Basic Overview of data:</i>	108
5.1.2 <i>Groundwater data:</i>	111
5.1.3 <i>Spring water data:</i>	112
5.1.4 <i>Stream water data:</i>	113
5.1.5 <i>Pipeline data:</i>	114
5.1.6 <i>Dam water data:</i>	115
5.1.7 <i>Canal water data:</i>	116
5.1.8 <i>Cave water data:</i>	117
5.1.9 <i>Discussion of isotope data:</i>	117
5.2 Chemical Data.....	122
5.2.1 <i>Groundwater:</i>	126
5.2.2 <i>Spring water:</i>	127
5.2.3 <i>Surface water:</i>	127
5.2.4 <i>Pipeline:</i>	127
5.2.5 <i>Dam water:</i>	127
5.2.6 <i>Canal water:</i>	128
5.2.7 <i>Cave water:</i>	128
5.2.8 <i>Discussion of data</i>	128
CHAPTER 6: CONCLUSION & RECOMMENDATIONS.....	132
6.1 Conclusion.....	132

LIST OF EQUATIONS

<i>Equation 3.1</i>	38
<i>Equation 3.2</i>	38
<i>Equation 3.3</i>	38
<i>Equation 3.4</i>	39
<i>Equation 3.5</i>	40
<i>Equation 3.6</i>	40
<i>Equation 3.7</i>	40
<i>Equation 3. 8</i>	40
<i>Equation 3.9</i>	41
<i>Equation 3. 10</i>	42
<i>Equation 3.11</i>	43
<i>Equation 3.12</i>	43
<i>Equation 3.13</i>	43
<i>Equation 3.14</i>	44
<i>Equation 3.15</i>	44
<i>Equation 3.16</i>	45
<i>Equation 3.17</i>	45
<i>Equation 3. 18</i>	56
<i>Equation 3.19</i>	58

<i>Equation 3.20</i>	81
<i>Equation3.21</i>	81

LIST OF TABLES

Table 1:	78
Table 2	96
Table 3	123

LIST OF FIGURES

<i>Figure 2.1: The Gerhard Minnebron with administrative boundaries.</i>	7
<i>Figure 2.2: Quaternary catchment boundaries with the Gerhard Minnebron.</i>	8
<i>Figure 2.3: Mean annual Precipitation of the area.</i>	9
<i>Figure 2.4: Regional Topography and Hydrology.</i>	10
<i>Figure 2.5: Map indicating two study areas.</i>	11
<i>Figure 2.6: Stratigraphy of the gold mines in WFS (Ngcobo, 2006)</i>	13
<i>Figure 2.7: Stratigraphic groups of the WFS area.</i>	14
<i>Figure 2.8: Geology of the WFS area.</i>	15
<i>Figure 2.9 Dolomitic compartments in WFS and dolomitic layers (Winde & Erasmus, 2011a).</i>	16
<i>Figure 2.10: Geology of GMB area</i>	18
<i>Figure 2.11: Borehole logs of boreholes 1 – 4</i>	19
<i>Figure 2.12: Groundwater occurrence in the area.</i>	21

<i>Figure 2.13: Relevant dolomitic compartments and springs.</i>	22
<i>Figure 2.14: Cross section of the dolomite to propose the compartments and springs from (Erasmus et al., 2011).</i>	23
<i>Figure 2.15: Digital Elevation Model (DEM) of the GMB.</i>	23
<i>Figure 2.16: Cross section to propose the ‘Mega-compartment’ with penetrated dykes (Erasmus et al., 2011).</i>	26
<i>Figure 2.17: Illustrating the “Mega-Compartment” with mine voids (Schrader et al. 2014a).</i>	27
<i>Figure 2.18: Map showing the effects of mining on the surface - and ground-water (Winde, 2010a)</i>	28
<i>Figure 2.19: Regional Land cover.</i>	30
<i>Figure 2.20: Land Cover of the study area.</i>	31
<i>Figure 2.21: Aerial photo of study area displaying land use.</i>	32
<i>Figure 2.22: Map showing possible contaminant sources and average and maximum Uranium levels (Winde, 2010b).</i>	33
<i>Figure 3.1: Atomic symbol.....</i>	34
<i>Figure 3.2 Example of Hydrogen isotopes.....</i>	35
<i>Figure 3.3 Chart displaying some elements, each square represents a nuclide (isotope specific atom) grey square are stable isotopes and white squares are unstable nuclides or isotopes. The arrows to the left show the shifts in proton and neutron numbers as a result of different decay mechanisms: a (beta decay), b (positron decay and beta capture), c (alpha decay) (Kendall & Caldwell, 1998b:53).</i>	36
<i>Figure 3.4 Isotope ratios of stable isotopes (White, 2013)</i>	39
<i>Figure 3.5 Displaying how fractionation occurs during evaporation due to differences in vapour pressure (Leibundgut et al. 2009).....</i>	41

<i>Figure 3. 6 The influence on equilibrium fractionation caused by temperature, at 0°C the phase transition from ice to water is displayed with a dashed line, and a step-in temperature equilibrium function is visible (Leibundgut et al. 2009).....</i>	42
<i>Figure 3.7 A concept showing the water-atmosphere exchange process (Leibundgut et al., 2011).....</i>	45
<i>Figure 3.8 Effects of temperature on isotope fractions (Leibundgut et al. 2009).</i>	46
<i>Figure 3.9 Influence of mean annual temperature on the isotopic compositions (Leibundgut et al. 2009).</i>	47
<i>Figure 3. 10 Effect of altitude on δ18O at Cyprus (Leibundgut et al. 2009).....</i>	48
<i>Figure 3.11: The stable isotopic depletion of meteoric water in the Western U.S. visualising the “Continental Effect” (Ingraham, 1998).</i>	49
<i>Figure 3.12: Global distribution of δ18O in precipitation showing the “Latitude effect” (Ingraham, 1998).</i>	50
<i>Figure 3.13: The Hydrologic cycle and its components (Encyclopaedia Britannica, 2020).</i>	52
<i>Figure 3. 14: δ18O – δ2H diagrams showing the effects of evaporation. In the bottom figure, an arrow indicates the isotopic composition of precipitation before evaporation (Leibundgut et al. 2009).....</i>	58
<i>Figure 3.15: Depth profile of δ2H in soil water in an unvegetated arid-zone (Gat, 2010).</i>	60
<i>Figure 3.16: Groundwater recharge in an arid and semi-arid environment and isotopic compositions (Gat, 1995).</i>	64
<i>Figure 3.17: Isotopic compositions of surface, ground, and rainwater (Maduabuchi et al. 2006).....</i>	68
<i>Figure 3.18: Sampling locations, Geology and drainage of the study area (Kumar et al. 2011).....</i>	69
<i>Figure 3. 19: Graph displaying RMWL and the geographical segregation of the stable isotope analysis (Kumar et al. 2011).</i>	71

<i>Figure 3.20: Stable isotope results for each separate geographical region, indicated by numbers 1, 2, 3 and 4 which, respectively, correspond to the highlands (n=20), b near the drains and canal adjoining region 1 (n=70), c direct recharge by the Yamuna River in its flood plain (n=20) and d evaporation-affected water in the flood plain (n=30) (Kumar et al. 2011).</i>	71
<i>Figure 3.21: Table displaying the results of stable isotopes of the four zones in the NCT of Delhi (Kumar et al. 2011).</i>	73
<i>Figure 3.22: Figure displaying major sources of recharge for different areas (Kumar et al. 2011).</i>	74
<i>Figure 3.23: Location of the study area (Mekiso et al. 2015).</i>	75
<i>Figure 3. 24: Cross plot of Deuterium and Oxygen-18 from the samples taken (Mekiso et al. 2015).</i>	76
<i>Figure 3.25: Isotopic compositions of surface and groundwater in the area (Mekiso et al. 2015).</i>	77
<i>Figure 3.26: Stable isotope concentrations from different sample sites within the study area (Nayak et al. 2016).</i>	80
<i>Figure 3.27: Tabulated slope and intercept for best fit line for different water samples (Nayak et al. 2016).</i>	80
<i>Figure 3. 28: Variation of $\delta^{18}O$ of the different sample locations (Nayak et al. 2016).</i>	82
<i>Figure 3. 29: Contribution of Precipitation and canals to the groundwater (Nayak et al. 2016).</i>	82
<i>Figure 3. 30: The locality of the boreholes and leachate sampling point at Boitshepo Landfill site with tritium values in TU. Arrows show inferred leachate migration (Levin & Verhagen, 2013).</i>	83
<i>Figure 3.31 Stable isotope data of Boitshepo relative to GMWL (Levin & Verhagen, 2013).</i>	84
<i>Figure 3.32: The locality of the boreholes and leachate sampling point at the Rooikraal Landfill site (Levin & Verhagen, 2013).</i>	85
<i>Figure 3. 33: Stable Isotope data with the GMWL (Levin & Verhagen, 2013).</i>	86

<i>Figure 3.34: Cumulative isotopic rainfall values from the two rain stations from 2010 till 2012 (Harris & Diamond, 2013).....</i>	<i>87</i>
<i>Figure 3.35: Weighted annual means for rainfall samples at the UCT site, and the springs (Harris & Diamond, 2013).....</i>	<i>88</i>
<i>Figure 3.36: Stable isotope plot for the water samples taken in the upper Crocodile River Basin (Abiye, 2013).....</i>	<i>91</i>
<i>Figure 3. 37: Plot showing d-excess and $\delta^{18}\text{O}$ from the study area (Abiye, 2013).....</i>	<i>92</i>
<i>Figure 4.1: Map of the study area displaying surface water samples.</i>	<i>97</i>
<i>Figure 4. 2: Map of the study area showing sampling locations of Groundwater.....</i>	<i>98</i>
<i>Figure 4. 3: Sampling locations with Quaternary Catchments and Dolomite.</i>	<i>99</i>
<i>Figure 4. 4: HDPE bottles used for sample collection (Researchers personal library).....</i>	<i>100</i>
<i>Figure 4. 5: Surface water example: Canal sampled (Researchers personal library).</i>	<i>101</i>
<i>Figure 4. 6: Groundwater sample: Ruptured extraction pipeline from a shaft (Researchers personal library).</i>	<i>102</i>
<i>Figure 4. 7: Picarro L2130i and components (Researchers personal library).....</i>	<i>103</i>
<i>Figure 4. 8: Schematic of CRDS and ring down measurement (Piccaro, 2015).</i>	<i>104</i>
<i>Figure 4. 9: Light intensity in CRDS, and how optical loss is rendered into time measurement (Picarro, 2015).....</i>	<i>105</i>
<i>Figure 4. 10: Picarro analyser bottles (Researchers personal library).....</i>	<i>106</i>
<i>Figure 4. 11: Picarro sample tray with standards, and sample spots (Researchers personal library).</i>	<i>106</i>
<i>Figure 4. 12: Picarro standard (Researchers personal library).....</i>	<i>107</i>

<i>Figure 5. 1: Graph showing all the isotope data collected GMWL from (Craig 1961), LMWL from (Mokadem et al 2021).</i>	109
<i>Figure 5. 2: Map indicating sample locations with sample ID's</i>	110
<i>Figure 5. 3: Graph showing all the groundwater data.</i>	111
<i>Figure 5. 4: Graph showing all the spring water collected.</i>	112
<i>Figure 5. 5: Graph showing all the surface water data.</i>	113
<i>Figure 5. 6: Graph showing all the pipeline water.</i>	114
<i>Figure 5. 7: Graph showing all the dam water data.</i>	115
<i>Figure 5. 8: Graph showing all the canal water data.</i>	116
<i>Figure 5. 9: Graph showing the cave data.</i>	117
<i>Figure 5. 10: Graph showing all data plots.</i>	118
<i>Figure 5. 11: Deuterium of samples.</i>	119
<i>Figure 5. 12: Map indicating stable isotope groups.</i>	121
<i>Figure 5. 13: Piper plot of data.</i>	126
<i>Figure 5. 14: Piper plot of data displayed as isotope groups.</i>	129
<i>Figure 5. 15: Composite bar chart of data</i>	131

CHAPTER 1: INTRODUCTION

1.1 Introduction:

Recent decades have proven that groundwater is one of the most important natural resources for many countries. Groundwater is considered as one of the best freshwater resources for multiple uses, mainly for its extensive availability and purity. Groundwater has several important advantages when compared to surface water as a source of water supply. The reason for this is because it's better protected from contamination and pollution, and less subject to fluctuations caused by seasonal and perennial changes; this results in an improvement of the quality in groundwater samples compared to other sources. In addition, groundwater is also available where there is no surface water available, and the groundwater is distributed more uniformly over larger areas than surface water. With these advantages, groundwater is also the sole supply of water for some countries and areas. Despite groundwater being one of the better protected resources, it is still exploited and experiences quality and quantity strains. One of the main influences of groundwater degradation is the improper management of water resources (Zektser & Everett, 2004: 13-17).

Groundwater makes up 30% of the earth's freshwater, from the remaining 70% there's 69% captured in ice caps, glaciers and snow. This indicates the crucial importance of groundwater sources and even though only 1% is made up of rivers and lakes, it is crucial to manage and protect it. The water on earth is part of the water cycle which in very basic terms says that all the water is connected, this means that by protecting and managing one resource the groundwater for instance is protecting and managing the surface water resource as well (IGRAC, 2021). While the management of just one resource isn't sufficient, it is a start that provides protection to some degree onto all the sources. The importance and effect of groundwater isn't always recognized and perceived due to its effects that aren't always clearly visible in surface water. Groundwaters baseflow contribution to surface water streams can't be seen but prevents surface streams from drying up during dryer conditions (IGRAC, 2021).

South Africa is considered a water-stressed country with an average annual rainfall of 500 mm, which is less than the world's average annual rainfall of 860 mm. The rainfall is increasing from west to east but overall, the country is considered semi-arid. The groundwater use in South Africa is estimated from 15% to over 65% over the surface of South Africa (Dennis & Dennis, 2012: 417). In a country that is water stressed and very reliant on water resources for food production and farming, protecting the groundwater and water resources is immensely important. The reason why the management and protection of water is not focused just on groundwater is that

groundwater forms part of the water cycle which connects all components as previously explained. This means that protecting a groundwater resource includes determining all the components and their extent that is part of the water cycle for that specific resource. Therefore, if we want to protect and manage the GMB, we need to determine the source of the groundwater because focussing on the GMB only would not be sufficient if the extent of the water feeding the GMB is beyond the management area.

1.2 Problem Statement:

South Africa has a very rich mining history and still has a lot of mines due to the country having so many valuable materials that can be mined. The large economic value of mines has led to vast economic growth which has become prioritised over environmental sustainability and resources. Groundwater and surface water have been negatively impacted by the mining industry. Some of the damage done to the groundwater has become irreversible and has resulted in becoming a source that could have negative health effects on the community (Winde & Erasmus, 2011a:292). It is thus very important to protect the water resources that are currently unpolluted.

Potchefstroom uses water from the Wonderfonteinspruit, Mooiriver and the Gerhard Minnebron. The Mooiriver and Wonderfonteinspruit both contain high levels of contamination yet surprisingly, the Gerhard Minnebron has considerably less contamination in comparison to the other two. The Gerhard Minnebron spring and aquifer is thus a valuable freshwater resource for Potchefstroom and the surrounding areas as the spring provides the area with high quality and quantity of water. The Gerhard Minnebron is improving the quality of the water when it mixes with the more contaminated water of the Mooiriver and Wonderfonteinspruit (Le Roux, 2005: 39). The level of contamination in the Gerhard Minnebron is inferred to slowly increase over time causing further deterioration of the aquifer (DWAF, 1998: 461). DWAF (1995: 45) implies that the deterioration of the Gerhard Minnebron aquifer will take place at a slower rate than the other aquifers in the Wonderfonteinspruit. The Gerhard Minnebron spring and aquifer is a crucial resource and the first step in managing and protecting the GMB is determining its water source. When the sources are determined, the extent of the area that needs managing and protection can be quantified.

1.3 Different methods:

To understand subsurface flows or determine sources, the best tools to utilise are tracers. Groundwater tracing or tracers is when a substance is added to water and can be detected and/or monitored to provide information about the flow of subsurface water. Tracers can be artificially added or naturally occurring substances that are already present within the water (Kincaid, 2003). Artificial tracers are a useful tool for characterizing the complex flow of water over surfaces,

hillslopes, in channels and artificial systems. Artificial tracers can track the flow through the soil and within aquifers. Artificial tracers are good tools because they aid in understanding the flow processes, estimating key hydrological properties and visualising effects that are not visible such as mixing of waters of unknown amounts.

Environmental tracers are useful tools for water resource estimations in catchments. Environmental tracers can also be used to identify past hydrological processes and integration of hydrological processes to great extents. When applied correctly both artificial and environmental tracers can be very useful in hydrogeological research (Leibundgut *et al.* 2009:5). Artificial tracers can be organic compounds or fluorescent dyes that can be added to water resources. Salts like NaCl, LiCl, KCl can also be added intentionally for the purpose of tracing. Natural tracers are isotope species of water and dissolved noble gasses, these are present in the surface and groundwater without adding them manually. These tracers could also be added manually (Kincaid, 2003).

To identify the source and recharge area of the aquifer a method that causes minimal contamination must be applied.

One method which causes minimum contamination is using stable isotope fractions as a fingerprint for the water because stable isotope fractions will be unique from different locations. Due to stable isotope fractions which are influenced by features such as location and elevation, a link can be established between the different samples. Identical stable isotope fractions from samples will establish if samples are related to the aquifer and could reveal their origins. Therefore, stable isotope fractions will be used to identify the sources of the Gerhard Minnebron aquifer, identifying the sources could help in protecting them from any future contamination and thus protecting Potchefstroom's water supply.

South Africa is experiencing increasing levels of water scarcity and quality problems. This is also compounded by problems caused by water-management structures, population growth issues and social and economic development (Dennis & Dennis, 2012: 417). This constant decrease in quantity and quality of groundwater resources in South Africa is why managing and protecting fresh groundwater resources like the Gerhard Minnebron is of such great importance.

1.4 Research Question and Objectives:

Aim:

The study aims to determine the origins of the water in the Gerhard Minnebron aquifer.

Objectives:

1. To determine the aquifer type of the Gerhard Minnebron spring.
2. To set up and implement a methodology for sampling, application, and analysing isotopes.
3. To identify the source of the GMB aquifer by identifying the main subsurface flow paths using stable isotopes.

1.5 Research Layout:

Chapter 1: Introduction

The introduction will give background about the research, the general problem, the objectives and research questions.

Chapter 2: Study area

This chapter will give a background on the study area and will do so by reviewing literature to give relevant information such as the physical, geological, climatic and historical characteristics of the area. The data and information from the area will all be used to identify all the features and factors that will influence the hydrology and geohydrology.

Chapter 3: Literature Review

This chapter will be divided into the following subsections to better identify and review certain features that are important to this research.

Isotopes: This subsection will give background on isotopes and stable isotopes, their uses and applications. This chapter will also review certain relevant literature on isotopes that will provide additional information on isotopes to better understand them and apply them more efficiently.

Case studies: This subsection will focus on studies done on either the same geology and hydrogeology or location. Studies that applied the same method or techniques that this research will utilise will also be included. These studies will be evaluated to improve the current research.

Chapter 4: Methodology

This chapter will discuss the methodology that will be developed to collect, analyse and interpret the results. A discussion of the type of data required, the data collected and from where or how the data was collected and the processed data will also be included in the chapter.

Chapter 5: Results

This chapter will include a discussion and analysis of the results. The results will also be compared to previous studies or other case studies where applicable. The results will be evaluated to determine if they are reliable or not.

Chapter 6: Conclusion

Chapter 6 will consist of the conclusions made from this study and the findings to identify if it was successful or not and recommendations to improve this research if it is repeated.

1.6 Research design and limitations:

The research approach is a Quantitative experimental research approach, with a well-developed methodology and procedure for data collection and data analysis. The data analysis is done in a controlled environment, and the process is repeatable. The results are time dependant and could be different from previous analysis.

Research limitations for this research are the following:

- (i) The number of samples that could be collected
- (ii) The different sources that were available for sampling
- (iii) The intervals between samples collected, because continuous data may provide more accurate results
- (iv) Only macro chemical constituents and stable Isotopes could be analysed. Additional constituents analysis may add more data and information that could improve the accuracy of the results.

CHAPTER 2: STUDY AREA

2.1 Location and history:

The GMB is one of the highest yielding springs in Southern Africa and yields on average 50-60 Ml³/day (Winde, 2006a). The spring earned the name "Gerhard Minnebron" from the first occupant that lived on the farm where the spring is located, the occupant's name was Gerhard Breytenbach. The farm on which the GMB is located was occupied by Gerhard in 1838 and in 1890 the pioneer Sammy Marks bought the farm. He was the first person to make use of irrigation canals that directed the water from the spring to the irrigation fields. This canal is now abandoned and no longer in use as water affairs constructed a new canal in 1962 and is currently used to provide irrigation water for many farmers downstream (Rural & Urban Exploration, 2016).

The spring is in the south eastern part of the North West province close to the border of the North West and Gauteng. The spring is in the north east of Potchefstroom and west of the Welverdiend. The spring is situated within the JB Marks Local Municipality as indicated by [Figure 2.1](#), which is in the Dr Kenneth Kaunda District Municipality. The GMB spring is located within quaternary catchment C23G and is within the Mooirivier Catchment. The Mooirivier catchment is part of the Upper Vaal Catchment area and contributes water to the Vaal River system through the Mooi River from which the GMB and the Wonderfontein Spruit are tributaries (Le Roux, 2005: 12).

The GMB is one of the largest contributing sources to the Mooi River which flows southwards to Potchefstroom. The water is mainly used for domestic purposes by the downstream community of Potchefstroom and for agricultural purposes by local farmers (Winde & Erasmus, 2011a:292). Underneath the GMB, there are dolomitic formations that are very large and extends further north and north east where they underlie the Wonderfontein Spruit (WFS). The GMB is well known because of the peat deposits near the GMB and the large gold mining activity which takes place near the GMB at the WFS. The gold mining activity has attracted frequent attention because of the high yielding gold mines, the uranium pollution in the groundwater and the dewatering of the dolomites coupled with sinkholes and large cave systems (Swart *et al.*, 2003:635).

The study area focuses on the GMB but from the following descriptions, it would be clear that the WFS and the dolomites of the WFS, have an impact on the GMB and should also be discussed. The larger study area including the WFS will thus be discussed at the applicable locations and topics.

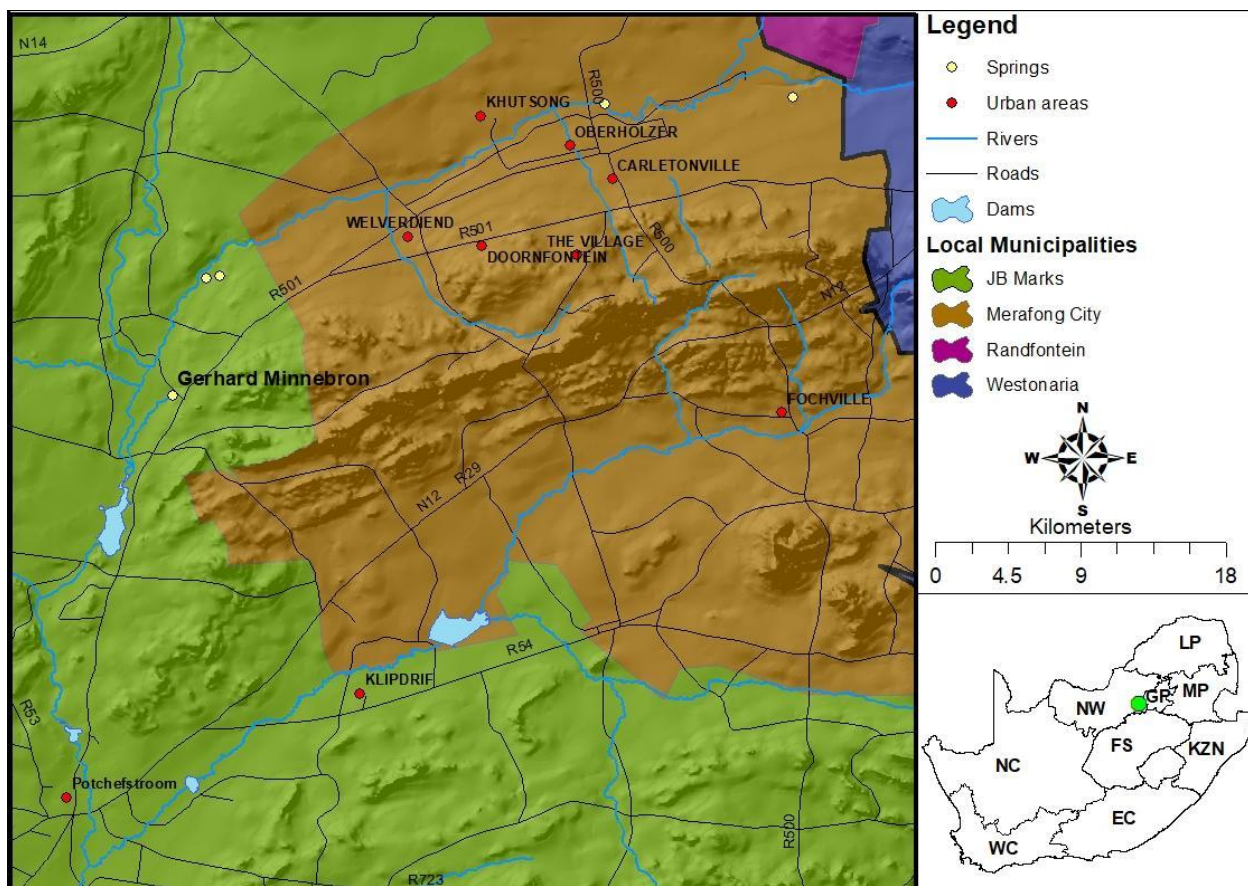


Figure 2.1: The Gerhard Minnebron with administrative boundaries.

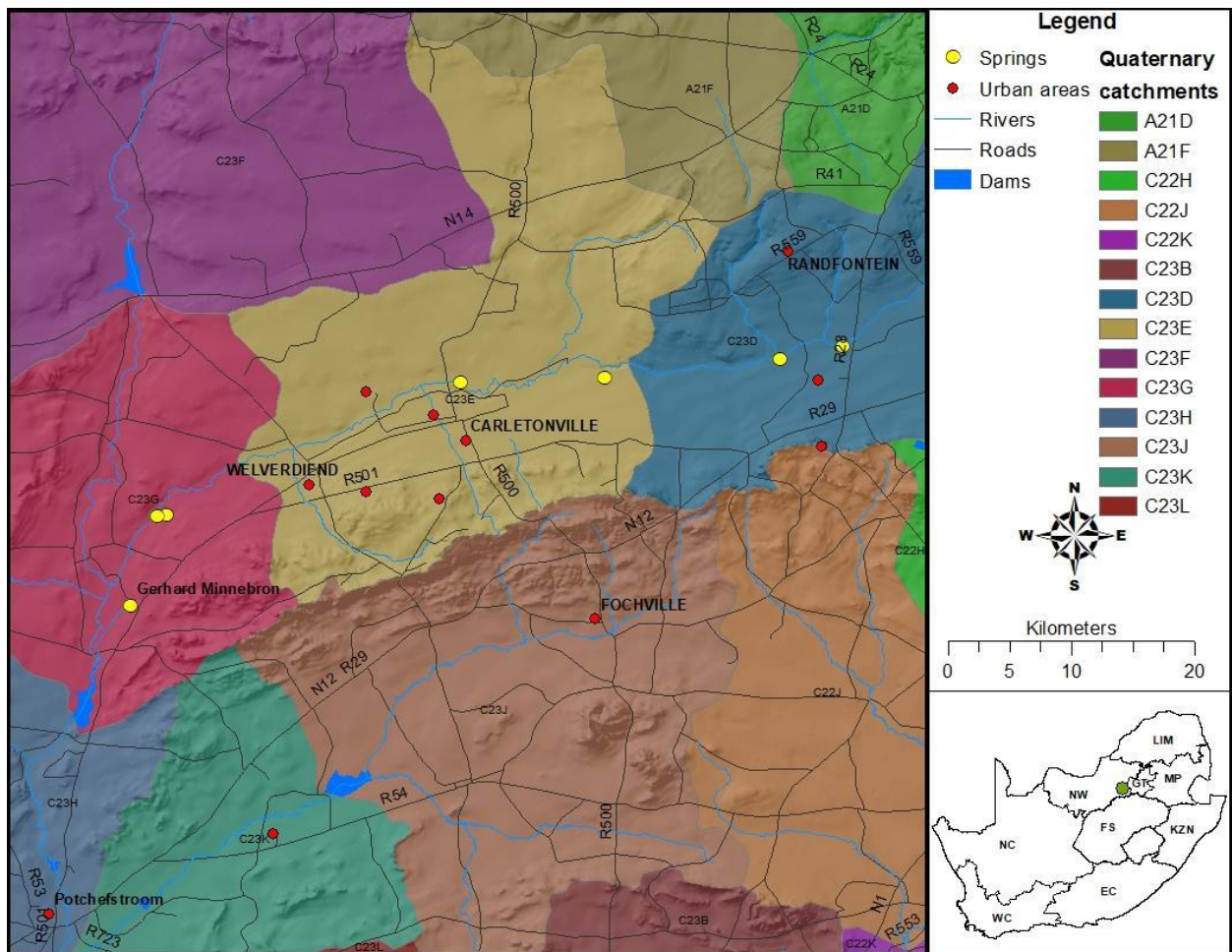


Figure 2.2: Quaternary catchment boundaries with the Gerhard Minnebron.

2.2 Physical Characteristics:

The study area and GMB is located within a semi-arid region, with summer rainfall and typically hot summers with convection thunderstorms which makes 90% of the rain events in the summer months of November until March. These summer rains deliver an annual precipitation of 597mm (WR2012, 2020), which increases to the east and decreases to the west as shown by [Figure 2.3](#). The winters occur in the months of June till August and are typically dry and cold with occasional frost and temperatures can be as low as 0 degrees in the early mornings. The area has an average annual temperature of around 19 degrees where midday temperatures can be as high as 33 degrees in the summer and as low as 10 degrees in the winter. The annual average evaporation is 1700 mm (WR2012, 2020) which indicates that it is a semi-arid climate.

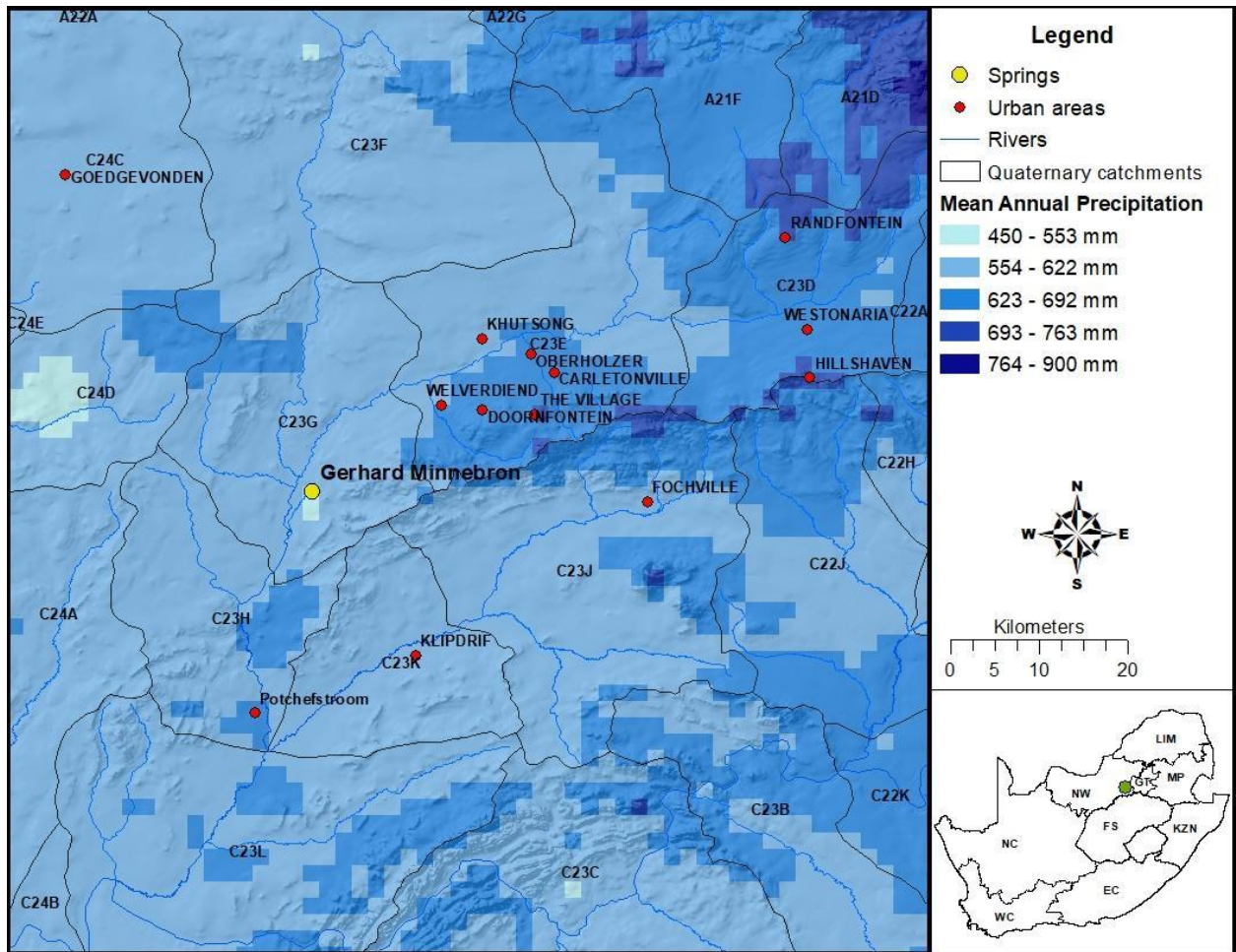


Figure 2.3: Mean annual Precipitation of the area.

2.3 Hydrology:

The topography and hydrology of the area can be seen in [Figure 2.4](#), from this it is visible that the surface water flows from the north eastern side to the south. The elevation has the same trend with the north east having the highest elevation with 1900 mamsl and the south east has the lowest elevation of about 1200 mamsl; the area is relatively flat with little steep slopes and mountains. The main river flowing through the area is the Mooi River. The Mooi River originates near Ventersdorp in the Mathopestad area and the stream originates out of Bovenste eye spring and the Klerkskraal eye’s just north of Klerkskraal dam. The Mooi Rivers main tributary is the Wonderfonteinspruit (WFS) which originates from the east of the area near Krugersdorp. The WFS flows west over an area with rocky ridges and large flat areas. The WFS flows into the Mooi River upstream where the Gerhard Minnebron’s (GMB) water also flows into the Mooi River. The study area has three large or major reservoirs, namely the Klerkskraal Dam, Boskop Dam and Potchefstroom Dam. The surface water in the area and the Mooi River drains to the south where it joins with the Vaal River (Barnard *et al.* 2013:656; Van Veelen, 2009:2).

The area has masses of dolomite underneath the streams where the relevance of these dolomites will be discussed later but they have an influence on the hydrology of the area. The dolomites create a direct link between surface water and groundwater. The interaction and effects of the dolomites on the hydrology and hydrogeology will be discussed later in the chapter.

There are some mountainous landscapes to the west of the study area that cause rainwater to collect and flow over the surface to the east. These rainwaters flowing overland have caused many seasonal streams to form and shape the landscape. Wetlands occur on the banks of seasonal streams, permanent streams and along the edges of larger bodies of water such as large ponds or dams. All the streams and the water of the spring flows to the Mooi River and south towards Potchefstroom.

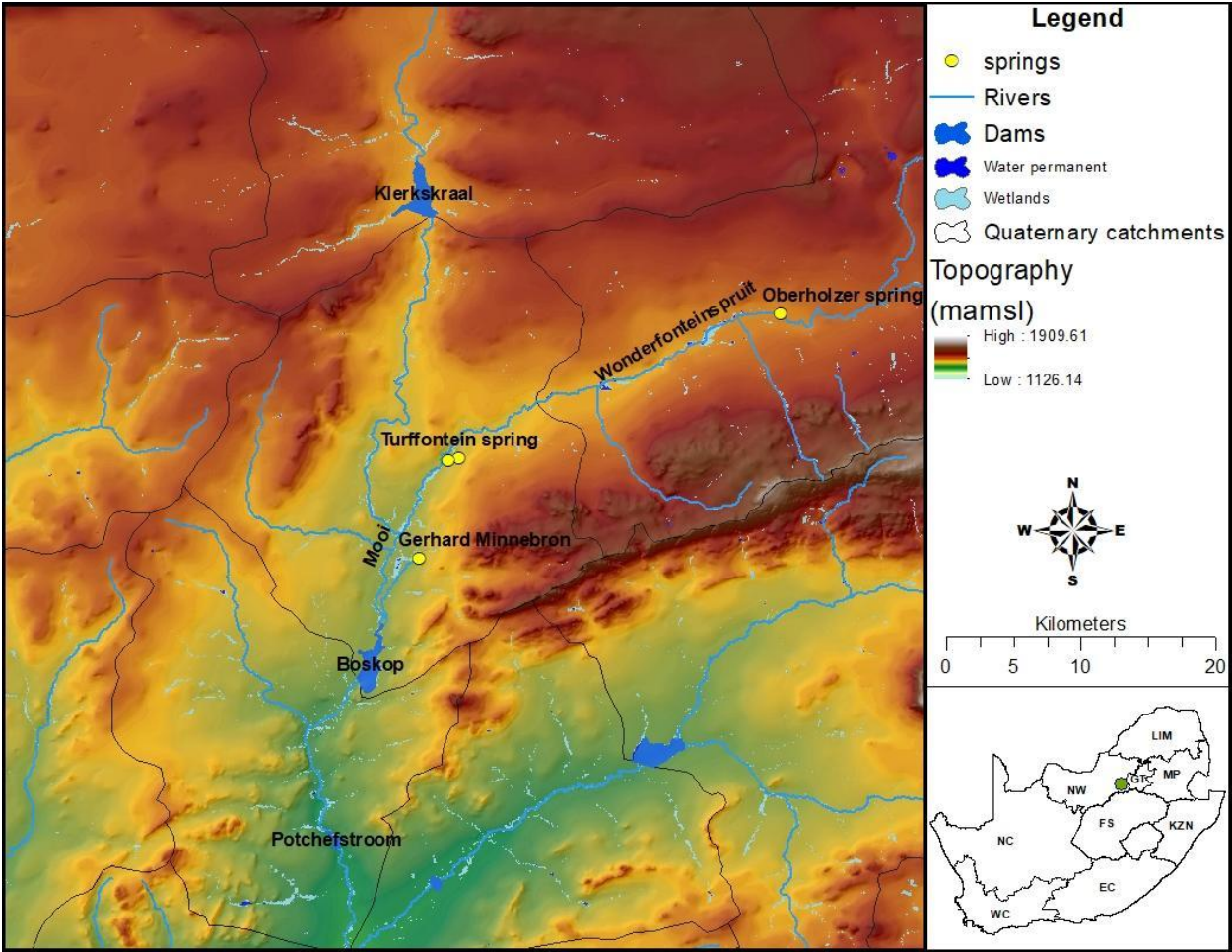


Figure 2.4: Regional Topography and Hydrology.

2.4 Geology:

The geology will be discussed in two areas, the main study area focusing on just the GMB. The bigger area will focus on the WFS as well, there is good reason to assume that this area has an influence on the smaller area and will be relevant for the research ([Figure 2.5](#))

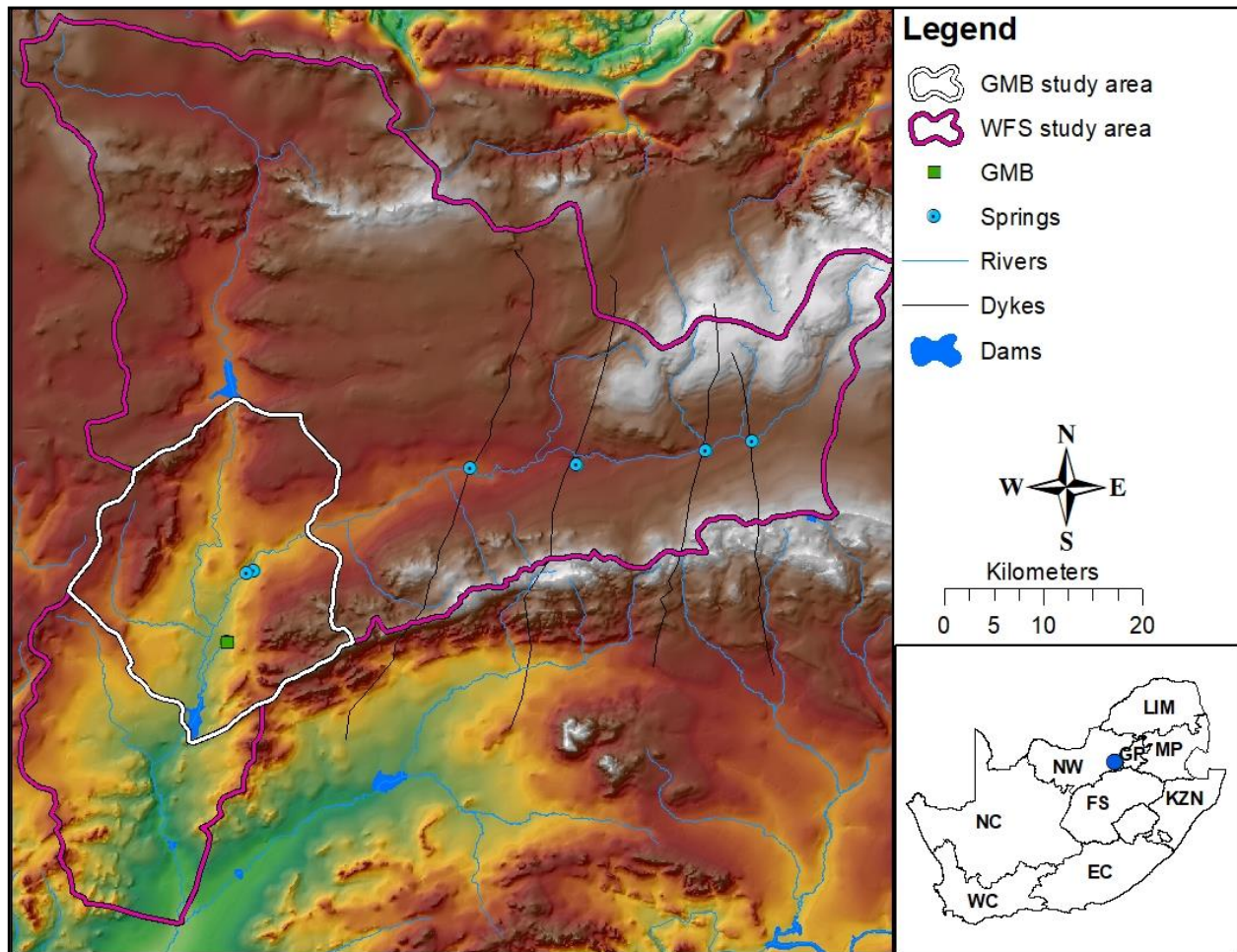


Figure 2.5: Map indicating two study areas.

Wonderfonteinspruit:

The Study area and surrounding area has a rich amount of different geological formations and a rich history in terms of the geological context. The geology in the area is straightforward, dominated by sedimentary formations with some igneous and metamorphic formations. To the south of the study area, the geology becomes more complex due to the influence of the meteorite impact of the Vredefort Dome. [Figure 2.8](#) shows that there is a very large dolomitic formation in the area, especially to the north and north east. The dolomite formation also makes up a very large part of the WFS where these dolomites occur there are high amounts of springs, caves,

sinkholes and voids within that area. These dolomites have intercalated chert bands that vary in thickness from 300mm to several meters thick and in some locations the dolomites are devoid of chert. The dolomites in the area have a relative thickness of 1,2km to 1,45km and they dip towards the south of the area at a 5° angle. The Syenite dyke intrusions that intruded these dolomites post Transvaal age are oriented in a north northeast to south southwest orientation, these syenite dykes form the boundaries of the dolomitic compartments (Swart *et al.*, 2003b:638).

The WFS area has geology that is rich in valuable material ore deposits and a very complex historical geology. Mines in this area produced some of the richest gold mines in the world (Winde, 2004:2-3). The dolomites which are of great importance in terms of water are lithostratigraphically at the base of the Transvaal Supergroup. The name Dolomite describes a sedimentary rock that consists of Calcium-Carbonates, Magnesium-Carbonates and Silica. To a lesser extent dolomites can contain Iron, Manganese and Aluminium. The Dolomites in the study area were formed during the early Proterozoic era and belong to the Malmani subgroup and Chuniespoort group (Swart *et al.*, 2003b:637-638).

The dolomites are divided into compartments by dykes but this will be discussed in the **2.5 Hydrogeology:** section. The deep level of mining in the WFS area and north east of the area have caused large scale dewatering, lowering the water table by as much as 1000m in some areas. The dolomites were also affected by the filling of caves and sinkholes with uriferous material where the discharge and seepage of large volumes of polluted effluents and fluid from the tailings, caused large amounts of water pollution in the area and surrounding areas.

The area is very layered in terms of geological formations as displayed by [Figure 2.6](#) The area has geological formations that are part of the Transvaal, Ventersdorp and Witwatersrand Supergroups, as indicated by [Figure 2.7](#). The areas that were targeted during the mining operations are on top of the Witwatersrand Supergroup or part of them and below the Ventersdorp Supergroup where it appears, thus forming the contact between these two Supergroups. These are then overlain by the Black reef formations and on top of this layer are the Chuniespoort dolomites. Pretoria Group sediments overlie these dolomites to the south and the different compartments in the dolomites were caused by the Pilanesberg syenite dykes (Swart *et al.*, 2003b:754 -755).

[Figure 2.6](#) and [Figure 2.9](#) indicate that the Malmani dolomites have four layers. Ngcobo (2006: 254), indicates that the four dolomitic layers that were deposited belong to the Eccles, Lyttleton, Monte Christo and Oak Tree formations in the order of youngest to oldest. As indicated by [Figure 2.9](#) and described by Winde and Erasmus (2011a:297 - 298), the layers are either chert rich or

chert poor. The chert rich dolomites are highly weathered and thus good aquifers, where the chert poor dolomites are not weathered and dry in terms of water.

THICKNESS	LITHOLOGY	FORMATION	SUB GROUP	GROUP	SUPER GROUP
200–500m	Andesitic lava and tuff	HEKPOORT ANDESITE		PRETORIA	TRANSVAAL SEQUENCE
50–200m	Quartzite	TIMEBALL HALL			
	Shale				
	Quartzite Chert Breccia	ROOIHOOGTE			
300m	Chert rich Dolomite	ECCLES	MALMANI	CHUNIESPOORT	TRANSVAAL SEQUENCE
150m	Dark Chert free Dolomite	LYTTLETON			
500m	Light Dolomite with Chert	MONTE CHRISTO			
100m	Dark Dolomite	OAK TREE			
10–20m	Carb. Shale with Quartzite Conglomerate	BLACK REEF			
400–500m	Amygdaloidal andesitic lava	EDENVILLE, LORRAINE, JEANETTE		KLIPRIVERSBERG	VENTERSDORP
100m	Non amygdaloidal aphanitic lava	ORKNEY			
250m	Porphyritic lava	ALBERTON			
0–40m	Komatiitic lava and tuff	WESTONARIA			
	Ventersdorp Contact Reef	VENTERSPOST CONGLOMERATE			
6m	Coarse light grey/green quartzite	ELSBURG QUARTZITE	TURFONTEIN	CENTRAL RAND	WITWATERSRAND
0–3m	Kloof reef Libanon reef	KIMBERLEY CONGLOMERATE			
0–80m	Shale and siltstone	BOOYSENS SHALE			
10–15m	Quartzite	KRUGERSDORP	JOHANNESBURG		
	Cobble reef	BIRD CONGLOMERATE			
3m	No. 5 Uppers				
90m	Quartzite	LUIPAARDSVLEI QUARTZITE			
40m	No. 4 Uppers	LIVINGSTONE CONGLOMERATE			
	Quartzite				
10m	No. 3 Upper reef	RANDFONTEIN QUARTZITE			
30m					
10–15m	No. 2 Upper reef	JOHNSTONE CONGLOMERATE			
90m	Quartzite	LANGLAAGTE QUARTZITE			
	No. 1 Upper reef				
60m	Middelvlei reef Greenbar Carbon Leader North Leader				
15m	Quartzite	MARAISBURG QUARTZITE			
	Jeppeshtown	ROODEPOORT			

Figure 2.6: Stratigraphy of the gold mines in WFS (Ngcobo, 2006)

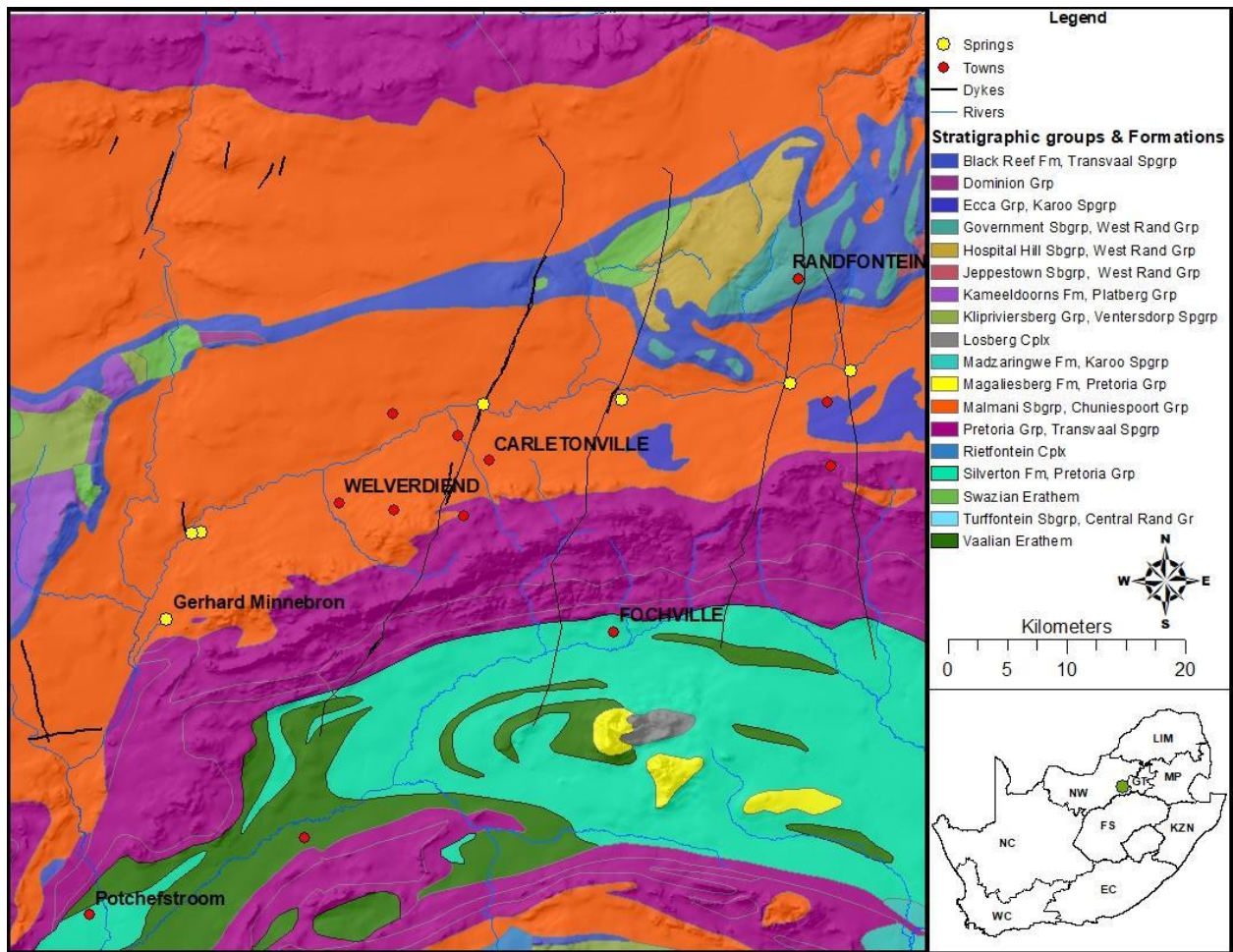


Figure 2.7: Stratigraphic groups of the WFS area.

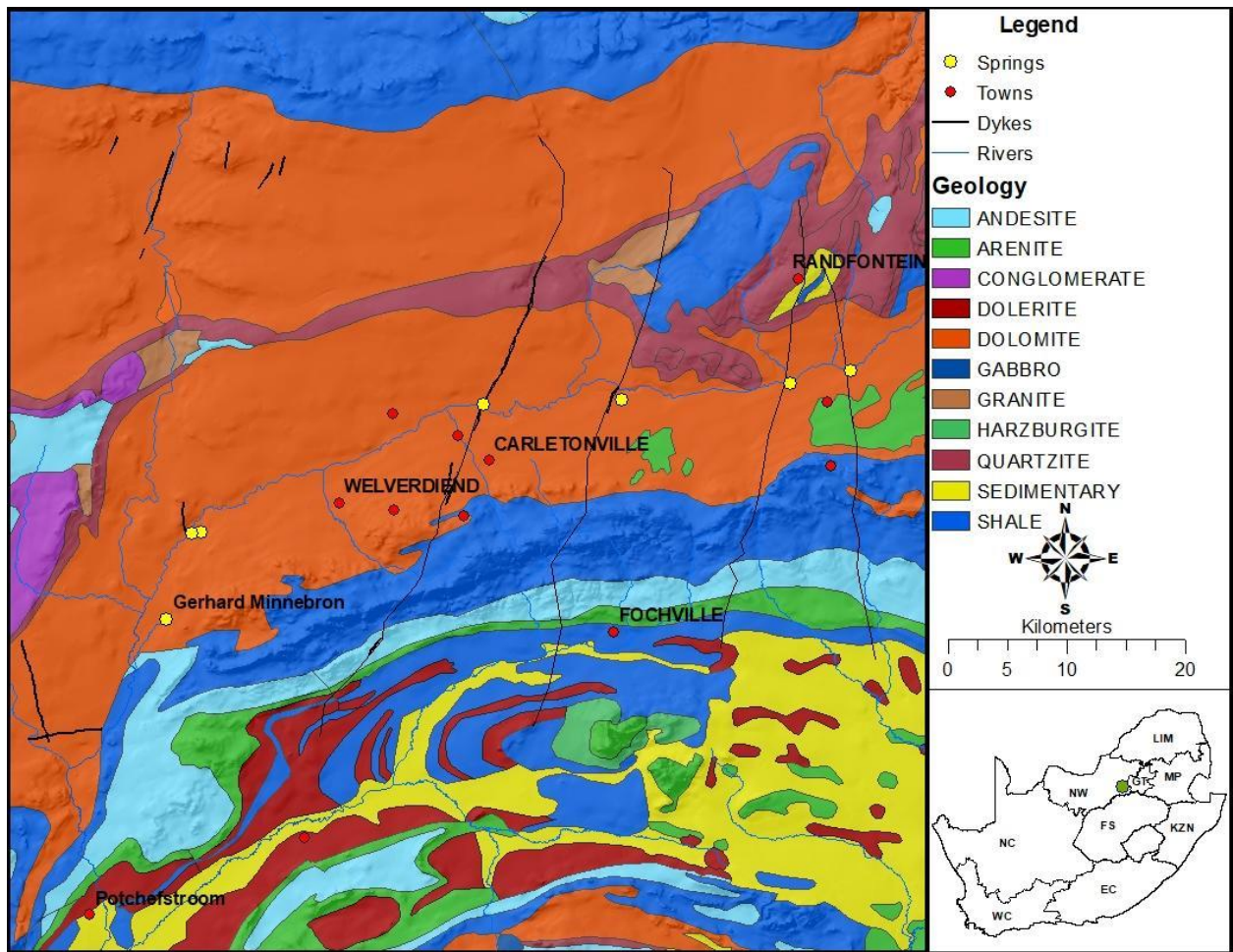


Figure 2.8: Geology of the WFS area.

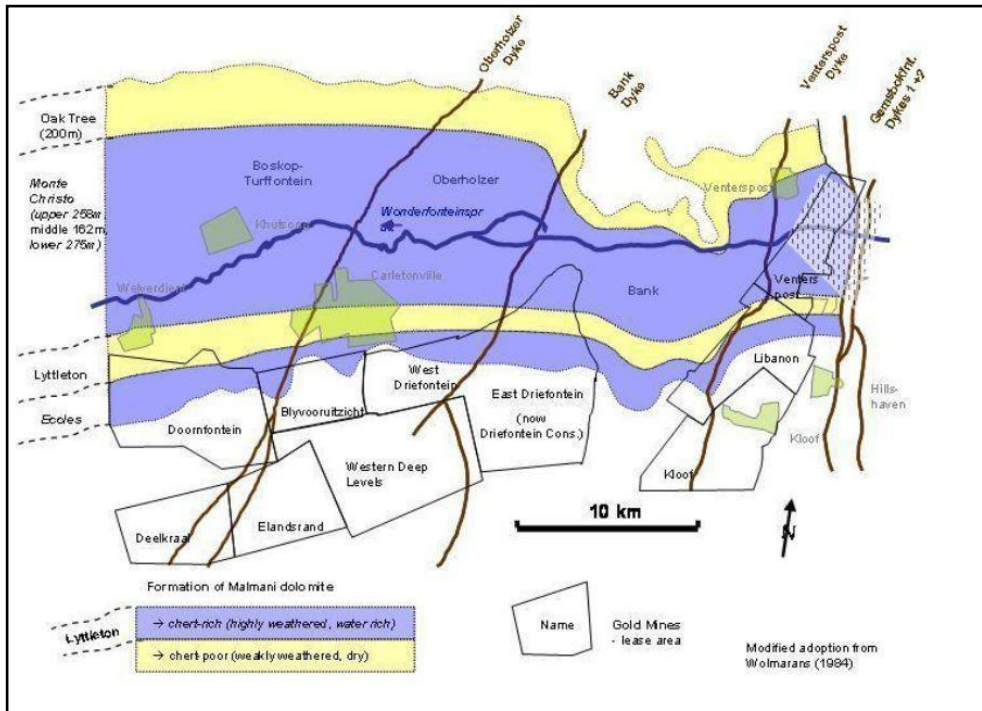


Figure 2.9 Dolomitic compartments in WFS and dolomitic layers (Winde & Erasmus, 2011a).

Gerhard Minnebron:

The GMB itself is located within the dolomitic formations. According to Winde and Erasmus (2011a:297), the spring is located within the Monte Christo dolomite formations and the dolomite formations dip 7° to the south. This is also indicated by [Figure 2.10](#), indicating formations of the Pretoria group with a mixture of sedimentary, igneous and metamorphic rocks. The formations overly the dolomites and form the border of the dolomitic aquifers on the southern and south-eastern side. [Figure 2.11](#) provides borehole logs of boreholes shown in [Figure 2.10](#), boreholes 1,2 & 4 all display only sedimentary rocks. The sedimentary formations are made up of dolomite, chert and shale. Borehole 3's log is also predominantly sedimentary formations with shale, banded ironstone and limestone. Borehole 3 also has diabase within the log which probably belongs to igneous intrusions that occurred post Transvaal sequence.

Brink *et al.* (2002) makes use of nine stages of geological formations and structural events to describe the GMB's geology.

The first stage took place after the west rand group geological formations. Tectonic movements and compressional force caused an anticline structure to be formed. The tension created by the folding and anticline formation caused a thrust fault to form.

During stage two below the thrust fault, an overfold formation is created due to an eastward tectonic movement. Lavas that flowed out over the surface cover the last of the Witwatersrand formations.

A westward and eastward tectonic movement occurred during stage three. The two opposing tectonic movements resulted in an extensional stress system which created listric faults. The lava that flowed over the Witwatersrand deposits were eroded only occurring in some places currently.

Stage four is the deposition of the Transvaal supergroup. The first formation to be deposited was quartzites of the Black Reef formation. On top of the Black Reef formation, the Malmani subgroup was deposited consisting of Dolomites and Chert. The final deposition was the Pretoria group on top of the Malmani subgroup.

Stage five is tectonic movement caused by the Vredefort meteor impact. The impact caused folding and faulting directed centrifugally away from the impact. The faulting occurred at the Black Reef formations layer.

Stage six was also caused by the meteor impact. The thrust force created by the impact caused previous faults zones to activate again and caused more faulting along previous faults. The folding also increased when compared to stage five and anticlinal folding increased.

A new thrust fault was created in stage seven. The Vredefort meteor impact's force caused the thrust fault to detach from the fault along the Black Reef formation fault upwards to the surface.

During stage eight the meteor impact caused a second thrust fault to sever from the Black Reef formation's fault. This thrust fault shifted the Ventersdorp supergroup formations and Transvaal supergroup formation over on to the Transvaal supergroup.

In stage nine centrifugal forces from the meteorite impact ceased and resulted in stress directed towards the centre of the meteorite impact. These stresses caused the fault created during stage eight to act as a second fault zone but this time as a rifting fault and shifted the layer back towards the centre of impact.

After stage nine erosion occurred until the present time with the Karoo supergroup sedimentation in some areas. The geology currently occurring is displayed in [Figure 2.10](#). Erosion of the folding caused the current visible geological formations to be seen on the surface along with some of the faulting that occurred.

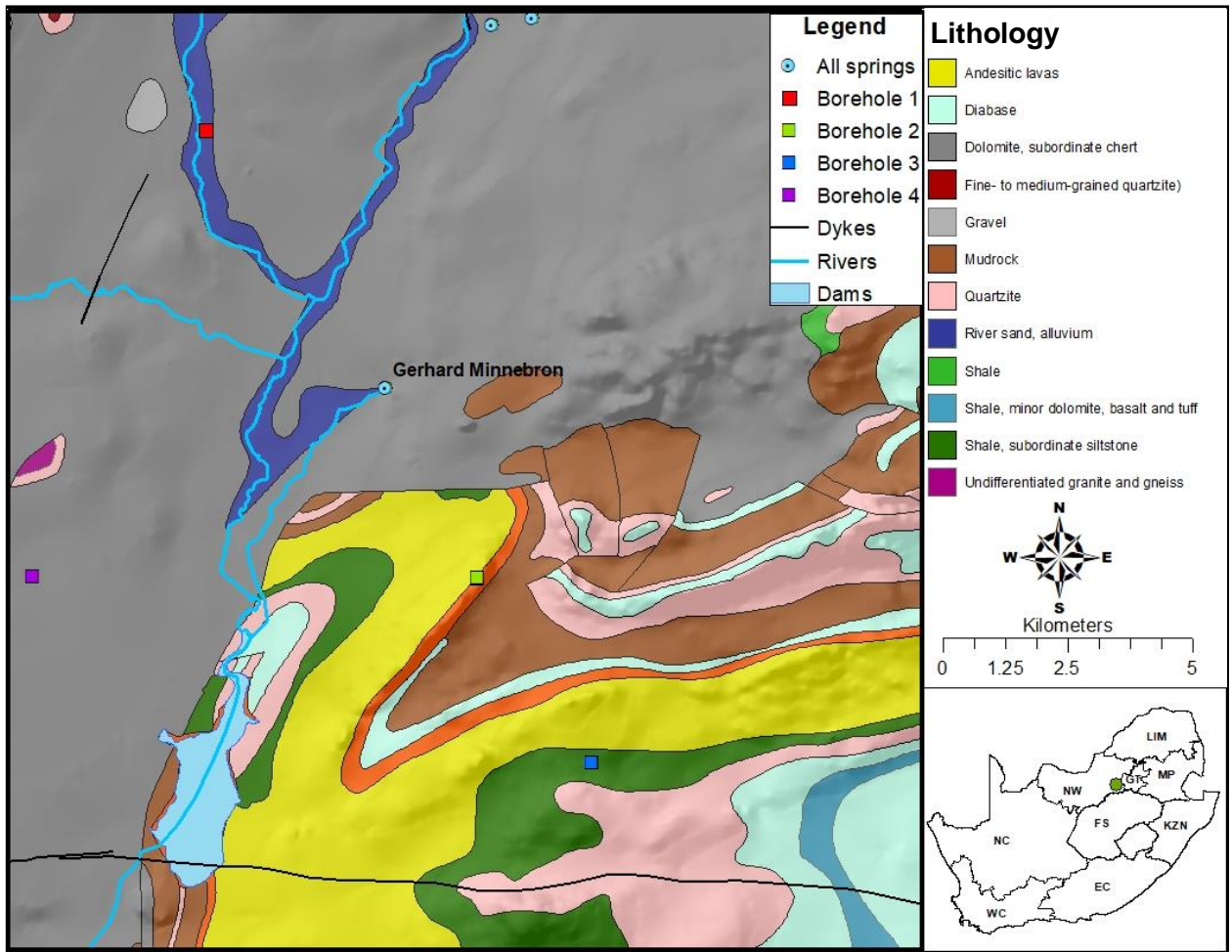


Figure 2.10: Lithology of GMB area

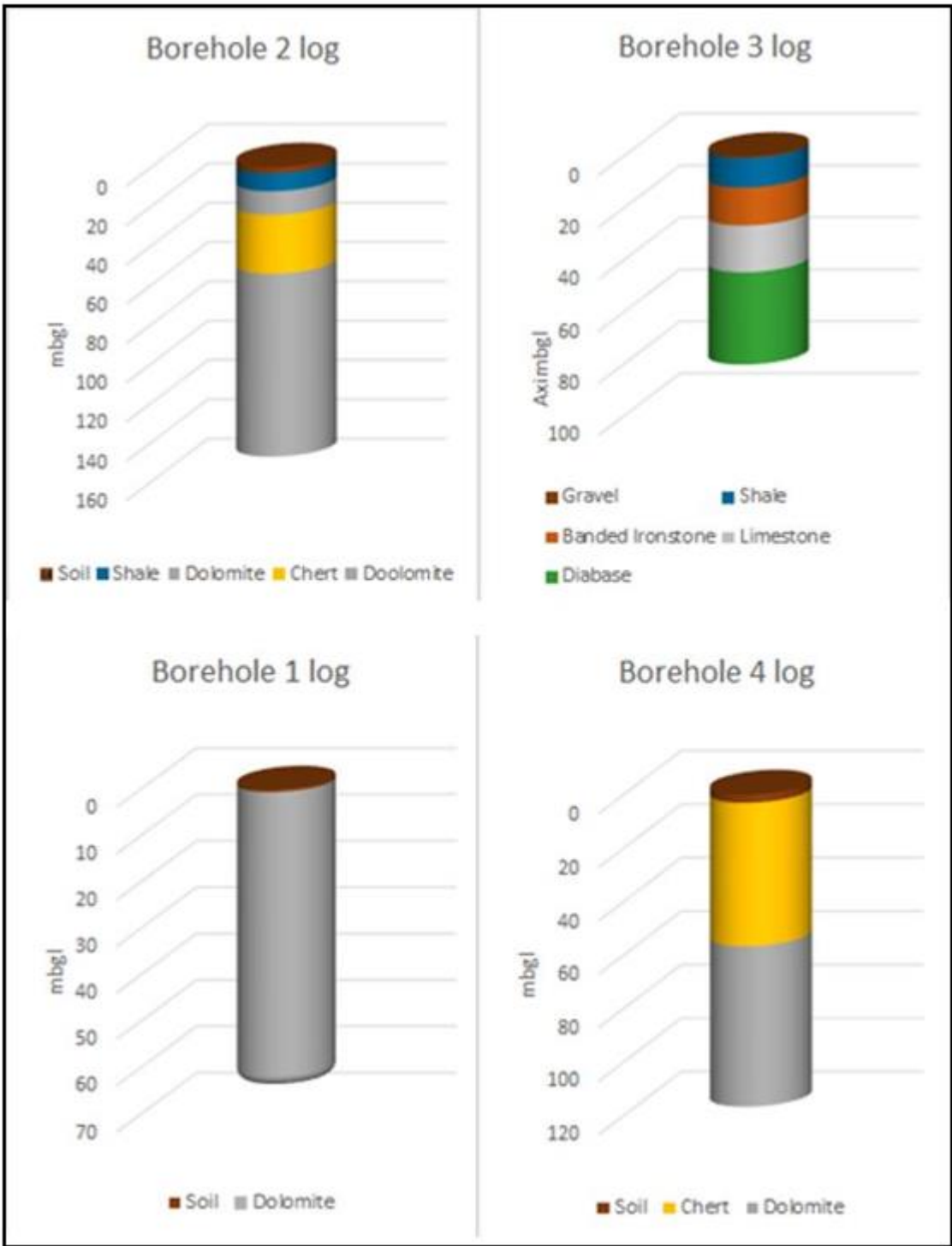


Figure 2.11: Borehole logs of boreholes 1 – 4

2.5 Hydrogeology:

The Hydrogeology of the area will be discussed in terms of two areas; the first area is the larger study area of the WFS which includes the GMB and the second smaller area is within the first area, but only focuses on the GMB itself. The reason that there is a larger study area is there is a possible link between the GMB and the WFS and the area cannot focus only on the GMB but needs to be described with the larger study area as well.

Wonderfonteinspruit:

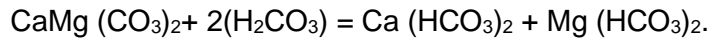
The area consists mainly out of dolomite and thus the main aquifers consist of dolomite and karsts as shown in [Figure 2.12](#) and [Figure 2.13](#). These dolomitic formations are divided into compartments by impermeable Syenite dykes that intrude in a north-south orientation. These form the eastern and western boundaries of the compartments; the northern boundaries are made up of the Black reef formation dipping southward and the southern boundaries are made up of dipping shales and quartzite of the Pretoria group which can be seen in [Figure 2.7](#) (Swart *et al.* 2003a:755–757). The locations of the springs can be seen in [Figure 2.13](#). Before the impacts of mine dewatering, impermeable syenite dykes would cause water to dam up upstream of the dykes. Where the built-up water level intersects the lowest point in the surface topography the water would flow out over the surface thus establishing a spring [Figure 2.14](#). The main surface and groundwater flow are expected to be from east to west (Swart *et al.* 2003b:639). The compartments and springs prior to mining and dewatering can be seen in [Figure 2.14](#).

Gerhard Minnebron:

The GMB is not caused by a dyke like the other springs in the area. The spring is at the foot of a 10–15m cliff in a relatively narrow valley as indicated by [Figure 2.15](#). It is inferred that the spring is caused by the sudden drop in relief, as the topography drops below the upstream groundwater table. The sudden drop in topography and the cliff is assumed to be products of a graben structure caused by the meteorite impact in the Vredefort Dome that caused the thrust faults to create the graben structure (Winde & Erasmus, 2011a:300 – 301).

[Figure 2.12](#) clearly shows the aquifers created by weathering of dolomites that also created karst environments and features. The Dolomites consist predominantly out of Ca and Mg in a ratio of 50:50 or in varying amounts like 47,5:52,5. Carbon dioxide in the atmosphere reacts with the water suspended in the air and forms a weak acid ($\text{H}_2\text{O} + \text{CO}_2 = \text{H}_2\text{CO}_3$). When this acid infiltrates

into the soil past plant roots it takes up additional acid which further increases the acidity of the groundwater. The acidity of the groundwater causes the dolomite to dissolve in the following reaction:



The above reaction creates karst environments within dolomites with very high volumes of water storage available. Dolomite without any weathering has a porosity of 0.3% (Swart *et al.* 2003b:639-640).

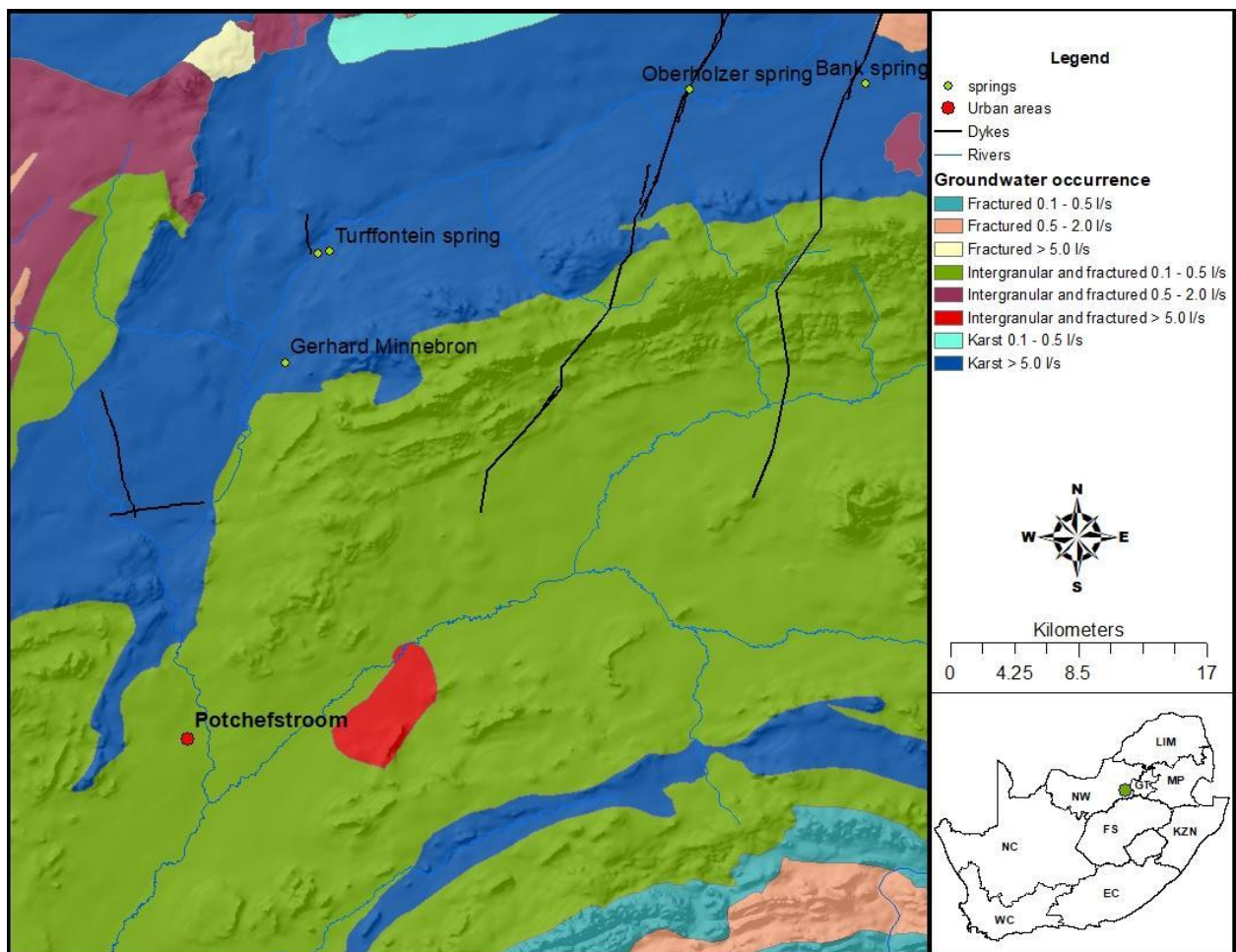


Figure 2.12: Groundwater occurrence in the area.

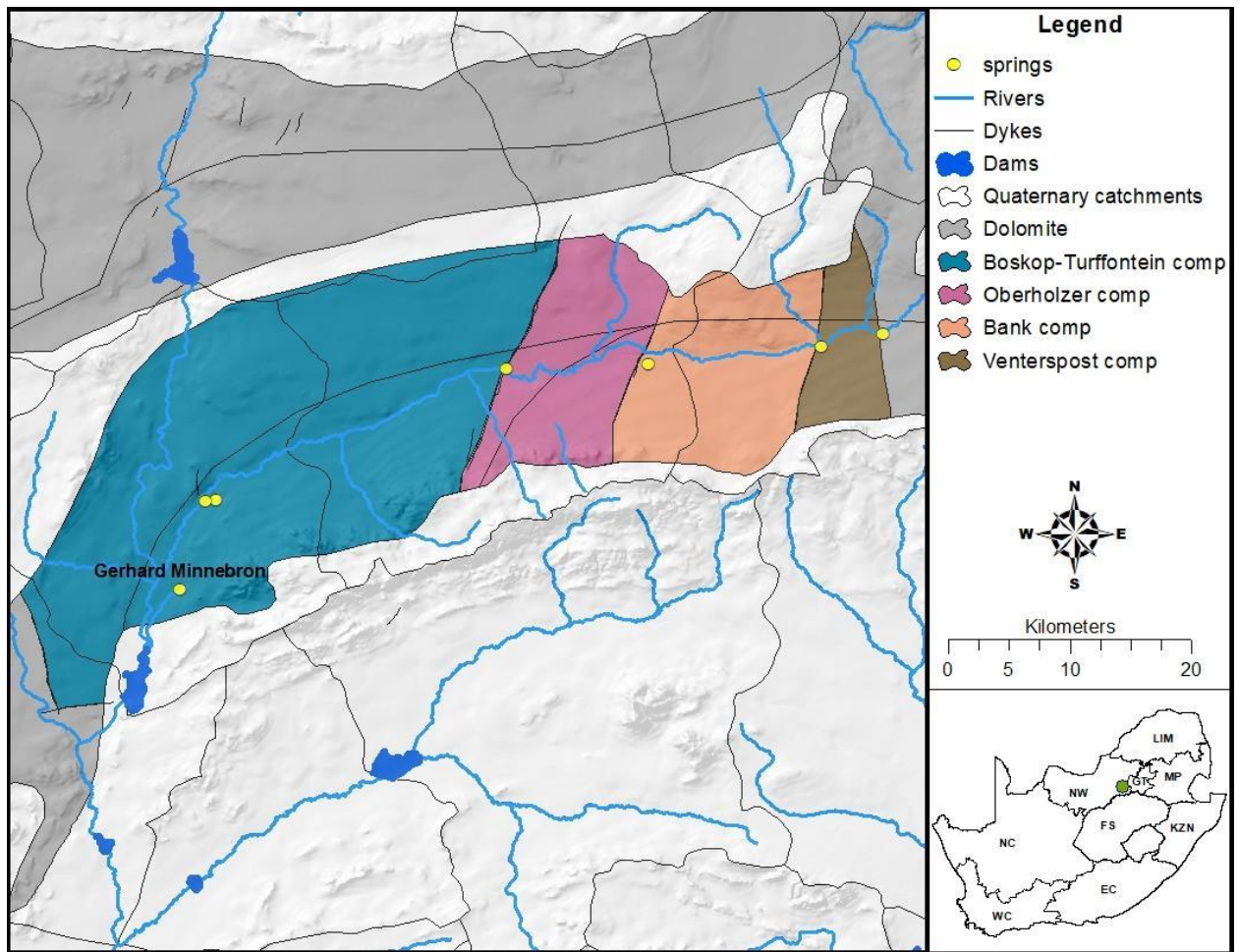


Figure 2.13: Relevant dolomitic compartments and springs.

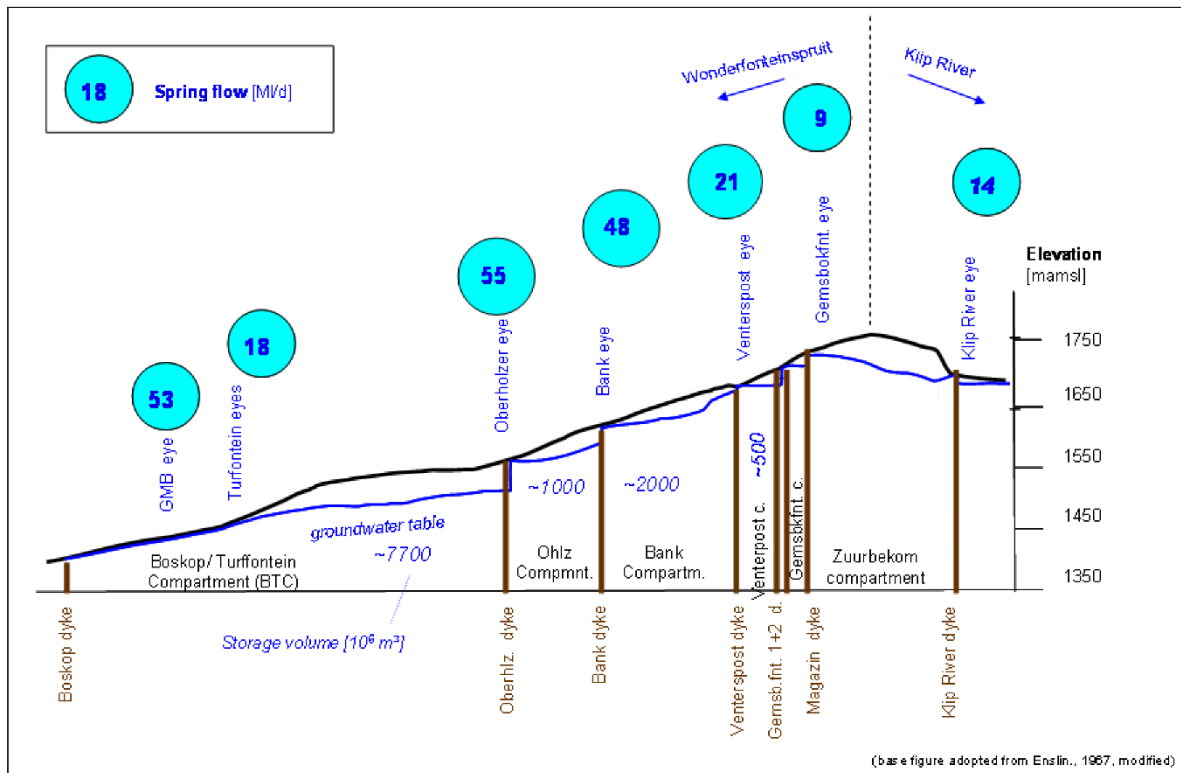


Figure 2.14: Cross section of the dolomite to propose the compartments and springs from (Erasmus et al., 2011).

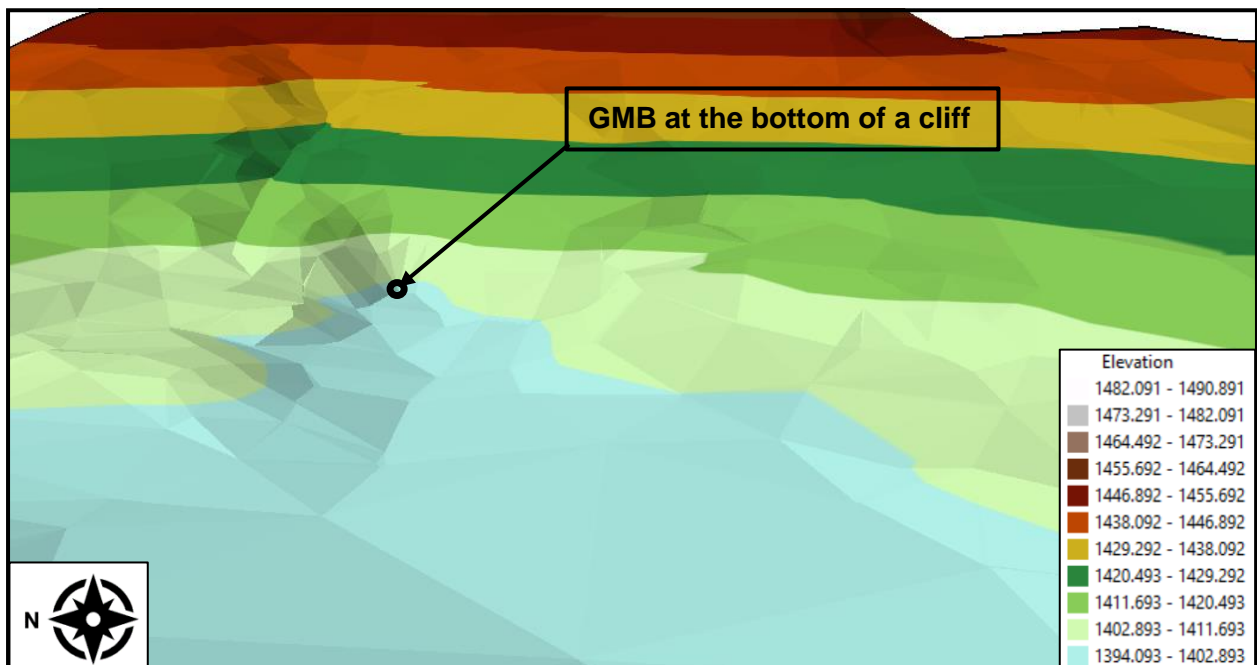


Figure 2.15: Digital Elevation Model (DEM) of the GMB.

2.7 Impacts of mining on the Hydrology and hydrogeology:

The study area is influenced by the mining activity within the Wonderfonteinspruit area and thus the impact mining has on the area will be discussed as well. In the eastern part of the WFS, the quartzite reefs have been mined since the 19th century at depths of up to 2000 meters below the surface, most of which are currently abandoned. Most of these mines are left neglected and unmonitored with sand dumps and slime dams that are heavily eroded. In the western part of the WFS, mining began about nine decades ago. As mining progressed, reefs at deeper depths could be mined as the target reefs dipped towards the west. The mining operations ventured deeper, infiltration of groundwater increased as depths of 4000 meters below the surface where mining was taking place (Winde, 2006a: 334 – 335).

With mining taking place at these depths large amounts of water started filling and flooding the mines and used various methods to curb the inflow of water into the mines but no success. The only affordable and effective solution was to dewater the whole dolomitic compartment and the mines got permission to go ahead with this from the government as it was seen as a greater economic benefit than what the agricultural sector offered them. The problem with dewatering a compartment was that water could not be pumped onto the surface because the streambeds had sinkholes in and the water would just flow back down into the mine voids, so the 1m-diameter pipeline was constructed.

The original purpose of the pipeline was to transport the water pumped out of the Venterspost mine across the Bank and Oberholzer Compartments into the Boskop-Turffontein compartment. However, due to the sinkholes that formed by the dewatering, it caused water from the WFS to gravitate into the underlying mines. Thus, they diverted the streamflow of the WFS to prevent recharge and save the mines millions in pumping costs and pumping the dewatered water into the Boskop-Turffontein compartment. Currently the dewatered compartments are the Gemsbokfontein West Compartment, Venterspost Compartment, Bank Compartment and the Oberholzer Compartment (Swart *et al.*, 2003b: 642-643). The dewatered compartments and 1m pipeline can be seen in [Figure 2.18](#).

The dewatering of these compartments have caused the drying up of four springs that had a total discharge of approximately 133 ML/d and as expected, the drying up of many irrigation boreholes and affecting agriculture. Large amounts of wide-spread sinkholes and dolines also appeared that had arguably the biggest influence on people's lives and infrastructure. Though the surface water was impacted immensely by the drying up of the spring and the diversion of natural streamflow

to accommodate for the large amounts of pumped water, the hydrogeological system was also impacted.

There are three scenarios regarding the hydrogeological impacts that dewatering the compartments had and what could occur after dewatering stops and rewatering starts.

The first scenario is described by Schrader *et al.* (2014a: 67-70) and Winde & Erasmus, (2011a: 303-304). It is estimated that the deep level mining with the large amounts of tunnels penetrated the impervious syenite dykes that separated the compartments, this is also applied to the Boskop-Turffontein compartment. Penetration of these dykes or boundaries creates a link between the compartments forming a new single, 'Mega-compartment'. The "Mega-compartment" is illustrated in [Figure 2.16](#). The mine voids and penetrated dykes are shown in [Figure 2.17](#). From the figure, it is clear that the dykes are still intact at the level of the water bearing dolomites. If the compartments ever rewater flow in the "Mega-compartment" will function like communicating vessels because the inter-compartmental ground flow will occur below the dolomites at the mine voids. If this is the scenario and the groundwater flow within the sub-compartments exceeds the amount of water through the natural recharge of each sub-compartments, the driving mechanism of the inter-compartmental flow is the difference in the groundwater head of the adjacent compartment. This driving mechanism or force would gradually decrease and disappear completely. Once this happens the water level would be on a single level elevation across all sub-compartments in this case and the water of the "Mega-compartment" would flow out of the lowest elevation springs namely the Gerhard Minnebron and Turffontein springs.

A second scenario is presented by Schrader *et al.*(2014a: 68-70). In this scenario, if the Inter-compartmental flow is reduced to be exceeded by recharge before the driving head of the adjacent compartment is reduced and the water level is equal. This would cause a difference in the head between adjacent compartments. The difference in head of adjacent compartments would be less than pre mining levels and the water table elevations would be at lower elevations as well. If this appears before the groundwater level reaches the surface there would be no spring flow and the compartments will be in between pre mining spring flow and a "Mega-compartment" scenario.

There is also a possibility that once the compartments are rewatered, they would proceed in functioning as normal or individually, due to it being suspected that the dykes are penetrated well below the dolomites and the lateral flow across penetrated dykes from the mine void in one compartment to the void in the next compartment will not be big enough to accommodate the naturally recharged groundwater, with the lateral flow and vertical flow through non-karstified

dolomite above (Winde & Erasmus, 2011a: 303-304). This normal or pre mining water levels and flow could also be achieved if the difference in the head of adjacent compartments is not enough to produce sufficient Intra-compartmental flow and once the compartments are filled with recharge up to surface level spring flow would resume at pre mining volumes and groundwater levels are expected to be at pre mining levels (Schrader *et al.* 2014a: 68-70).

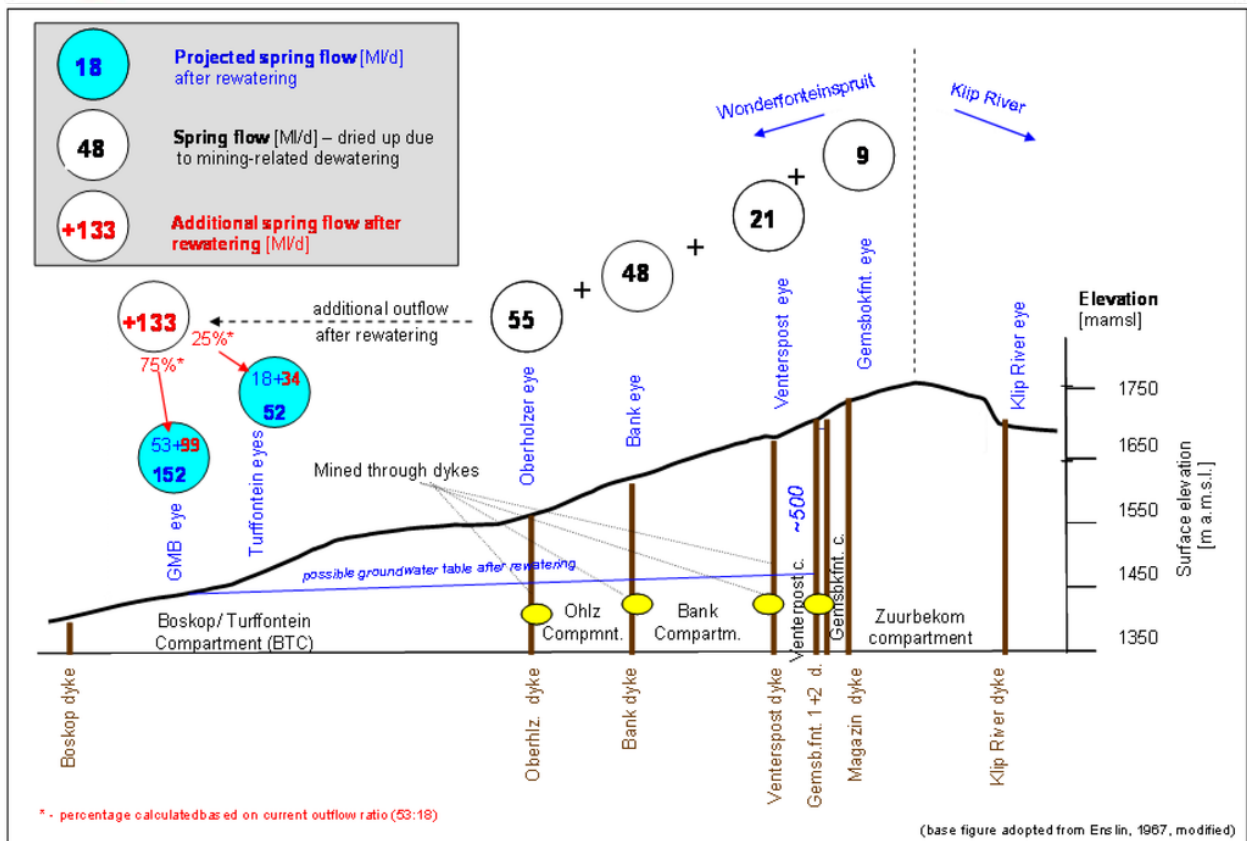


Figure 2.16: Cross section to propose the 'Mega-compartment' with penetrated dykes (Erasmus *et al.*, 2011).

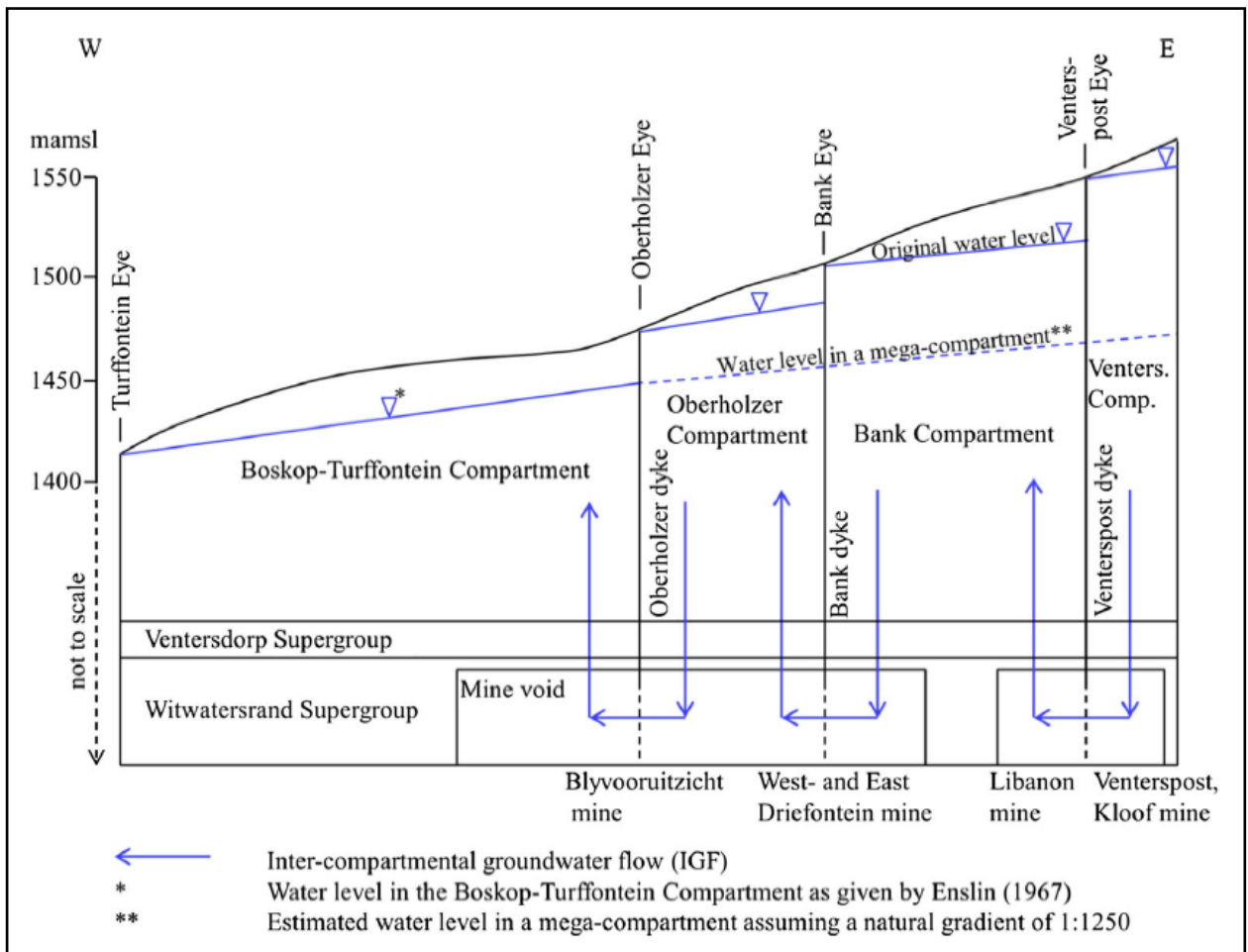


Figure 2.17: Illustrating the “Mega-Compartment” with mine voids (Schrader et al. 2014a).

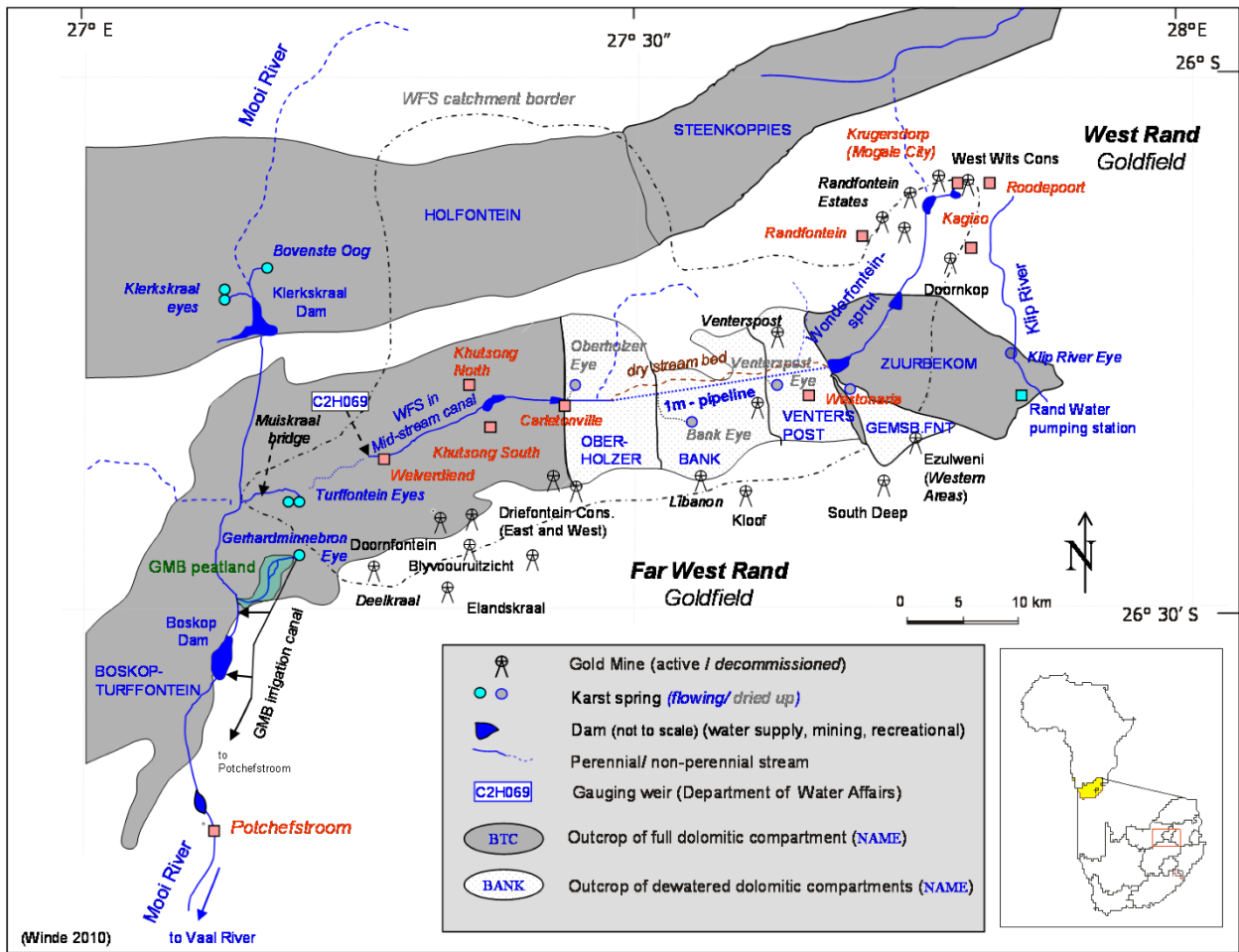


Figure 2.18: Map showing the effects of mining on the surface - and groundwater (Winde, 2010a)

2.8 Land cover:

The land cover of the study area will focus on two areas. The first area is the larger area including Potchefstroom and the far west Wonderfonteinspruit. The second area is the GMB and the surrounding area.

Wonderfonteinspruit:

The study area is primarily rural, with most of the population condensed within the towns. The primary contributors to the area economically are the mines and the secondary contributors would be the agricultural sector. The agricultural sector also covers the largest percentage of the area, which consists mainly of livestock in the grassland areas and then also cultivated and irrigated agriculture. The biggest part of the area is still within a natural state and very little urban development, which has all been aforementioned and can be seen in Figure 2.19. According to Barnard *et al.* (2013:656), the majority of the land usage is for grazing and crop farming purposes.

The soils and climate in the area are appropriate for a range of different agricultural practices such as crops of maize and sunflowers, grazing for cattle, sheep, and goats. The agricultural land use has accelerated the inputs of salts into the soils and has removed the natural vegetation and cover. The consistent agricultural development for over 75 years has changed the soil structure and has led to erosion increasing and the topsoil being removed. Mining of the peatland at the Gerhard Minnebron has also decreased the habitat of the surrounding area (Barnard *et al.* 2013:656).

The soil in and around the study area is relatively fertile with unaltered areas showing dense brush and lush grasslands, near the surface waters there're very dense and lush vegetation. The soil is also very commonly used for crop production, such as maize. The areas that have access to pivots or irrigation also plant fruits, vegetables and grains in large quantities. The moderate rainfall, warm temperatures and humid summers cause the area to be densely vegetated, in open flat plains it is predominately grass with small brushes and on steeper hills and rocky areas there are small to large dense brushes and trees.

Gerhard Minnebron:

The immediate land cover around the GMB can be seen in [Figure 2.20](#). Downstream of the GMB, or to the west of the spring, there are a lot of wetlands along the banks of the stream of the GMB and along the Mooiriver. Surrounding the wetlands are woodlands and, in some cases, cultivated fields. Downstream of the GMB and Mooiriver are the cultivated fields that increase in number and cultivated pivots occur. To the north of the GMB, the wetlands continue along the banks of the Mooiriver and to the east of the GMB, there are large areas of surrounding grasslands that are used for livestock grazing. The previously mentioned features are also visible in [Figure 2.21](#). The Plantations, wetlands, woodlands and grasslands can clearly be seen from the aerial photographs.

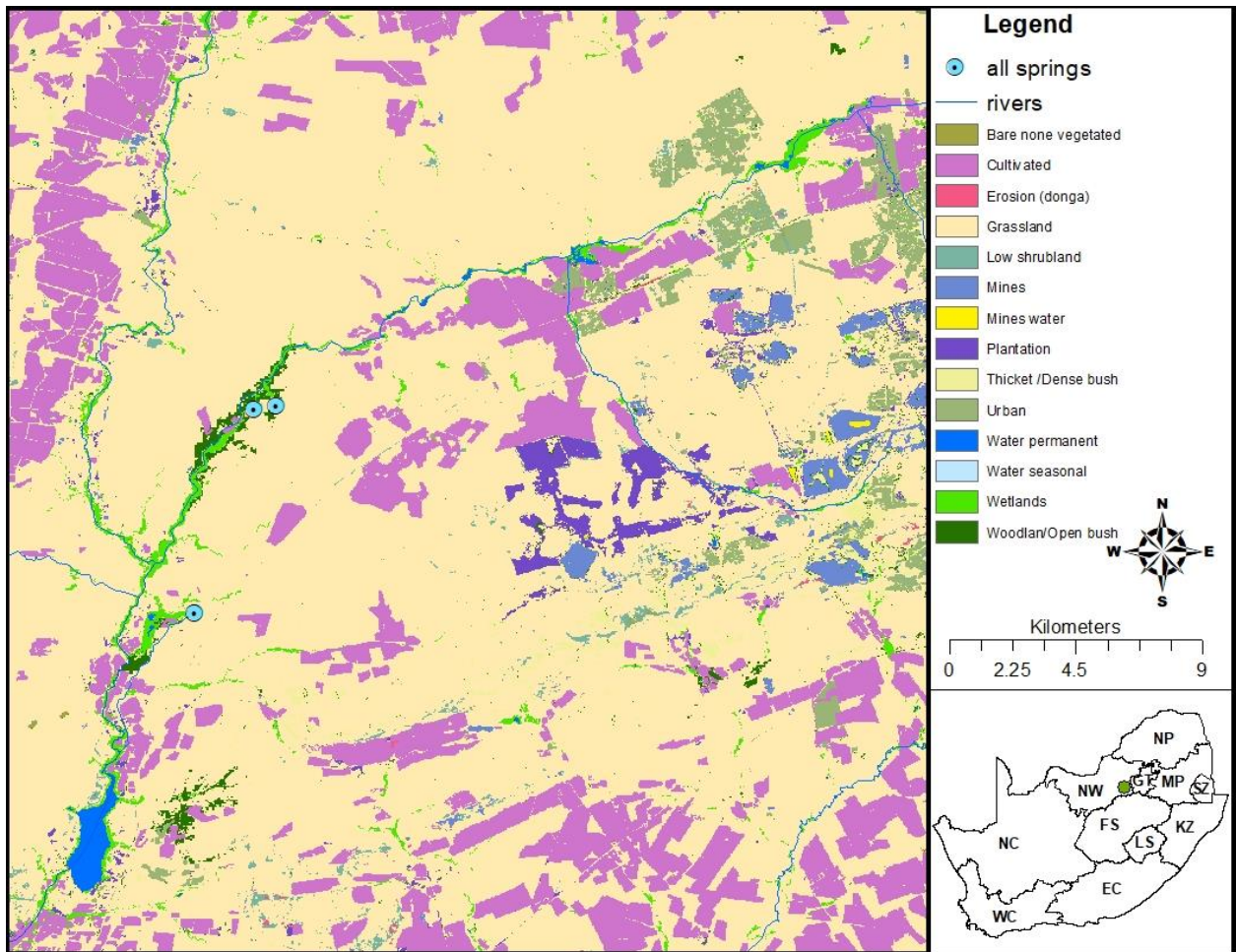


Figure 2.19: Regional Land cover.

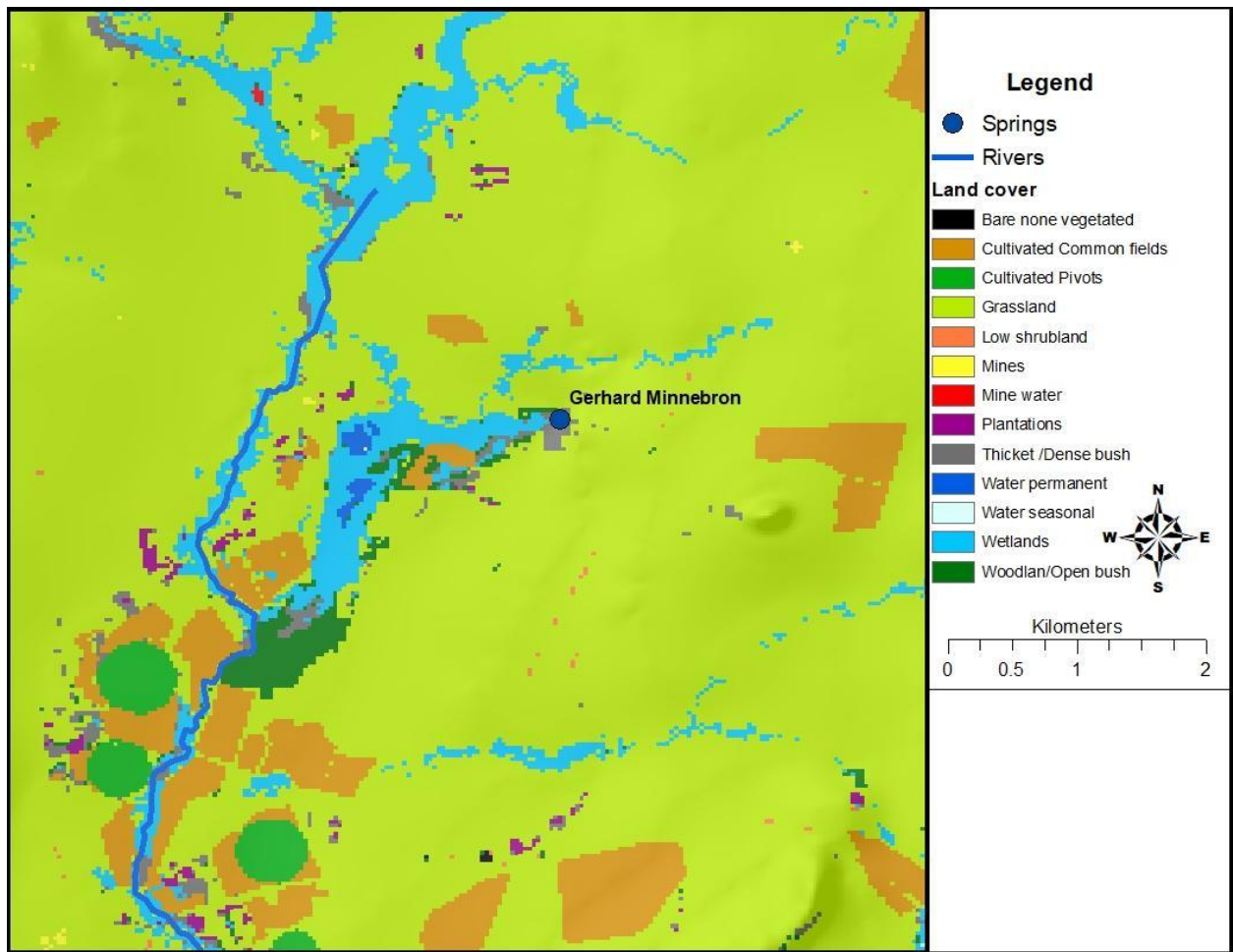


Figure 2.20: Land Cover of the study area.

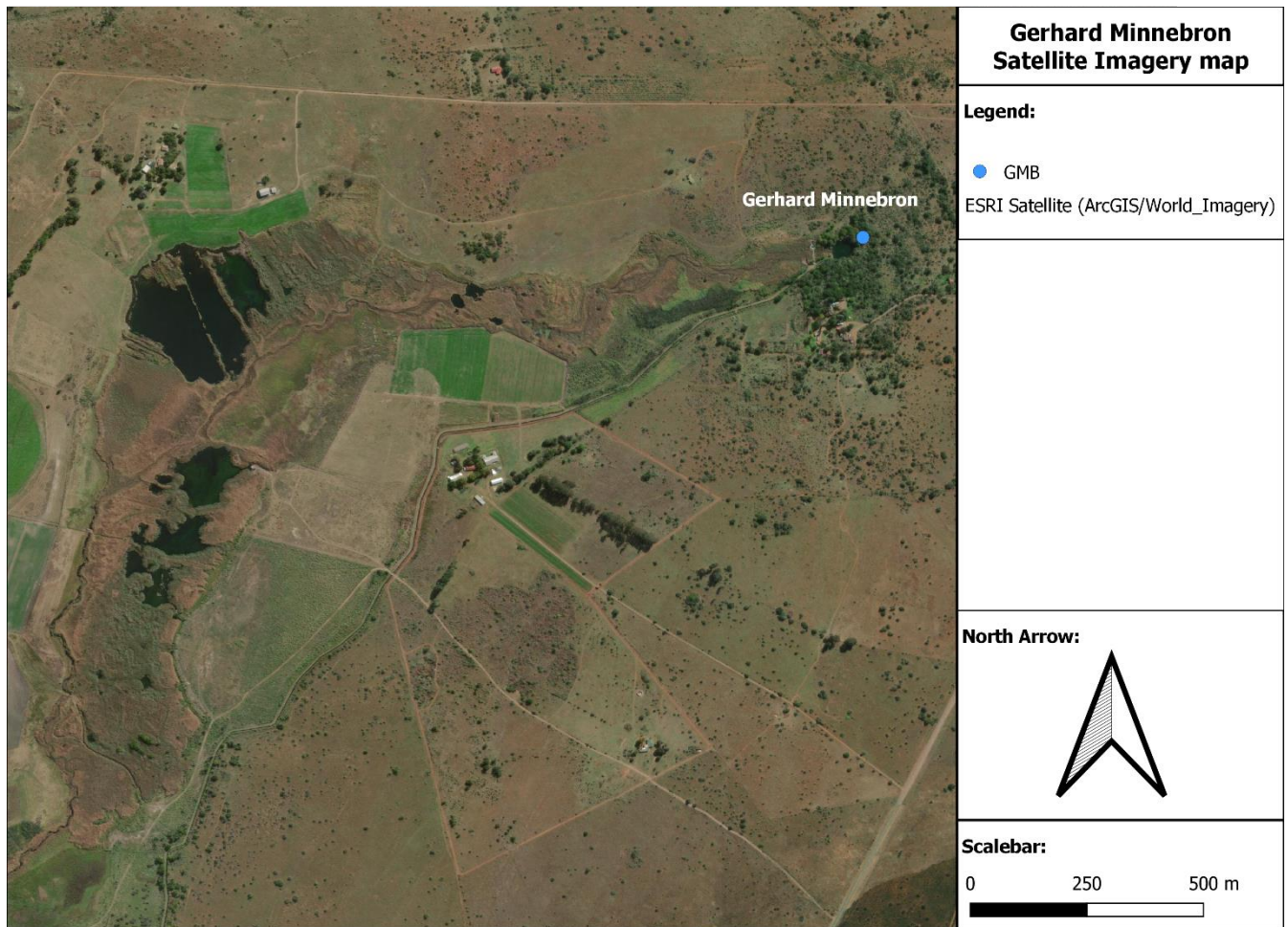


Figure 2.21: Aerial photo of study area displaying land use.

2.9 Water quality:

The inflow of groundwater and rainwater that flow into the mines and onto the TSF's have a big influence on the quality of the water. The hydrogen and oxygen dissolved in the water reacts with the pyrite in the TSF and forms sulphuric acid. The low pH that prevails causes heavy metals, trace elements and radionuclides to remain in a dissolved state, as the groundwater and surface runoff water flows and interacts with the environment. These pollutants are also then transported downstream to more water bodies (Van Veelen, 2009:3-5). According to Coetzee and Ntsume (2004:67), the following elements are polluting the area: Sulphate, Chromium, Cobalt, Nickel, Copper, Arsenic, Cadmium and Uranium, with Uranium and Cadmium poisoning posing the biggest threat to the environment. One major contributing factor to radiological contamination by Uranium is the disposal of slimes material onto dams that are placed on top of dolomites or too close to waterways as indicated in [Figure 2.22](#). The poor management of these TSF and disposal

CHAPTER 3: LITERATURE REVIEW.

3.1 Introduction to Isotopes:

Isotopes are variant atoms of a specific chemical element that differ in the number of neutrons they possess. [Figure 3.1](#) shows how the elements are described with the element, the mass number and atomic number, and how those values are calculated.

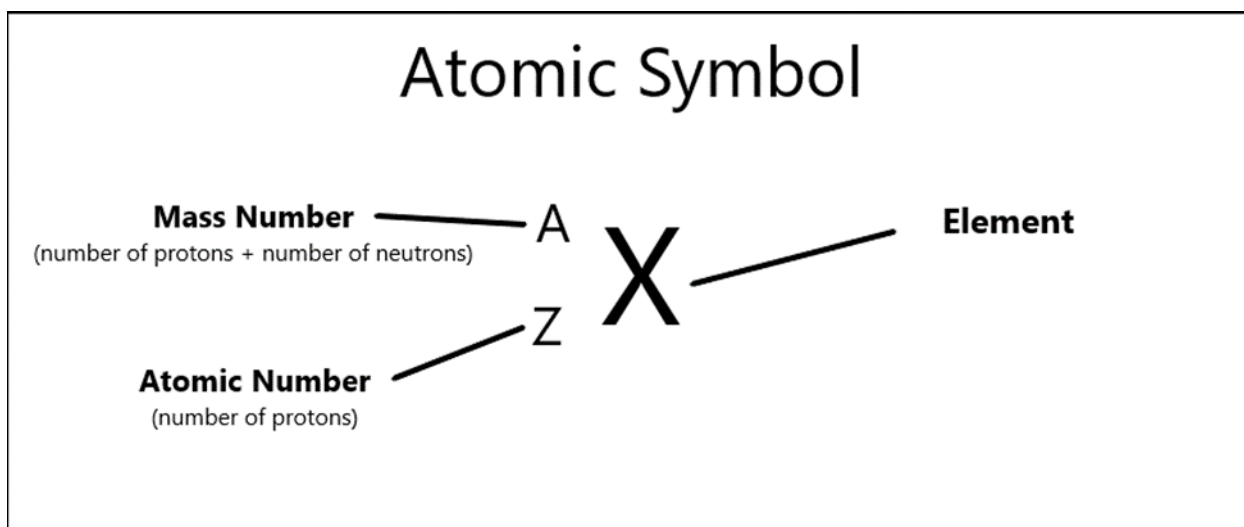


[Figure 3.1: Atomic symbol.](#)

All isotopes of a given element have the same number of protons but different numbers of neutrons in each atom and thus a different mass, this is visualized in [Figure 3.2](#). Protium is the most common isotope of the element hydrogen and has only one proton and zero neutrons. Deuterium (D or 2H) has one neutron and one proton, deuterium thus has a mass number of 2 double that of protium, where tritium (3H) has one proton but two neutrons double that of deuterium and then a resulting mass number 3. It is evident within the above figure ([Figure 3.1](#)) and in [Figure 3.2](#), these are all the same elements because they all have the same atomic number (number of protons) but they are isotopes of the same element because they have varying amounts of neutrons resulting in a different Mass number (Kendall & Caldwell, 1998b:53).

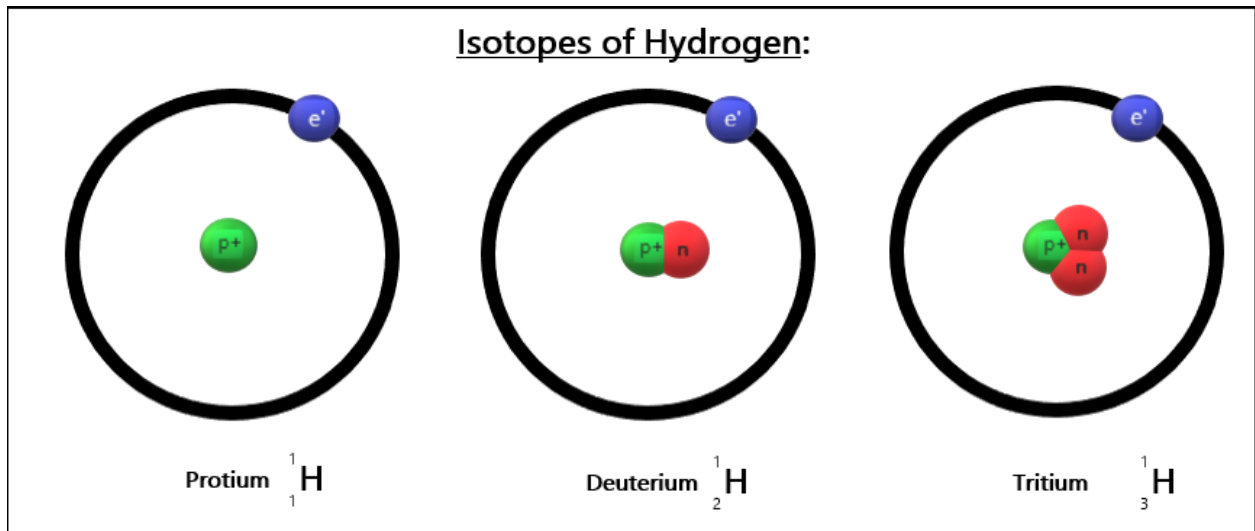


Figure 3.2 Example of Hydrogen isotopes.

Nuclear processes in the stars created the original isotopic compositions of the planetary systems. With the elapse of time, these original isotopic compositions of terrestrial environments changed due to processes such as radioactive decay, cosmic rays, mass-dependant fractionations accompanied by biological and inorganic reactions, anthropogenic actions like nuclear fuel processing, reactor accidents and nuclear-weapons testing. Radioactive or unstable isotopes are nuclides that over time spontaneously disintegrate into other isotopes while emitting alpha or beta particles and sometimes gamma rays. Stable isotopes are nuclides that do not decay to other isotopes on geological time scales, but they could be products of radioactive decay of unstable isotopes, thus the product of unstable isotopes decaying sometimes are stable isotopes (Kendall& Caldwell, 1998b:53).

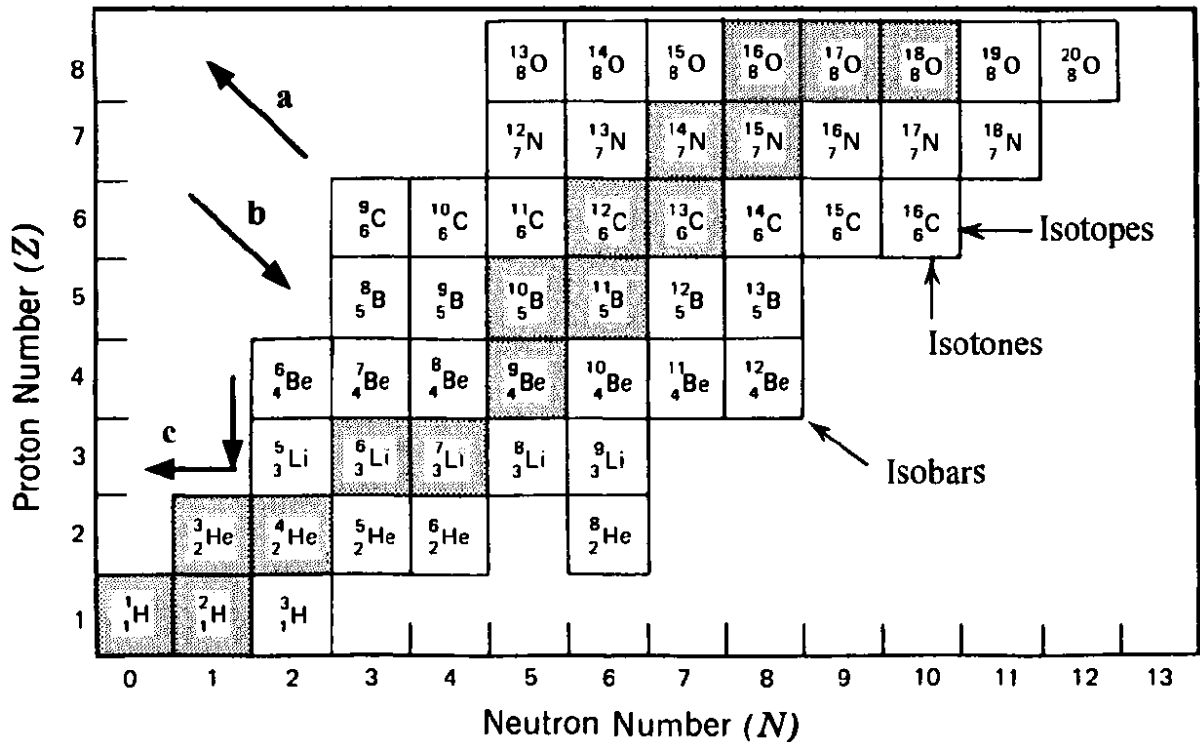


Figure 3.3 Chart displaying some elements, each square represents a nuclide (isotope specific atom) grey square are stable isotopes and white squares are unstable nuclides or isotopes. The arrows to the left show the shifts in proton and neutron numbers as a result of different decay mechanisms: a (beta decay), b (positron decay and beta capture), c (alpha decay) (Kendall & Caldwell, 1998b:53).

Naturally occurring nuclides express a path in the chart of nuclides, equivalent to the greatest stability of the neutron/proton (N/Z) ratio. For elements or nuclides of low atomic mass when the number of neutrons is close to or equal to the number of protons (N=Z) the greatest stability will be achieved and thus result in so-called stable isotopes, indicated in [Figure 3.3](#) by the grey squares. As atomic mass increases, the ratio for stable isotopes increases until the ratio (N/Z) is equal to 1.5. Radioactive decay thus takes place when the ratio (N/Z) of neutrons to protons is too large or small. Radioactive decay will occur then as changes in the protons (z) and neutrons (N) of an unstable nuclide will result in the transformation of one nuclide to that of another, more stable nuclide. This process described is radioactive decay and these elements are called unstable nuclides shown as the white squares in [Figure 3.3](#) (Kendall & Caldwell, 1998b:54).

Atoms are called radiogenic if they are created by the radioactive decay of other nuclides. Cosmogenic nuclides are nuclides that are produced by cosmic ray bombardment of stable nuclides. New nuclides can be formed by the addition of neutrons from alpha decay from other nuclides, alternatively adding a neutron can displace a proton in the nucleus thus resulting in a

nuclide of the same atomic mass but a lower atomic number. These two processes create nuclides that are termed lithogenic. If the product of a decayed nuclide is radioactive, the product or daughter nuclide will decay to another more stable nuclide, this process will continue until a stable nuclide or isotope is formed (Kendall & Caldwell, 1998b:54). Nuclides can change in varying ways, but the most common mechanism that causes a change in the number of neutrons is the following:

- *Beta decay* is when a nuclide deficient in protons transforms a neutron into a proton and an electron, the electron is then ejected from the nucleus as the negative beta particle (β^-), this action increases the atomic number by one while the number of neutrons is reduced by one.
- *Positron decay* is when nuclides short of neutrons transform a proton into a neutron, electron and neutrino. This causes the atomic number to decrease by one and increases the number of neutrons by one. Both processes leave isobars because the daughter nuclides are isotopes, meaning that they are nuclides of equal mass as the parent nuclide but still are different elements.
- *Beta capture* (electron capture) is the process when nuclides deficient in neutrons transforms a proton into a neutron and a neutrino by capturing an electron with a proton. This action causes a decrease in the number of protons in the nucleus by one, thus also creating a daughter nuclide that is an isobar of the parent nuclide.
- *Alpha decay* is the process when elements with atomic numbers (Z) are equal to or above 83, and these nuclides emit an alpha particle which consists out of Helium nuclei which is two neutrons, two protons with a positive two charge. The daughter nuclei of this process are not isobars because the mass of the daughter nuclei is four times less than the mother or original nuclei (Kendall & Caldwell, 1998b:54).

Notation:

To further define isotopes, a ratio was created because it is easier to measure the ratio of the rare isotope to the common isotope than to measure the concentration of the rare isotopes. The ratio is an isotopic abundance ratio (R), this ratio is defined by

Equation 3.1:

Equation 3.1

$$R = \frac{N_i}{N}$$

N_i is the less abundant isotope species and N is the more abundant isotope species. These ratios can also be expressed in terms of mole fractions.

Equation 3.2

$$m = \frac{N}{N+N_i} \quad \& \quad m_i = \frac{N_i}{N+N_i}$$

The most common and accepted way to display isotope values are with the delta (δ) notation, these values or δ notations are reported in parts per thousand or ‰ (per mille) relative to a standard. These Delta values are calculated with the following formula (where R is the ratio of the relevant isotopes):

Equation 3.3

$$\delta = \left(\frac{R_{sample} - R_{standard}}{R_{standard}} \right) \times 1000$$

These standards are set and there are different standards for different elements. *Figure 3.4* shows a few standards of elements that can be used in a delta calculation (Gat, 1996:227; Kendall & Caldwell, 1998b:55-56; Leibundgut *et al.* 2009:15-16; White, 2013:361-362).

Element	Notation	Ratio	Standard	Absolute Ratio
Hydrogen	δD		SMOW	
Lithium			NIST 8545 (L-SVEC)	
Boron			NIST 951	
Carbon			PDB	
Nitrogen			atmosphere	
Oxygen			SMOW , PDB	
			SMOW	
Sulfur			CDT	

Figure 3.4 Isotope ratios of stable isotopes (White, 2013)

Fractionation:

The fractionation process is a process that causes changes in the isotopic composition and the process takes place because of a physical or chemical process that causes the isotopic abundance ratio to change. The isotopic fractionation can be due to kinetic or equilibrium effects. The strength of chemical bonds is influenced by different isotopes because isotopes of the same elements cause different strength bonds. This could be surprising because it is expected that the chemical properties of an element are dictated by its electronic structure and that the nucleus plays no role in chemical interactions. In the following content, the mass of an atom affects the vibrational motion, as well as rotational and translational motions which all influence the strength of chemical bonds (White, 2013:363).

To describe fractionation, α the fractionation factor is used:

Equation 3.4

$$\frac{dR}{R} = \frac{\left(\frac{dNi}{dN}\right)}{\left(\frac{Ni}{N}\right)} = \alpha$$

And for specific reactions at full equilibrium, it can be expressed as:

Equation 3.5

$$R_{A \leftrightarrow B} = \frac{R_A}{R_B}$$

Where R_A and R_B represent isotopic ratios of two phases, A is for instance water and B is vapour. The equation can also be rewritten in the form of δ values:

Equation 3.6

$$R_{A \leftrightarrow B} = (1000 + \delta_A) / (1000 + \delta_B)$$

In terms of parts per thousand or ‰ (per mille) the enrichment factor $\epsilon_{A \leftrightarrow B}$ is used and the equation looks as follow:

Equation 3.7

$$\epsilon_{A \leftrightarrow B} = \left(\frac{R_A}{R_B} - 1 \right) \times 1000 = (\alpha_{A \leftrightarrow B} - 1) \times 1000$$

For small enrichment values the equation is a bit different because, for small enrichment factors, the approximation exists that: $\ln \alpha \approx 1 - \alpha$ when $\alpha \approx 1$ this leads to this equation:

Equation 3.8

$$\epsilon_{A \leftrightarrow B} = \delta_A - \delta_B = 1000 \ln \alpha_{A \leftrightarrow B}$$

For the stable isotopes of water, phase transitions are very important because the fractionation between the different phases of H₂O results from differences in physical properties of the molecules that contain different isotope species of hydrogen and oxygen. The water vapour pressure of species with the lighter isotopes like ¹H₂¹⁶O can differ by about 1% at 20°C compared to the heavier isotopes like ¹H₂¹⁸O. This difference in the physical properties of H₂O then causes the following phenomena: When evaporation occurs over an open body of water, the water source

will be enriched with the heavier isotopes and the vapour or gaseous phase will be depleted in the heavier isotopes as displayed in [Figure 3.5](#) (Leibundgut *et al.* 2009:17).

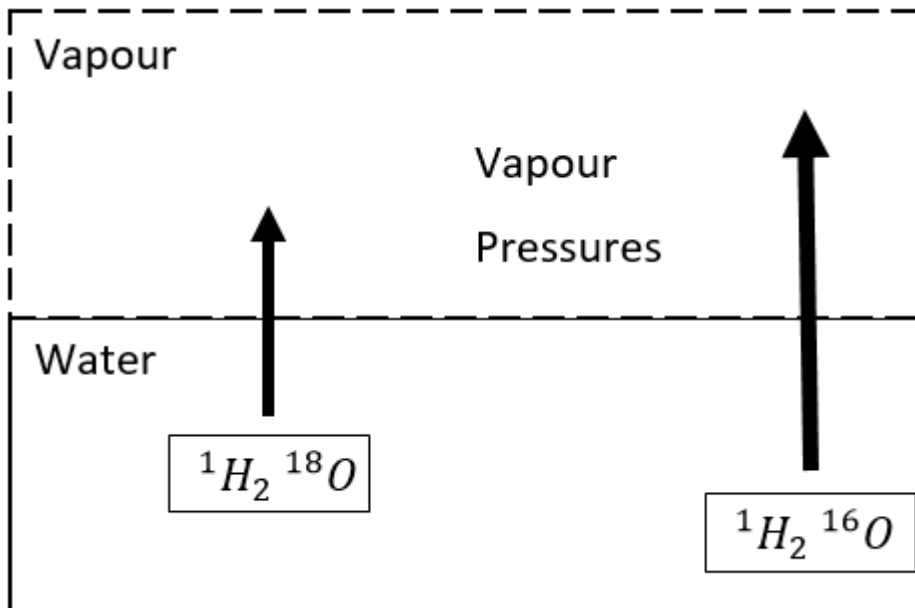


[Figure 3.5](#) Displaying how fractionation occurs during evaporation due to differences in vapour pressure (Leibundgut *et al.* 2009).

Isotope equilibrium fractionations are influenced by temperature and according to Leibundgut *et al.* (2009), the fractionation factor $\alpha_{A \leftrightarrow B}$ can be defined with the following equation:

Equation 3.9

$$10^3 \ln \alpha_{A \leftrightarrow B} = \frac{10^6 a}{T^2} + \frac{10^3 a}{T} + c$$

Where T is the ambient temperature of the water in terms of K and a, b, c is known as constants. From water to vapour equilibrium exchange, fractionation is lower at high temperatures than at low temperatures. [Figure 3.6](#) shows how temperature influences the equilibrium fractionation. This influence of temperature is the main process of a few in hydrological systems that cause macro effects such as altitude effect, latitude effect, continental effect, seasonal effect and amount effect.

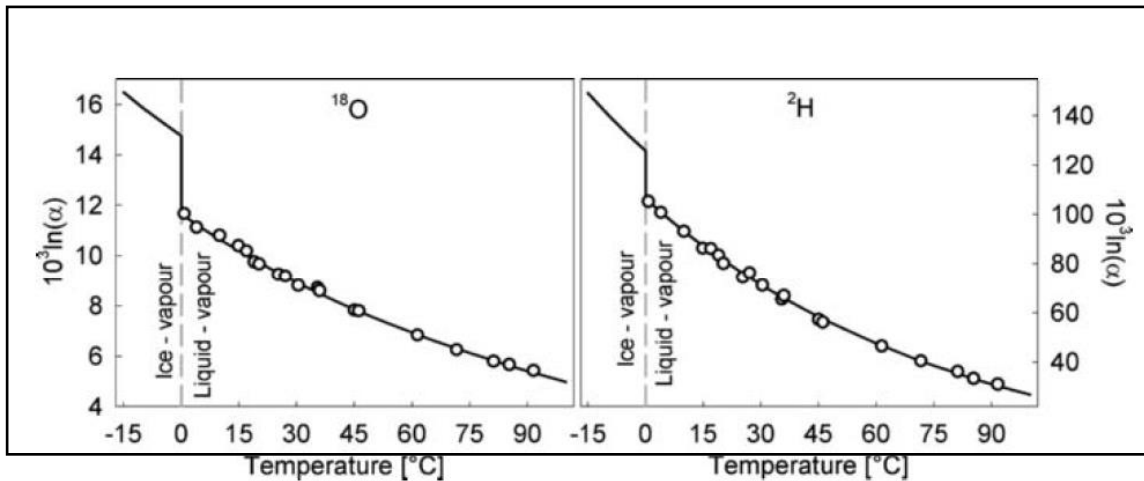


Figure 3. 6 The influence on equilibrium fractionation caused by temperature, at 0°C the phase transition from ice to water is displayed with a dashed line, and a step-in temperature equilibrium function is visible (Leibundgut et al. 2009).

Kinetic fractionation will take place as isotopic equilibrium is not met, this could be caused by a rapid change in temperature or the removal or addition of either the product or reactant while the reaction is occurring. Two major non-equilibrium hydrological processes are Rayleigh distillation and diffusive fractionation. Diffusive fractionation occurs because of processes such as water vapour diffusing into the air. The diffusive fractionation is a result of different molecular velocities caused by different isotopes. The molecular velocities are influenced by temperature and the mass of the atom or molecule. The following equation describes this relationship or influences (Leibundgut et al. 2009:18-19).

Equation 3.10

$$v = \sqrt{k \times \frac{T}{2\pi \times m}}$$

In the above equation, **k** equals the Boltzmann constant $k= 1.3806504 \cdot 10^{-23} \text{ J/K}$ and **T** is the absolute temperature (*Kelvin*) and **m** is the molar mass (*kg*) the calculated value is velocity and is expressed in (*m/s*). This equation allows us to derive the diffusion of two isotopes of different masses in a vacuum. From the equation above it can be derived that in a vacuum the diffusion rates for an ideal gas are just inversely proportional to the square root of the mass of the particles. Where m_A and m_B are molecular weights of different substances.

Equation 3.11

$$diffusion\ air\ (A-B) = \sqrt{\frac{m_B}{m_A}}$$

This principle is called Graham's Law of Effusion. If this law is applied to dry air the molecular mass of the air needs to be considered. The molecular mass of dry air can be calculated from its gas composition and molecular weight of the different elements as seen in the equation below:

Equation 3.12

$$diffusion\ air\ (A-B) = \sqrt{\frac{m_B * (m_A + 28.8)}{m_A * (m_B + 28.8)}}$$

The fractionation factors can be described and derived into an isotope difference by making use of Equation 3.7, but Equation 3.12 is only true for dry air conditions with a humidity of 0%. The fractionation by diffusion is stronger with oxygen than with hydrogen (deuterium), as seen that the kinetic effect of diffusion is 32.3‰ for H₂¹⁸O/H₂¹⁶O and 16.6‰ or ²H₂O/¹H₂O. But in the natural world with real hydrological systems, the equation should account for atmospheric humidity and turbulence. Gat (1970), Merlivat (1978) and Vogt (1976) have conducted Studies to include these effects and it has been found that isotopic differences caused by kinetic fractionation are much smaller when compared to diffusive fractionations.

Thus, experiments were carried out to examine the process of evaporation from natural open-source waters into the atmosphere with relative humidity (*h*) in terms of %, and it was found that for H₂¹⁸O/H₂¹⁶O empirical values between 13 and 28.5% were found. Empirical values are generally used to state the fractionation factor that is expressed as per mille (‰) and these values are proportional to (1- *h*) where *h* is the relative humidity (Leibundgut *et al.* 2009:19).

Equation 3.13

$$\Delta\epsilon_{18O} = 14.2 \times (1 - h) [‰]$$

$$\Delta\epsilon_{2H} = 12.5 \times (1 - h) [‰]$$

Deuterium also indicates that kinetic fractionation has a higher yield than diffusion (16.6 to 12.5 ‰). For real and actual systems, a ratio of the coefficients changes to $(\frac{D_A}{D_B})^n$ and *n* is the turbulence parameter which is $0 \leq n \leq 1$, with many datasets fitting with *n* = 0.5 which is also the square-root of the diffusion coefficients ($\sqrt{\frac{D_A}{D_B}}$).

The pure diffusion process described by these equations are however not what takes place, thus a kinetic fractionation has to be defined by turbulent diffusion. In a closed system, water vapour assemblage would equilibrate as shown by *Equation 3.13*, but in open systems, there is an additional kinetic fractionation. If we want to define this process, then resistance is inversely proportional to the diffusion coefficients D_A and D_B ($\pi_i \sim 1/D_i$). Because of the statement that resistance influences the flux of isotopes, the following equation is applicable:

Equation 3.14

$$kinetic (water-vapour) = (1 - h) \times \left(\frac{p_i}{p} - 1 \right)$$

The slope of an evaporation line is also influenced by the humidity during evaporation. For instance, at high humidity (> 85%) the slope is steeper approaching that of the meteoric water line and the opposite is true where at low humidity the slope is dropping. In nature these processes are more complex as can be seen in *Figure 3.7*, this is a concept that evaporation, in reality, is a function of various processes namely, equilibrium, diffusion, mixing and re-equilibrium. *Figure 3.7* also indicates that the concept estimates that equilibrium fractionation happens in a thin liquid-vapour interface layer above the water that is saturated with vapour. The isotopic composition of the layer is initially caused by temperature dependent equilibrium fractionations.

After this, the vapour diffuses from this saturated layer and this process is caused by molecular diffusion. The diffusion is influenced by humidity in the layer and the mass ratio of isotopes as discussed. After this the vapour enters the turbulent mixing zone and here the vapour mixes with an advanced vapour of given isotopic composition, it is expected that in the turbulent boundary layer no fractionation occurs. The vapour that is mixed partially re-enters the layer where diffusion takes place, and then vapour can re-precipitate on the surface of the water leading to molecular exchange. This concept does allow us to describe the process of fractionation, in steps but this also causes the integration to become very complex as seen in the equations below.

Equation 3.15

$$E = (c_{liquid} - c_{air}) \times \frac{1}{p} \text{ with } h = \frac{c_{air}}{c_{liquid}} \text{ relative humidity}$$

$$E = (c_{liquid} - h \times c_{liquid}) \times \frac{1}{p} = c_{liquid}(1 - h) \times \frac{1}{p}$$

Equation 3.15: is the evaporation, h is relative humidity and c_{liquid} is the absolute moisture or vapour pressure above an open source of water, c_{air} is the absolute moisture or vapour pressure in the atmospheric layer and ρ is the resistance coefficient for the fluctuation of moisture (Leibundgut *et al.* 2009:19-21).

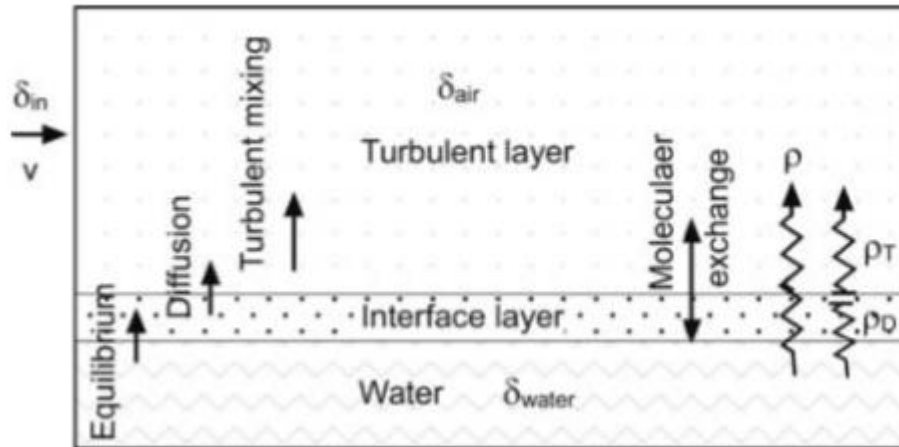


Figure 3.7 A concept showing the water-atmosphere exchange process (Leibundgut *et al.*, 2011).

Equation 3.15 can also be improved by adding the isotopic ratios R , R_{liquid} and R_{air} , the equation then looks like this:

Equation 3.16

$$E = c_{liquid} \left(\frac{R}{\alpha} - h \times R_{air} \right) \times \frac{1}{pi}$$

Where pi is the specific resistance coefficient of an isotope.

Another important fractionation process is the Rayleigh distillation, which is also a kinetic fractionation process. The Rayleigh process can be used to describe systems where the reactant is being removed, an example of such a process is rain-out or evaporation. Equation 3.17 can be created that states that R is the isotopic ratio and is a function of the initial ratio R_o , and f the fraction of remaining water in the reservoir.

Equation 3. 17

$$R = R_0 f^{(\alpha-1)}$$

$$\delta \simeq \delta_0 f^{(\alpha-1)}$$

When the residual water fraction values start decreasing the fractionation increases strongly. The Rayleigh formula is aimed at describing the distillation process. The differential equation shows that change in mass is related to the fractionation factor, this is only applicable if the fractionation factor is constant or can be approximated by a constant value. The differential equation can thus be used with an integrated variable of temperature to describe the condensation process that causes altitude effects (Kendall & Caldwell, 1998b:61; Leibundgut *et al.*, 2011:21-22).

3.2 Factors that influence Isotope fractions:

3.2.1 Temperature effect:

As mentioned previously, it was briefly discussed that temperature affects fractionation, especially at low temperatures the fractionation from water to vapour is affected. The result of this occurrence is that rainfall in colder environments is more depleted in isotopic composition when compared to warmer environments. [Figure 3.8](#) clearly shows the influence that temperature has on isotope fractions which is true for ^{18}O and ^2H and by combining these two, a thermometer can be created (Coplen *et al.* 2000:87; Leibundgut *et al.* 2009:23).

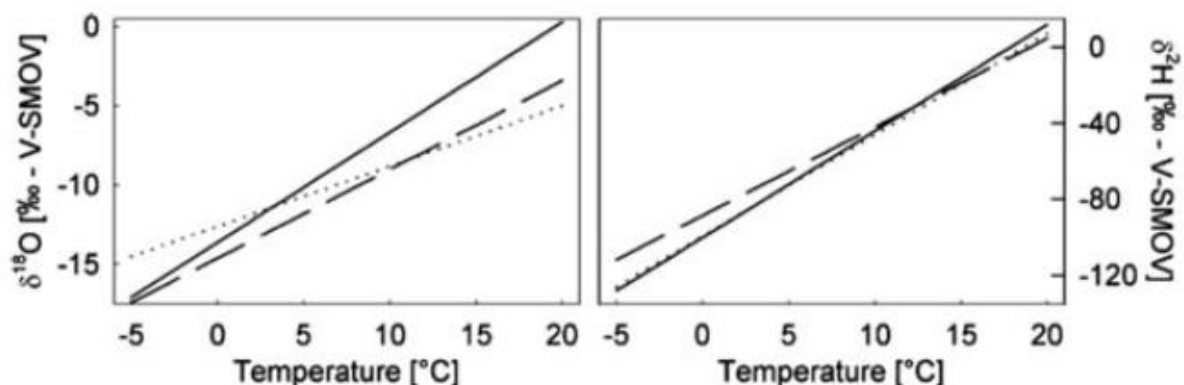


[Figure 3.8](#) Effects of temperature on isotope fractions (Leibundgut *et al.* 2009).

The thermometer reveals the ambient temperature of different sites because the temperatures can be estimated with the stable isotope values, this can be seen in [Figure 3.9](#).

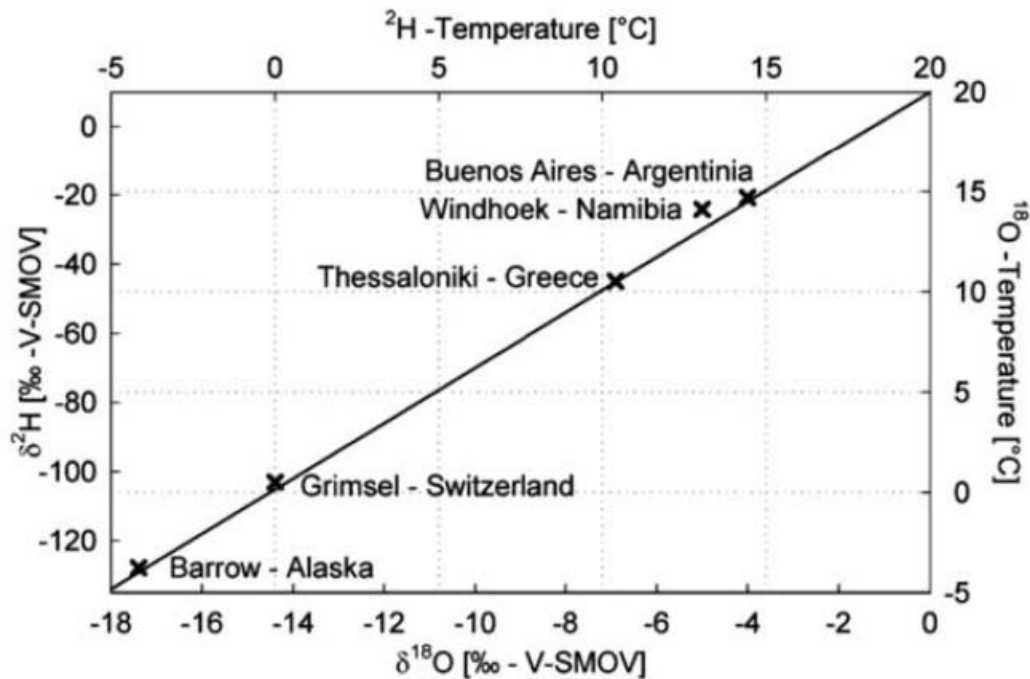


Figure 3.9 Influence of mean annual temperature on the isotopic compositions (Leibundgut et al. 2009).

3.2.2 Seasonal effect:

With the seasons changing, there also comes a change in the isotopic composition of rainfall with basic changes. Some of these basic changes are the change of the ocean's temperature with a change in seasons, the air-sea interaction, changing temperatures that lead to changes in the extent of rain-out and the sources of summer and winter precipitation differ that could lead to large changes in the Delta values (δ). The changes can all be described as seasonal fluctuations of the stable isotope ratios caused by temperature effects, different movement of air masses and a change in the source area and different atmospheric moisture. This leads to the fact that winter precipitation is usually depleted in ^2H and ^{18}O when compared to summer precipitation (Coplen et al. 2000:86; Gat, 1996:245; Leibundgut et al. 2009:24-25).

3.2.3 Altitude effect:

The altitude or elevation effect is the effect that in general precipitation at higher elevations are more depleted in stable isotopic compositions than at lower elevations or altitudes. This is assumed because of continuous pseudo-adiabatic cooling. This causes isotopic depletion of rain

and is assisted by increasing fractionation between liquid and vapour at cooler temperatures. **Figure 3.10** clearly shows the effects of altitude on stable isotope compositions, there exist several observed altitude effects and ranges in calculations that can be derived from the adiabatic cooling rate of air temperature. In some cases, though other factors influence the composition of the precipitation at different altitudes, the altitude effects need to be verified for each region (Ingraham, 1998:101; Leibundgut *et al.* 2009:25-26).

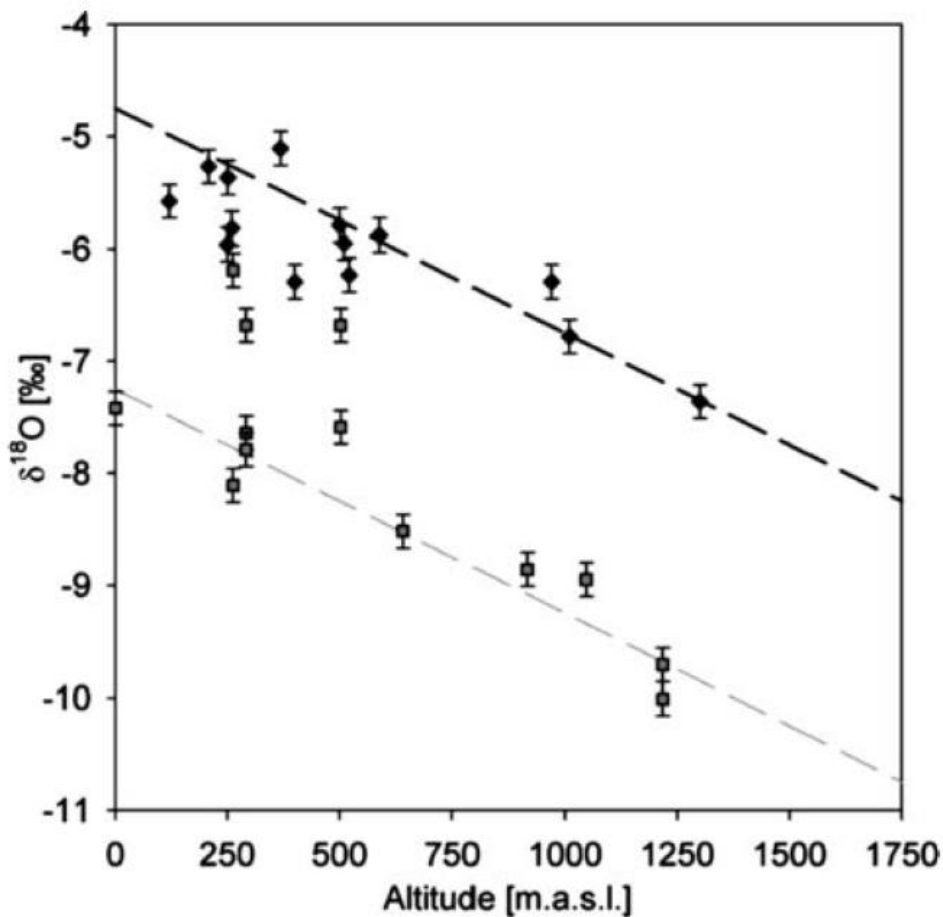


Figure 3. 10 Effect of altitude on $\delta^{18}\text{O}$ at Cyprus (Leibundgut *et al.* 2009).

3.2.4 Continental effect:

The continental effect is visible in **Figure 3.11**, and it is observed that ^2H and ^{18}O contents of meteoric water is being depleted the further away it is from its source or the coast. The precipitation from condensation is more enriched than the vapour remaining due to the fractionation of the stable isotopes. This causes the water in the clouds to become more depleted in heavy isotopes every time a condensation or precipitation event takes place. Each condensation and precipitation event that happens at a given temperature leads to the fractionation of isotopes. This also causes the depletion of the air mass in heavy isotopes as the

air moves inland or further away from its source. This inland depletion effect is reduced by transpiration and re-evaporation on the continent (Coplen *et al.* 2000:86; Ingraham, 1998:100; Leibundgut *et al.* 2009:27-28).

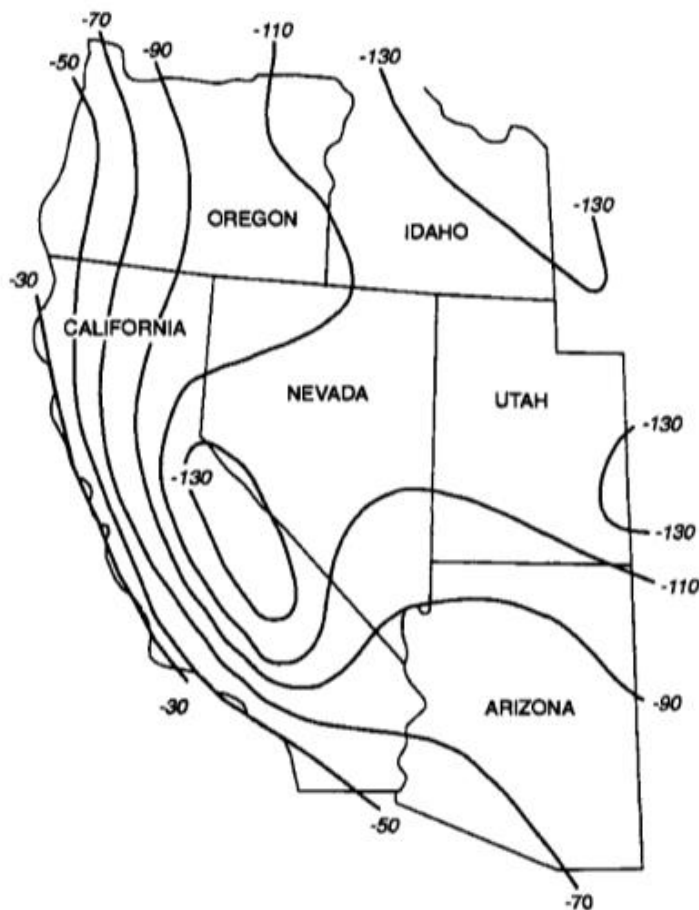


Figure 3.11: The stable isotopic depletion of meteoric water in the Western U.S. visualising the “Continental Effect” (Ingraham, 1998).

3.2.5 Latitude effect:

The ^2H and ^{18}O contents in air masses decrease with rainouts. This is because of an increase in rainouts at higher latitudes and greater fractionation at the cooler temperatures than is expected at higher latitudes. The fractionation does not occur linearly with the increase in latitude. **Figure 3.12** shows the latitude effect on precipitation; this is however also just one effect of many that contribute to the isotopic composition at a specific site (Coplen *et al.* 2000:86; Ingraham, 1998:102).

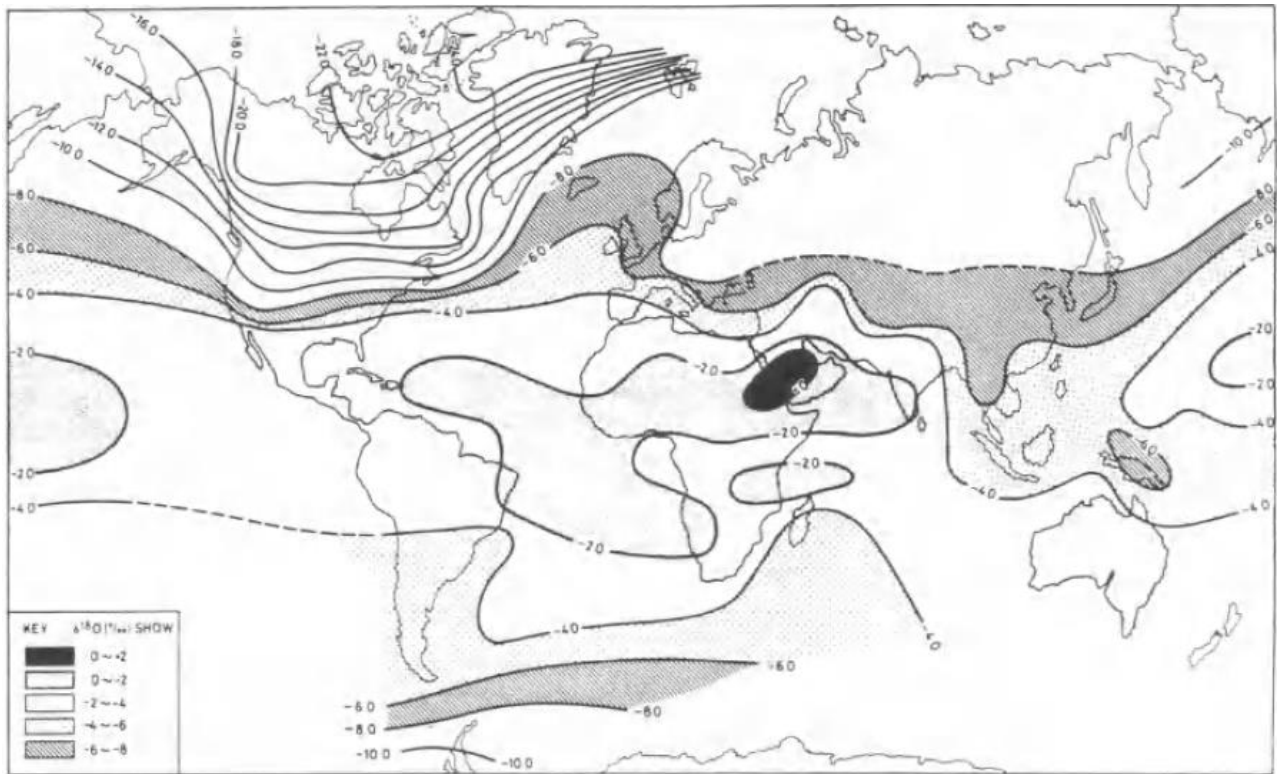


Figure 3.12: Global distribution of $\delta^{18}\text{O}$ in precipitation showing the “Latitude effect” (Ingraham, 1998).

3.2.6 Amount effect:

The amount effect is the observation that precipitation is more enriched with isotopes the smaller the precipitation event is, meaning that larger rainstorms are less enriched in ^2H and ^{18}O than the smaller rainstorms. Rain evaporates as it falls to the ground through an atmosphere of relative humidity. This causes evaporation to have a bigger influence on small rainstorms and the early part of a rainstorm because the atmosphere below the clouds becomes saturated. The saturation that occurs when rain falls causes less evaporation of the rain, and the longer the rainstorm continues the more depleted the raindrops become. This explains why long rainstorms are more depleted than short or small rainstorms (Coplen *et al.* 2000:87; Ingraham, 1998:102).

3.3 Hydrologic Cycle:

The Hydrologic or water cycle is the interaction and circulation of water between different sources of water. The interaction and circulation of water is a constant global process that takes place between and in all the different spheres of the earth, namely the atmosphere, lithosphere,

hydrosphere and biosphere. Water constantly circulates between these spheres in varying phases and processes (Balasubramanian & Nagaraju, 2015:1; Encyclopaedia Britannica, 2020).

3.3.1 Concept of Hydrologic Cycle:

The Hydrologic cycle is just the change in the form or phase of water that takes place. This can be described by the following: water is transformed from liquid to solid, solid to liquid, liquid to vapour, vapour to liquid and vapour to solid states, where there is a constant change in the phases of water within the hydrologic cycle. Factors that make these changes possible and regular are the following: the sun's radiation, gravity that causes acceleration and several properties of water such as the ability to flow. The main input of water to the earth's sources is precipitation.

Precipitation can be in many different forms, such as rain and snow. The precipitation falls on the earth's surface and infiltrates, percolation moves the water towards the groundwater systems. Some water flows towards the sea as runoff, some water is caught in surface water bodies where it will be evaporated into the atmosphere. Vegetation takes up ground water or soil moisture through their roots and transpires the collected moisture back into the atmosphere. Water enters the atmosphere as vapour, and when the vapour collects and accumulates clouds are formed. As more vapour is added to the cloud's, precipitation will take place, and the cycle starts again, this is an endless continuous cycle (Balasubramanian & Nagaraju, 2015:2).

3.3.2 Components of the Hydrologic Cycle:

This hydrological cycle consists of two phases; the first is the atmospheric phase and secondly is the terrestrial phase. The atmospheric phase describes the movement of water within the atmosphere in the forms of gas (water vapour), liquid (rain) or solid(snow). The terrestrial phase describes the movement of water in, over and through the earth. The terrestrial phase can be further described by two phases; a surface water phase consisting of processes such as streamflow and runoff. The second phase is the groundwater phase that consists of processes such as infiltration, percolation, and recharge. As seen in [Figure 3.13](#) many processes form part of the cycle and they will be discussed below (Easton & Bock, 2015:2).

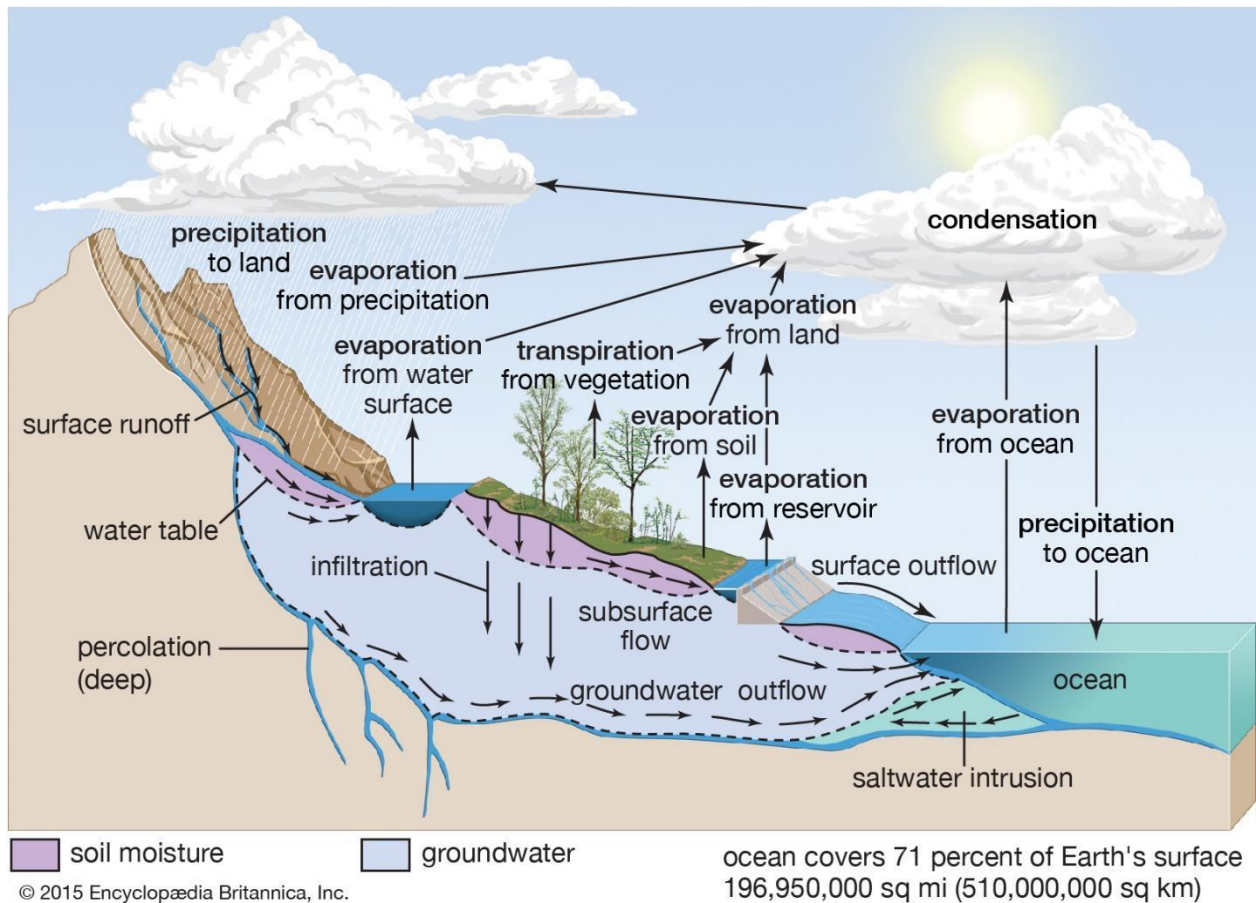


Figure 3.13: The Hydrologic cycle and its components (Encyclopædia Britannica, 2020).

Condensation:

Water vapour is the main form of water within the atmosphere; the vapour is the main source of moisture for dew, frost, fog, clouds, and precipitation. The process that causes the change from vapour to these phases is condensation or the change from the vapour phase to a liquid phase (Encyclopædia Britannica, 2020). Small particles in the air with an affinity for water known as hygroscopic nuclei surround the condensation nuclei. Once condensed masses of water vapour collect the water molecules form precipitation (Balasubramanian & Nagaraju, 2015:3).

Precipitation:

Precipitation is the process where condensation causes water vapour to accumulate and fall to the earth because of gravity. Precipitation can be a liquid or solid depending on the air temperature, some forms of precipitation include mist, rain, fog, hail, sleet, and snow. Precipitation that falls to the earth is evaporated mid-air or when the precipitation forms surface water. Interception also occurs which is when vegetation and plant intercept precipitation before it reaches the ground. Some of the precipitation infiltrates the soil and contributes to groundwater

and could later percolate into surface bodies of water. The precipitation can also become surface runoff molecules (Balasubramanian & Nagaraju, 2015:3-4; Easton & Bock, 2015:2).

Evaporation:

Evaporation is when water in the form of a liquid or solid is transformed into a gas or vapour. The change from a liquid to gas takes place once the molecules have collected enough kinetic energy to eject from the water's surface. Factors that affect evaporation are temperature, humidity, wind speed, and solar radiation. If a solid evaporates to a gas, then it is called sublimation. Evaporation can take place on open surfaces of water, like oceans, rivers, and lakes, but evaporation also occurs within the soil, ice and snow (Encyclopaedia Britannica, 2020).

Transpiration:

Transpiration is when a plant releases water in the form of vapour from the stomata in its leaves. Plants collect the soil moisture or water through their roots and then the water moves to all the different parts of the plant through osmotic pressure and eventually releases the water through their stomata (Balasubramanian & Nagaraju, 2015:3-4).

Evapotranspiration:

Evapotranspiration is the combined effect of evaporation and transpiration because they almost always occur simultaneously. Evapotranspiration mainly takes place in the summer months and hotter climates (Easton & Bock, 2015:4).

Runoff:

Runoff is when precipitation falls onto an area and the precipitation is rapidly discharged over land through stream canals. Runoff can however be more complex and described by two types of runoff:

Firstly, infiltration excess runoff: This type of runoff occurs when the rate of precipitation is higher than the rate of infiltration. This will occur with thunderstorms or on soils with slow or poor infiltration such as clays, compacted soils or urban areas. Surface depressions will be filled by the accumulating water as the precipitation rate is higher than the infiltration rate. When these surface depressions are full then the water will start to flow either overland or in defined channels.

Secondly, runoff can be saturation excess runoff: This will occur when the soil profile is saturated with water and infiltration will cease. Once the soil profile is saturated all the remaining precipitation will become runoff soil depth and topography largely affects this type of runoff. Soils that are prone to producing saturation excess runoff are soils where there are shallow restricting

layers and areas or landscapes that are prone to being flat areas that drain large upslope contributing areas as the interflow from the upslope area can no longer be transmitted through the soil profile. Saturation excess runoff is not dependable on the intensity of precipitation or soil infiltration rate, but dependable on the landscape and features (Easton & Bock, 2015:6-7).

Infiltration:

Infiltration has previously been mentioned and it plays a major role in the hydrologic cycle. Infiltration is the process where water moves down into the soil due to gravity. The amount of water that can infiltrate the soil and the tempo of infiltration is determined by many factors and soil properties. Some of the factors are soil moisture content, soil texture, soil bulk density, organic matter content, permeability, porosity and the presence of any restrictive layers in the soil. Permeability is the measure of how fast water can flow through soil and porosity is the number of voids within a soil that can be filled with water. Higher porous soils like gravels and sands will have greater permeability and infiltration. The infiltration rate of soil changes during a precipitation event and will decrease as saturation of the soil occurs. Infiltration of soil can be improved by organic matter within the soil or vegetation and organisms living within the soil. Better infiltration will cause less runoff over an area (Easton & Bock, 2015:4-5; Balasubramanian & Nagaraju, 2015:7).

Percolation & Recharge:

Once the water has infiltrated the soil and avoided plant uptake and has gone beyond the reach of plant roots, percolation will take place. Percolation is the downward movement of water through the soil to geological formations below and recharges groundwater aquifers (Easton & Bock, 2015:5).

Interflow:

Interflow is the horizontal flow of groundwater; this will occur if there is a confining or restricting layer that stops percolation from taking place. Interflow can also recharge aquifers, emerge on the surface and become runoff or it can contribute to spring, rivers or other surface water bodies (Easton & Bock, 2015:6).

Discharge:

Water that has infiltrated and percolated down to aquifers can either be stored in the aquifer or in some cases the water will be discharged once the aquifer is saturated. The discharge will take place to a surface water body such as a river, lake, or stream. If the aquifer discharges onto the

earth's surface a spring would appear and the discharge to surface water bodies would be the base flow of those surface bodies of water (Easton & Bock, 2015:5-6).

3.4 Hydrologic cycle in karst environments:

The hydraulic cycle in karst environments isn't a separate cycle, it is still part of the global hydrological cycle. The same components and features still exist for the cycle in karst environments, the processes are still the same, the only difference is the impact that the karst features have on the movement of the water in the cycle. The features of karst environments will be described and their impact on the hydrological cycle to better understand the cycle in karst environments.

Karrens – Karrens are small linear cavities that occur on the surface and beneath the surface. They are different shapes and forms varying in size from a few centimetres to metres and are caused by dissolution. When karrens are connected and interlinked or occur together in a large area they create a karrenfield (Stevanovic, 2015:36). Karrens will reduce runoff of surface water after precipitation and increase infiltration as it creates an ease of access for surface water to infiltrate the soil and reach groundwater.

Dolines & Sinkholes – Dolines and sinkholes are elliptical closed depressions with varying appearances and sizes. Dolines can be small or very large and when they are densely together, they can create a whole collapsed basin. Dolines are created by dissolution and mechanical processes like erosion, landslides and frost wedging to name a few. Once a doline is formed it acts as a source of preferential water absorption. When dolines continue to grow, colluvium is created and the colluvium fills the depressions (Gilli & Fandel, 2015:37-39). As seen by the structures created, dolines and sinkholes will greatly improve infiltration and decrease runoff. These structures can also improve groundwater interflow and if a doline is filled with compacted colluvium or soils it can create surface water bodies and marsh environments and thus increase evaporation.

Caves - Caves are large voids and caverns beneath the earth's surface and sometimes have openings on the surface. Caves in karst environments are mainly formed by dissolution. Because caves are large voids within the earth surface they act as underground lakes and cause mass amounts of interflow. Caves could also distribute water to the surface through springs and thus create surface water bodies. Caves would increase interflow in groundwater and could link

different aquifers, create surface water bodies and thus add to evaporation and atmospheric moisture. Cave openings could also decrease runoff as they can cause direct quick infiltration into the subsurface.

When taking into effect these few components of a karst environment it is visible that karst environments can increase the infiltration rate and decrease runoff, thus increasing recharge of the area. Karst environments can also be very good aquifers with all the possible subsurface voids created by dissolution, the base flow and interflow could also be increased in karst environments. The springs that are commonly found in karst areas can add surface water bodies which would increase evaporation and thus air moisture content.

3.5 Isotopes in Hydrology:

3.5.1 Stable isotopes in rainfall:

The fractionation processes described previously that occur naturally in the hydrological systems causes certain patterns in stable isotopes within the rainfall. These patterns in rainfall reveal the rainfalls' seasonal and geographic distribution. It is accepted that for global scale description of surface water in terms of $\delta^{18}\text{O}$ and $\delta^2\text{H}$ the following equation is accepted:

Equation 3.18

$$^2\text{H} = 8\delta^{18}\text{O} + 10\text{‰}$$

This *Equation 3.18* was developed for the SMOW (Standard Mean Ocean Water) and defines the global meteoric water line (GMWL). This GMWL is created by using long-term isotopic concentrations in precipitation at various locations all over the globe. This relationship is a good representation of the isotopic composition of precipitation in the humid regions for most continental stations. There are however deviations from this relationship on a regional scale and thus in a certain instance, a regional meteoric water line (RMWL) can be used to describe the local meteoric local water line (LMWL). It is visible that there are a lot of features that have an influence on the isotopic compositions of water from different areas. To carry out detailed stable isotope studies within a certain geographic area, an LMWL should be established to properly interpret isotopic data from surface and subsurface waters (Coplen *et al.* 2000:87; Gat 1996:242-246; Leibundgut *et al.* 2009:22-23).

3.5.2 Evaporation:

Evaporation causes fractionation to occur, when evaporation takes place the lighter isotopes are being evaporated and the heavier isotopes are not. This results in the remaining surface water being enriched with heavier isotopes (^2H & ^{18}O). Evaporation is evidently a very important factor in isotope fractionation, especially with open surface waters. **Figure 3.14** shows the effects of evaporation on the water in terms of ^2H and ^{18}O isotopes. From the figures, it is visible that evaporation enriches the remaining water and causes a slope that is less than the GMWL's slope. Isotope data from different aquifers are often dispersed as seen in **Figure 3.14** (Top). However, samples that experience the same conditions and are from the same source will show a characteristic evaporation line as seen in **Figure 3.14** (Bottom). Evaporation can remove water from open sources through vapour diffusion, but it can also remove moisture from soil columns by diffusion (Leibundgut *et al.* 2009:30).

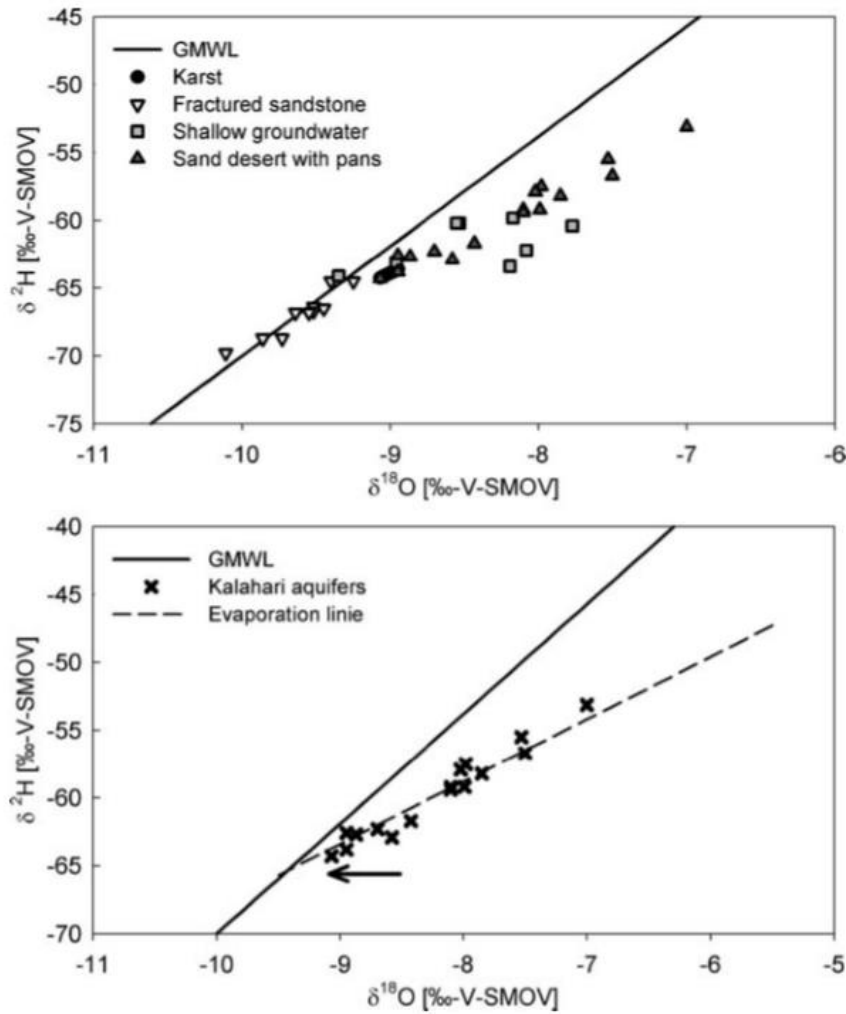


Figure 3. 14: $\delta^{18}\text{O} - \delta^2\text{H}$ diagrams showing the effects of evaporation. In the bottom figure, an arrow indicates the isotopic composition of precipitation before evaporation (Leibundgut et al. 2009).

To correct the effects of evaporation Equation 3.19 can be used. This equation shows the values that would exist before evaporation takes place or if it never occurred. The equation thus indicates where the evaporation line intersects the GMWL.

Equation 3.19

$$^{18}\text{O}_{\text{correct}} = \frac{\delta^2\text{H}_{\text{measured}} - e \cdot \delta^{18}\text{O}_{\text{measured}} - d}{8 - e}$$

In the above equation, e is the slope of the evaporation line, d is the excess of deuterium in global precipitation ($d = +10\text{‰}$). If $\delta^{18}\text{O}$ is calculated the equation for the GMWL can be solved to calculate the corresponding $\delta^2\text{H}$. This method utilising this equation is very useful when investigating flow paths of surface and groundwater that has been affected by evaporation. Once the evaporation has been corrected it can be determined whether the original water is the main source or if it's mixing with other sources and thus causing different $\delta^{18}\text{O}$ values (Leibundgut *et al.* 2009:32).

3.5.3 Stable isotopes in soil:

When water collects on the surface of soil whether, from precipitation or overland flow, the water will infiltrate into the voids within the soil. This infiltration rate can vary depending on the type of soil, it can be as low as 0.5 mm/hour for heavy clay soils and as high as 100 mm/hour for sandy soil. It is evident that water moves downward at very different rates, because of different pore sizes and in some cases the water infiltrates through cracks, fissures or macro pores. When the rate of precipitation exceeds the rate of infiltration the excess water will accumulate in soil depressions and/or impoundments which will, over time be emptied by evaporation and infiltration. The composition of water that infiltrates the soil varies at different depths as seen in [Figure 3.15](#).

This difference in fractionation or composition of the isotopes in the water can be attributed to several processes that take place in the soil. One of these processes is the selective abstraction of soil water by plants. This selective abstraction removes different fractions of the infiltrated rainwater, and thus changes the average composition of the remaining soil water. This previous process also occurs with evaporation within the topsoil, these two effects cause an enrichment in the heavy isotopes in the residual waters. At some depth, however, an evaporation front develops. The movement of water above the evaporation front as indicated in [Figure 3.15](#) is predominantly vapour transport and below the front, it is mainly liquid. The enriched water in the topsoil is flushed down the soil by successive rains and thus altering the composition of the deeper soil and ground waters (Gat, 1996:250-252; Gat, 2010:106-112; Leibundgut *et al.* 2011:35).

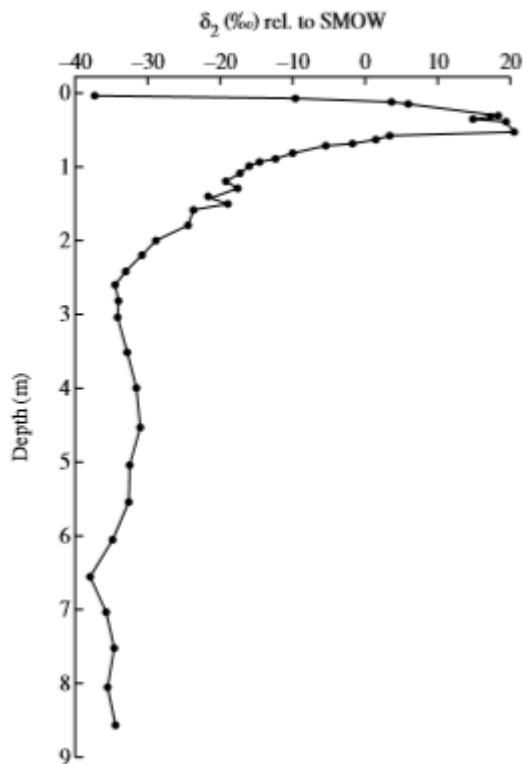


Figure 3.15: Depth profile of δ^2H in soil water in an unvegetated arid-zone (Gat, 2010).

3.5.4 Stable isotopes in surface & groundwater:

The water that precipitates onto the soil's surface can be divided into three parts. The first part is groundwater; this is created by precipitation or surface water that infiltrates into the ground and becomes groundwater. The second part is surface water, if the precipitation rate exceeds the infiltration rate precipitation becomes runoff and then flows into surface water bodies like streams, rivers, dams or lakes. The final part of precipitation is the part that returns to the atmosphere through various processes like evapotranspiration and evaporation (Gat, 1995: 409).

The isotopic composition of precipitation which is the main source of groundwater and surface water is altered by many effects and factors these factors are discussed in **3.2 Factors that influence Isotope fractions**: These factors cause weighted averages of isotopic compositions from precipitation and groundwater to differ and to be biased. This takes place if selective recharge occurs. Selective recharge is when groundwater is recharged by a specific event that has a specific isotopic composition. An example of this is that when flash floods recharge groundwater in arid conditions it is found that compared to rain, the water is isotopically depleted and has a clear isotopically different signature compared to the rainwater. Over time the difference between the actual average isotopic composition of precipitation and the groundwater indicates

that the groundwater was recharged with precipitation that was created during periods of different conditions and thus resulted in different isotopic compositions of the groundwater (Leibundgut *et al.* 2011:38).

3.5.4.1 Surface water:

Surface water is typically rivers and lakes, these waters normally reflect the isotopic composition of the precipitation over the catchment basin. Surface runoff is a large part of surface water. Surface runoff combines to form rivulets. These rivulets then later flow into larger river systems and surface water bodies like lakes and dams. Surface runoff interacts with other water sources that alter the isotope compositions, further altering the runoff composition is water loss due to evaporation and possible precipitation. Runoff's isotope composition is complex, some interactions and effects cause isotope enrichment and others cause depletion (Gat, 2010: 81).

Rivers and river systems also make up a big part of surface water. An undisturbed flowing river's isotopic composition is an amount weighted average composition of the river surface, sub-surface and tributary inflows. The river systems continually experience evaporation causing an increase in heavy isotopes in the river. The river systems reflect seasonal patterns through the isotope compositions because one of the biggest factors affecting isotope composition is seasonal effects (Gat, 2010: 83). While river systems still experience evaporation, stagnant water bodies like pans and lakes are influenced more by evaporation. The evaporation causes the residues in the water bodies to be enriched with heavy isotopes and thus creating a unique signature for large surface water bodies allowing them to be traced in the specified system based on isotopic compositions. Such surface bodies are however not that simple, there are three distinct types of systems that occur in surface water.

The first is a throughflow system, inflows and outflows are present in this system. The isotope composition of the system will continue to enrich as evaporation persists until a steady state is reached. Hydraulic steady state is achieved when the inflow is equal to the outflows plus evaporation. The second is a terminal system, this system has no outflows. A steady state in this system is achieved when the evaporation equals the inflows. Due to no outflows in this system, the salts in the water source would accumulate, and when salinity increases the isotopic build up and evaporation changes. The final system is a drying system, no hydraulic steady state can be achieved, but an isotopic steady state can be achieved (Gat, 2010: 87-100).

Another surface water example would be that if the basin is mostly mountainous terrain, then the water will be more depleted in heavy isotopes because of the altitude effect. This will also lead to the fact that the groundwater will be even more depleted in heavy isotopes than the surface water. Surface water isotopic compositions are also largely influenced by seasonal factors. One factor is the effect that heavy rains have on surface waters after a dry period. In this example, the distinct difference between the surface waters and groundwater is because of the direct contribution from the rain to the surface waters.

All the different forms of surface waters are largely influenced by evaporation. An example is that waters in lakes are being enriched with heavy isotopes as the evaporation removes the lighter isotopes. This is especially true for a closed lake, where there is no removal of the water except for evaporation. Evaporation also influences the water in the river even though they are constantly flowing. It was found that the water in rivers is enriched within regards to heavy isotopes when compared to adjacent ground waters (Gonfiantini *et al.* 1998: 206).

3.5.4.2 Groundwater:

Groundwater or sub-surface water is water that is found beneath the surface and within the lithosphere, in a variety of hydrological environments. The upper part of the soil or rock zone where the voids and structures are is only partially filled with water is the vadose zone. In this zone, water movement is mainly vertical, with downward movement driven by drainage of water when the water exceeds the layers holding capacity, and upwards movement is driven by evaporation and moisture. Whenever the voids are all saturated with water, the water bodies are formed.

These water bodies can be on top of impermeable layers (aquiclude) or still within the vadose zone (perched groundwater). Water in large groundwater bodies or aquifers also follow pressure gradients and will emerge as springs or as seepage into surface water bodies. Stagnant groundwater can be encountered deep below the earth's surface where a water body encounters no inflows like recharge and no outflows like drainage. This can happen if the inflow and outflow of these water bodies are stopped by either climatic or environmental changes. A good example of the mentioned ground waters is paleo waters where their inflow and outflows have been stopped for long periods (Gat, 2010:132). Typically, environments with mild and humid climates will have stable isotopic compositions of groundwater that correlates with the precipitation that recharges the groundwater. Cases that are exempt from this is when surface water such as lakes that have undergone significant evaporation are major contributors to the groundwater. Except

for this instance, the precipitation and recharge waters will obey the meteoric water relationship. This means that many processes will alter the isotopic composition of precipitation before it recharges the groundwater. This shift in isotopic composition will cause a shift of less than 1‰ in δ values. Because these processes change the composition before and during recharge, typically enriching the water with heavy isotopes.

The groundwater would shift away from the Meteoric Water Line, but the effects would not be so great because the local precipitation is the dominant contributor to groundwater. The isotope compositions of groundwater can thus be used to identify recharge sites, identify mixing patterns, and identify encroachment patterns. The reason isotopes are so powerful for aquifer source identification is because the composition of water is not changed or altered beneath the capillary fringe. Even when chemical compositions of the groundwater are changed due to rock and aquifer geochemical interactions, the isotope composition stays unaltered and will stay practically unchangeable if the temperature stays below 60°C. When groundwater mixes the composition is also changed, an example of subsurface mixing is additional recharge or aquifer leakage from adjacent aquifers. The isotopic compositions will be influenced, but the isotopic composition in the mixed groundwater is just the amount-weighted average of all the inflows (Gat, 1996:253-254; Gat, 2010:130-134; Leibundgut *et al.* 2011:39-40).

3.5.5 Sources & Mechanisms of recharge:

Various sources can recharge groundwater in a basin. Any water that falls on the surface and does not get evaporated or taken up by plants or animals can recharge groundwater. The sources that recharge the groundwater can be determined with stable isotopes and an example of this is the altitude effect previously discussed and the windward side of mountains. These factors will cause water to be depleted in ^2H and ^{18}O , in this instance the recharge is from precipitation on mountains. Another application is the continental effect that can be used to determine what the source of the recharge is. The sources can vary from precipitation only to rivers, runoff, and lakes that all recharge the groundwater. The mechanism in which recharge takes place differs a lot at different locations with varying conditions. In semi-arid and arid regions, the recharge water would have a long residence time, and evaporation can thus occur in the topsoil. Different recharge mechanisms like recharge during flood events which are rapid recharge will have different isotope compositions than for instance water infiltrating slowly during light rains where evaporation has a bigger influence. The different mechanisms of recharge and sources will all have different isotopic compositions, but because the isotopic composition of the groundwater is a combination of all the recharge events. It will reflect a mixed isotopic signature, but it will still be in proportion to the

amounts of recharge from the different mechanisms. Some of these mechanisms and their effects can be seen in [Figure 3.16](#) (Coplen *et al.* 2000:89-90).

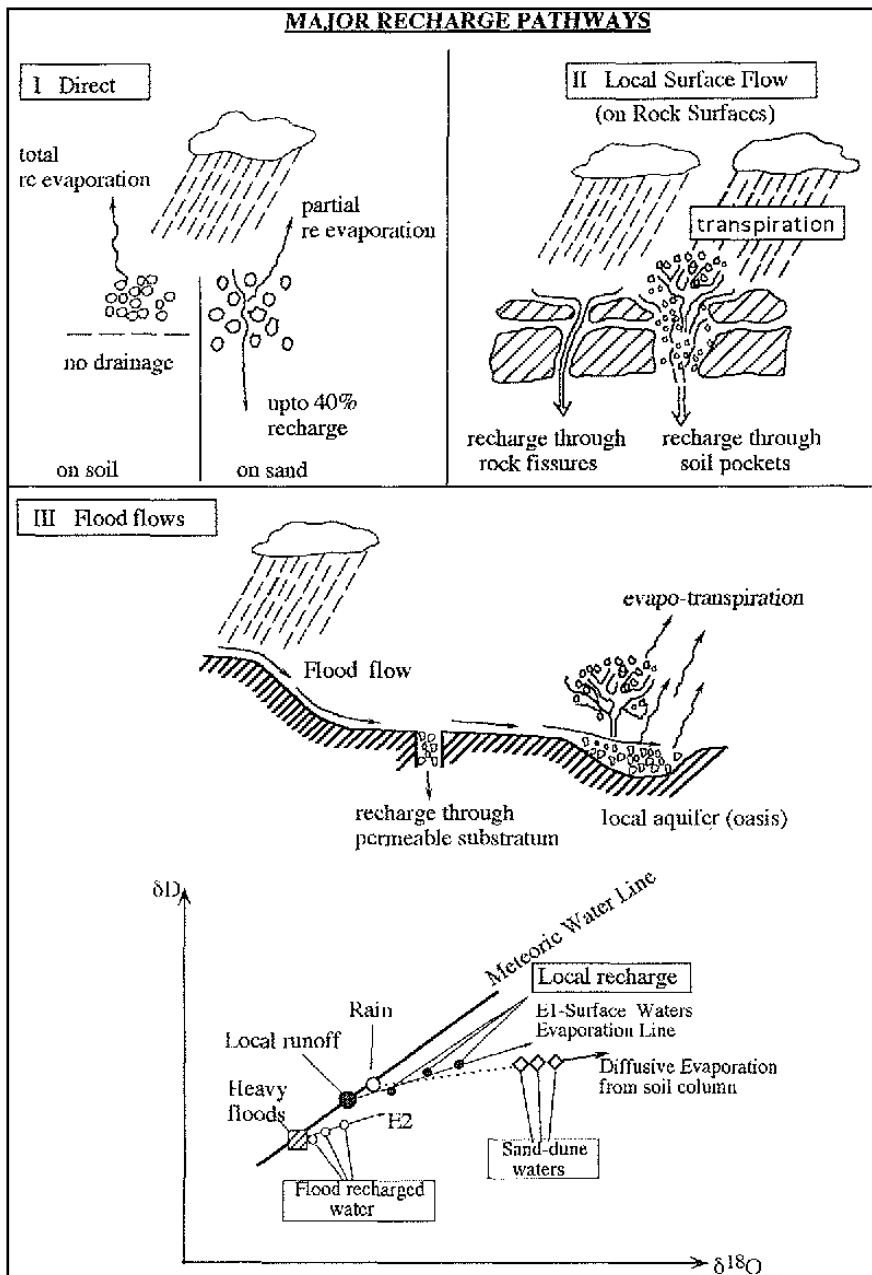


Figure 3.16: Groundwater recharge in an arid and semi-arid environment and isotopic compositions (Gat, 1995).

3.6 Isotopes in Karst environments:

Isotopes do not change when they are in karst environments. The same processes and effects that affect isotopes normally are the same ones that occur in karst environments. The stable isotopes of H₂O are also not affected or contaminated by any geological formations. Even the

dissolution of carbonates that causes changes in CO₂ has very little to no effect on the isotropic compositions (Palmer, 2010:146).

3.7 Applications of Stable Isotopes:

From the above descriptions of stable isotopes, it can be presumed that stable isotopic compositions vary significantly based on environment and climate. This variation is due to the factors that influence these stable isotopic compositions, and these factors are different and different combinations in different areas. This ultimately causes every area to have a unique stable isotopic composition if the environmental conditions differ. According to Leibundgut *et al.* (2011), the stable isotopes of H and O can be applied to:

- Groundwater, where the application of isotopes can determine groundwater origin and recharge. The groundwater also refers to soils and the saturated and unsaturated zone, here stable isotopes can be used to determine transport and filtration through soils which are important in groundwater protection as this could predict pollutant migration.
- Surface water can be in many types and forms and thus the application of stable isotopes and their function can vary depending on the type of surface water. An example would be isotopes in lakes, these isotopes can be used to determine water balances, groundwater exchange, residence times, stratification and mixing. In rivers, isotopes can be used to determine connections with groundwater, determine flow patterns, predict mixing and tracing of pollutants.
- Glaciers can also be termed as surface water bodies as it is on the surface and when melting occurs the meltwater will interact with the surface. In glaciers, an application of isotopes could be to determine the impact melting glaciers have with surface and groundwater, and the source of the glacier's ice.
- Catchment scale, the catchment scale refers to all water that is in contact or has an influence on the catchment and thus includes water in the atmosphere (precipitation). On a catchment scale, all the above applications can be used but additionally, Surface to groundwater interactions can be determined.

Gat (1996) states that in addition to all the above-mentioned applications, stable isotopes can also be used for palaeoclimatology and paleo waters in identifying them and describing the

conditions when those specific waters were formed and the processes that occurred. Gat (2010), also adds the function of climate change evaluation and identification with stable isotopes.

All the mentioned stable isotopes of H and O have been used a lot over the last decades and will continue to be used as new applications are uncovered. But these isotopes are so functional and considered an ideal tracer because they physically form part of the water molecule and thus follow the physical movement of water. They give information on recharge and discharge processes and can be used to delineate the recharge areas, identify mixing and the fractions of mixing between different sources of water whether surface or groundwater. They can also be used to provide valuable information about the past and the possible conditions at certain times (Coplen *et al.* 2000:105).

3.8 Land use impacts on isotopes:

The reason Stable isotopes is such a good tracer is that land use has minimal impact on stable isotopes. The only impact land use has on stable isotopes is the enrichment of isotopes by causing water to experience more evaporation. When evaporation occurs all the factors discussed in section **3.2 Factors that influence Isotope fractions:** will also take place. Irrigation is an example of how land use impacts stable isotopes. In the process of irrigation, groundwater is brought to the surface and used to irrigate plants, once the water encounters the atmosphere evaporation will occur. The evaporation causes an enrichment in heavy isotopes when compared to the origin of the water. The change in isotopic composition is not negative, because a sample of the water would display the change. Land use cannot impact isotopes to the extent that they are useless or give inaccurate results, on the contrary isotopes can display the changes that a certain source experienced (Buttle, 1998: 36 – 37).

3.9 Case Studies:

The case studies that will be presented are case studies that focus on the use of stable isotopes, and relevant hydrology.

3.9.1 Case study 1:

Location & Background:

Maduabuchi *et al.* (2006) conducted a study in the Chad Sedimentary Basin Nigeria, where they used stable isotopes to identify sources and deep groundwater mixing. There are three aquifers in the area, the upper, middle, and lower aquifer. The upper aquifer is made up of alluvial deposits

of lake margin origin as well as alluvial fans or deltaic sediments. The aquifers are recharged by rainfall and runoff and are predominantly used for domestic use and watering of vegetables and drinking water for livestock. The middle aquifer is the most encountered aquifer in the area and compared to the upper aquifer has mineralized water. The aquifer also has abstraction rates as high as 10^6 m³/day, and 70% of the wells are artesian wells with discharge varying from 0.12 to 90m³/h in some wells and the head pressure of up to 21 m above the surface. The lower aquifer consists mainly of alternating Continental Terminal sands and clays. The discharge in the artesian wells varies from 7 to 17m³/h.

Methodology:

To reach the aims of the project, ample amounts of samples had to be collected from the three distinct aquifers. The sampling had 38 wells that were sampled, with 15 in the upper, 14 in the middle and 9 in the lower aquifer, additionally, there were 10 sampling wells in the control zone. Samples for the second sampling campaign consisted of 47 wells, surface water from Lake Chad, rivers and Aludam reservoir and rainwater from 28 events. The samples for stable isotope analysis were collected in 1 litre bottles and stored at 4°C. The stable isotope samples were determined with mass spectrometry and calibrated with the V-SMOW standard.

Results & Discussion:

The rainwater collected during the 28 events showed that there was no specific trend between the amount and duration of the event and the isotopic signature. Despite the rainfall's inconsistent isotopic signature, the linear array formed by the data however appears very close to the GMWL. The samples collected from the surface waters like Lake Chad, rivers and the Aludam reservoir plotted on a linear regression line of $\delta^2H = 5.2 \times \delta^{18}O + 2.1$ ($r^2 = 0.99$) indicates enrichment in isotopes for the surface waters, with the rivers being less enriched than the Lake and Reservoir. The data from the shallow aquifer created the line equation of $\delta^2H = 6.7 \times \delta^{18}O - 0.23$ ($r^2 = 0.93$) that does not deviate significantly from the GMWL this indicates that the groundwater for the shallow aquifer has not undergone significant kinetic fractionation. The wide range of groundwater could be because of the wide range of isotopic compositions in the rainfall, and the heterogeneity of the recharge conditions. Deeper samples in the top or upper aquifer showed values with a negative trend and plotted more to the right of the GMWL indicating that it could potentially be a paleo recharge.

The stable isotope concentrations of the middle and lower aquifers were within a narrower range. In [Figure 3.17](#) the middle and lower aquifer shifted more to the negative trend, but with the same slope as the GMWL indicating paleo-recharge water. Seepage between the middle and lower

aquifer can be possible as the values are relatively similar. The comparison of the stable isotope values and the GMWL also indicates that the lower and middle aquifers have paleo climatic origins. The depleted isotope values in these aquifers correspond better with a wetter and cooler climate than the present day. The recharge zone of the shallow and middle aquifer is still unknown, and more research could be done to determine this.

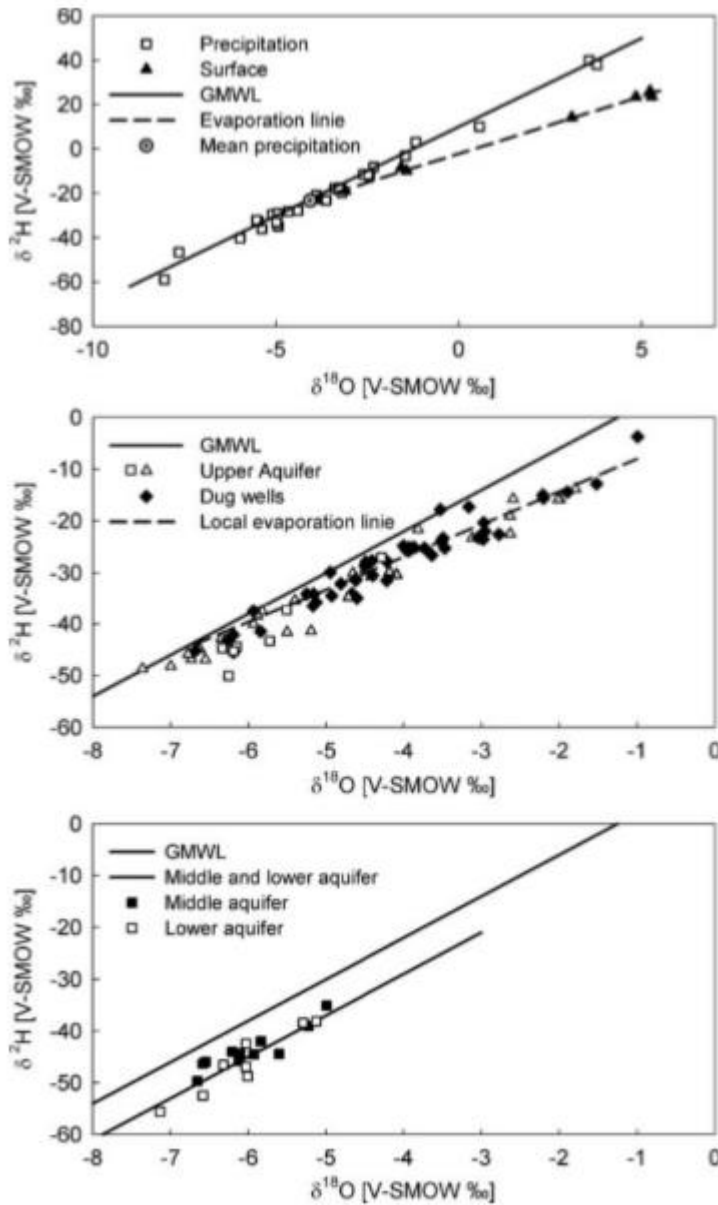


Figure 3.17: Isotopic compositions of surface, ground, and rainwater (Maduabuchi et al. 2006).

3.9.2 Case study 2:

Location & Background:

Kumar *et al.* (2011) did a study where aquifer recharge zones and sources were identified making use of stable isotopes. The study took place in the NCT (National Capital Territory) of Delhi India. The study area is part of the Indo-Gangetic Alluvial Plain with elevation varying from 198 to 263 mamsl, the surface area is 1483 km². During the months of June to September, the area experiences the main climatic seasonal influence of the monsoon rains which mainly contribute to the mean annual rainfall of 612 mm. The area has four major exposed morphological units:

- 1- The Delhi Ridge which is composed out of quartzites.
- 2- The Chhatarpur alluvial basin is occupied by alluvium from the adjacent ridge.
- 3- Alluvial plains on the eastern and western sides of the ridge.
- 4- Yamuna floodplain deposits.

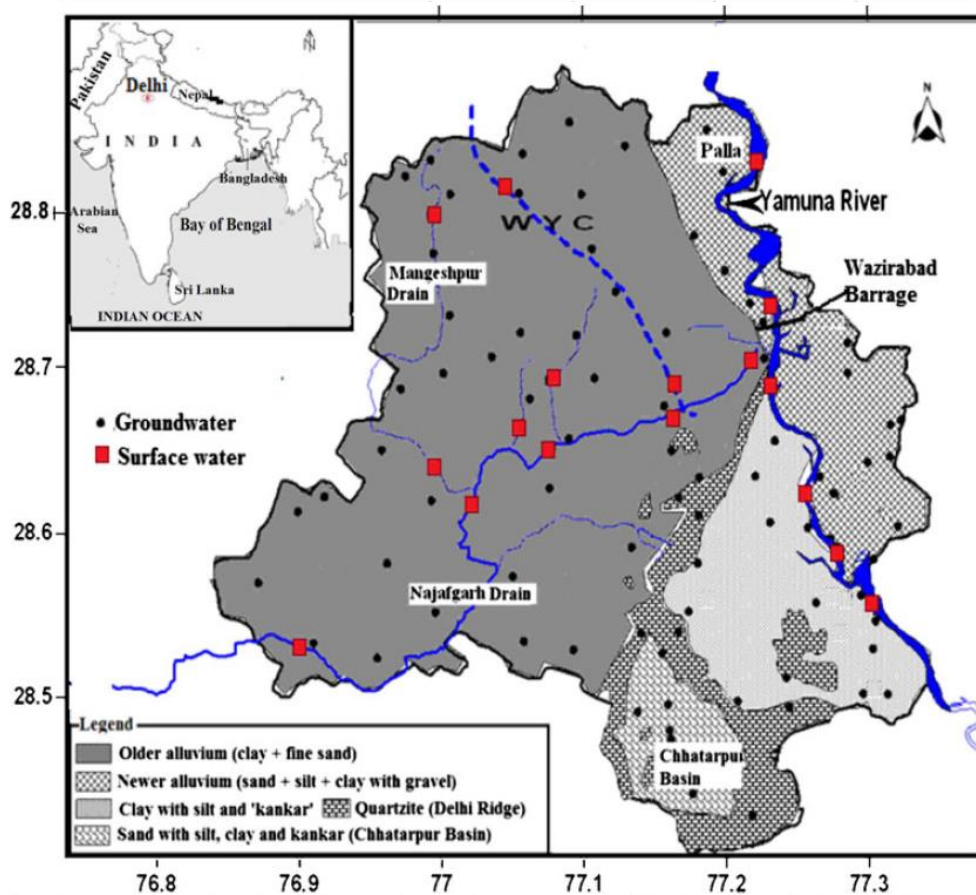


Figure 3.18: Sampling locations, Geology and drainage of the study area (Kumar *et al.* 2011)

The surface and groundwater in the area experience a lot of stress, as the surface waters are constantly polluted because the treatment plants can only treat 54% of wastewater. The extraction of groundwater exceeds the resources by 85%. The geology that makes up the bedrock of the area is primarily quartzite with interbedded mica schist. Quartzite does occur at the surface and

this is shown in [Figure 3.18](#) where the quartzite appears in the central and southern parts, Quaternary sediments cover the rest of the area composed out of older and newer alluvium. The older alluvium consists of silt and clay mixed with calcite carbonate nodules (Kankar), where the newer alluvium is composed of unoxidized sands, silt and clay. The newer alluvium creates an unconfined aquifer with water levels at 2.5 to 7 mbgl. The newer alluvium creates an aquifer with good potential and can be used for tube wells, due to seasonal variations the groundwater level changes but falls within the 0.5 to 2 mbgl range.

Methodology:

To reach the aim of this research, samples were collected from 2002 until 2005 with 480 water samples. The sampling locations and wells were selected to represent the different depths within the aquifer. These sites comprised out of publicly owned wells and government wells where government wells represented the greater depths, more than 30 mbgl and the publicly owned wells the shallow and intermediate depths. To make sure stagnant water wasn't sampled, the wells were pumped for 10 minutes and then sampled thus obtaining a representable sample. Stable isotope analysis was conducted on 140 samples within the same year. The samples were all collected and sealed in high-density polyethylene (HDPE) bottles and stored at low temperatures to avoid fractionation of the isotopes within the samples.

Kumar et al., (2011) used a dual-inlet isotope ratio mass spectrometer (Isoprime with Masslynx software Ver. 4.0) to analyse the oxygen and hydrogen isotopes. Three aliquots of each sample were also taken for statistical consistency. The Oxygen analysis made use of a CO₂ equilibration method, and the Hydrogen made use of hydrogen gas in the presence of platinum as a catalyst. The values were expressed in the Delta (δ) notation relative to the VSMOW standard.

Results & Discussion:

These analyses found the following, $\delta^{18}O$ ranged between -9.6 and -1.99‰ and the δD ranged between -60.8 and -20.8‰. To determine the recharge zones geographical segregation of the data was required. Geographical segregation is depicted in [Figure 3.19](#), and the results of the four zones are displayed in [Figure 3.20](#). In [Figure 3.19](#) the point where the line of each zone intersects with the RMWL identifies what the isotopic values of that water were during precipitation. The annual averages of stable isotope values for rainfall at Delhi ranges from -8.37 to -4.18‰ for $\delta^{18}O$ and from -60.52 to -24.21 ‰ for δD .

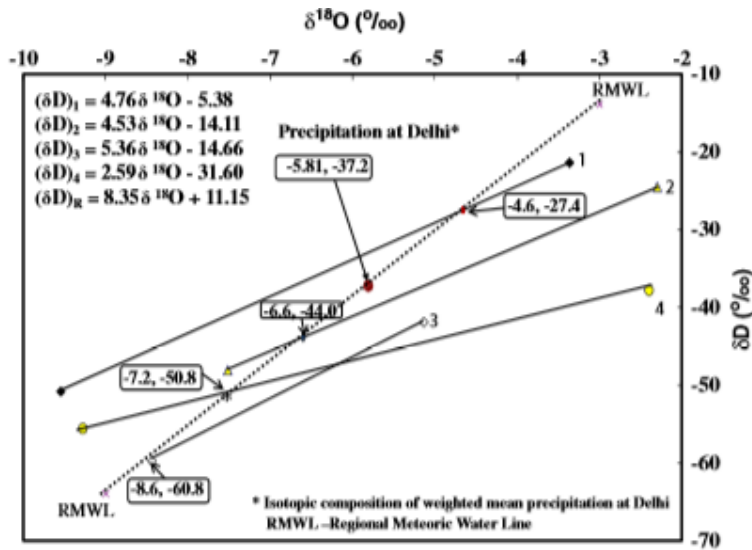


Figure 3. 19: Graph displaying RMWL and the geographical segregation of the stable isotope analysis (Kumar et al. 2011).

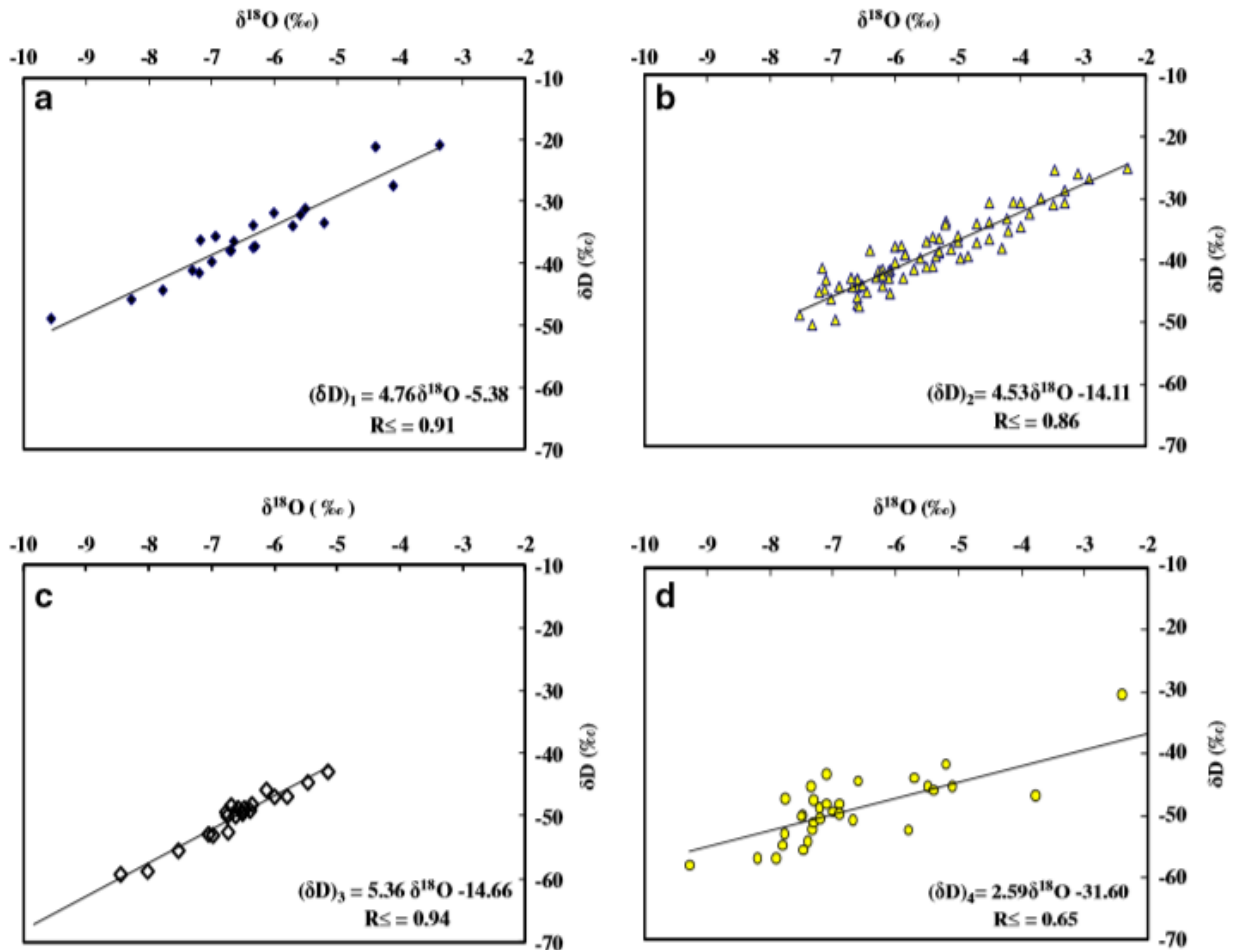


Figure 3.20: Stable isotope results for each separate geographical region, indicated by numbers 1, 2, 3 and 4 which, respectively, correspond to the highlands (n=20), b near the drains and canal adjoining region 1 (n=70), c direct recharge by the Yamuna River in its

flood plain (n=20) and d evaporation-affected water in the flood plain (n=30) (Kumar et al. 2011).

It is expected that the groundwater stable isotope concentrations are equivalent to the average weighted stable isotope concentrations at the recharge sites; any deviation from this can be attributed to a specific effect, such as evaporation, water logging or climate change. This feature of isotopes makes it possible to trace and identify recharge sources (Kumar *et al.*, 2011). The results of the stable isotopes are described in *Figure 3.19*, *Figure 3.20* and *Figure 3.21* all these figures divide the study area into four groups and are interpreted as follows:

1(a) - These results represent the highland area, the data plot on the left side of the RMWL in *Figure 3.19* thus indicating recirculation of moisture as secondary precipitation. This is caused by the high elevation of this area and thick forest cover.

2(b) – These data points are distributed near drains and canals and do not show signs of secondary precipitation. Mixing with canal and or drain water is identified in a more negative intercept in *Figure 3.19*, this negative intercept is characteristic of water from the Yamuna River.

3(c) – The data that makes up line 3 in *Figure 3.19* is groundwater that represents the Yamuna floodplain. The data causes a high negative intercept, but the slope is relatively maintained at a moderate level when compared with the other groundwater. The cause for this is the temperature in the part, the temperature remains low during most of the year and thus causes less evaporation than the other regions.

4(d) – This line intersects the RMWL at a more negative location than what the isotopic composition of the regional rainfall is (-5.81 , -37.2), this is comparable with groundwater formed from the Yamuna River, thus the composition is probably due to Western Yamuna Canal or the Yamuna River water. The very low slope and high negative intercept suggest that the groundwater was recharged from water that experienced great evaporation. This corresponds with water that would fall on the low-lying marsh lands.

The four isotopic lines intersect the RMWL at different locations, and in descending order to intersect it is 1,2,4,3. In general, the δ values decrease with an increase in altitude of precipitation and thus assuming this the average elevation of the recharge increases in the order of 1,2,4,3. The data represented by line 4 is groundwater flowing in from a northern direction, and the source of this is high altitude origins such as Western Yamuna Canal or the Yamuna River of Himalayan

origin. The large range of Delta values for Oxygen and Deuterium can be attributed to continuous evaporation in bank storage regions, slow continuous groundwater recharge, and or the effect caused by cumulative evaporation on multiple recharge cycles through irrigation return flow. The overlapping of lines 3 and 4 shows that these two waters are mixed. Deducted from this the isotopic data of the groundwater is formed from three types of water:

- Precipitation is the major contributor in the highland area, with the minimum flow towards the plains, and is least affected by evaporation.
- Surface water, these are primarily the surface water flowing north to south and recharge through canals, drains, rivers (Yamuna River), and subsurface inflow from the north.
- The final type is a mixture of precipitation and surface water that is the final contributor.

Equation	Data range (‰)		Mean composition (‰)		Spatial distribution of recharge zone
	Min ($\delta^{18}\text{O}, \delta\text{D}$)	Max ($\delta^{18}\text{O}, \delta\text{D}$)	$\delta^{18}\text{O}$	δD	
$(\delta\text{D})_1 = 4.76\delta^{18}\text{O} - 5.38$	(-8.27, -45.8)	(-3.36, -20.8)	-6.21	-35.07	Highland area
$(\delta\text{D})_2 = 4.53\delta^{18}\text{O} - 14.11$	(-7.9, -46.9)	(-2.3, -25.1)	-5.48	-38.24	Area being recharged by drain and canal
$(\delta\text{D})_3 = 5.36\delta^{18}\text{O} - 14.66$	(-9.95, -68.82)	(-5.14, -42.88)	-6.89	-50.9	Direct recharge by Yamuna River in its flood plain
$(\delta\text{D})_4 = 2.59\delta^{18}\text{O} - 31.60$	(-9.28, -58.0)	(-2.4, -30.4)	-6.45	-48.32	Evaporation-affected canal/river water near the flood plain

Figure 3.21: Table displaying the results of stable isotopes of the four zones in the NCT of Delhi (Kumar et al. 2011).

The stable isotope data were used to determine the sources of the groundwater, and the results are displayed in [Figure 3.22](#).

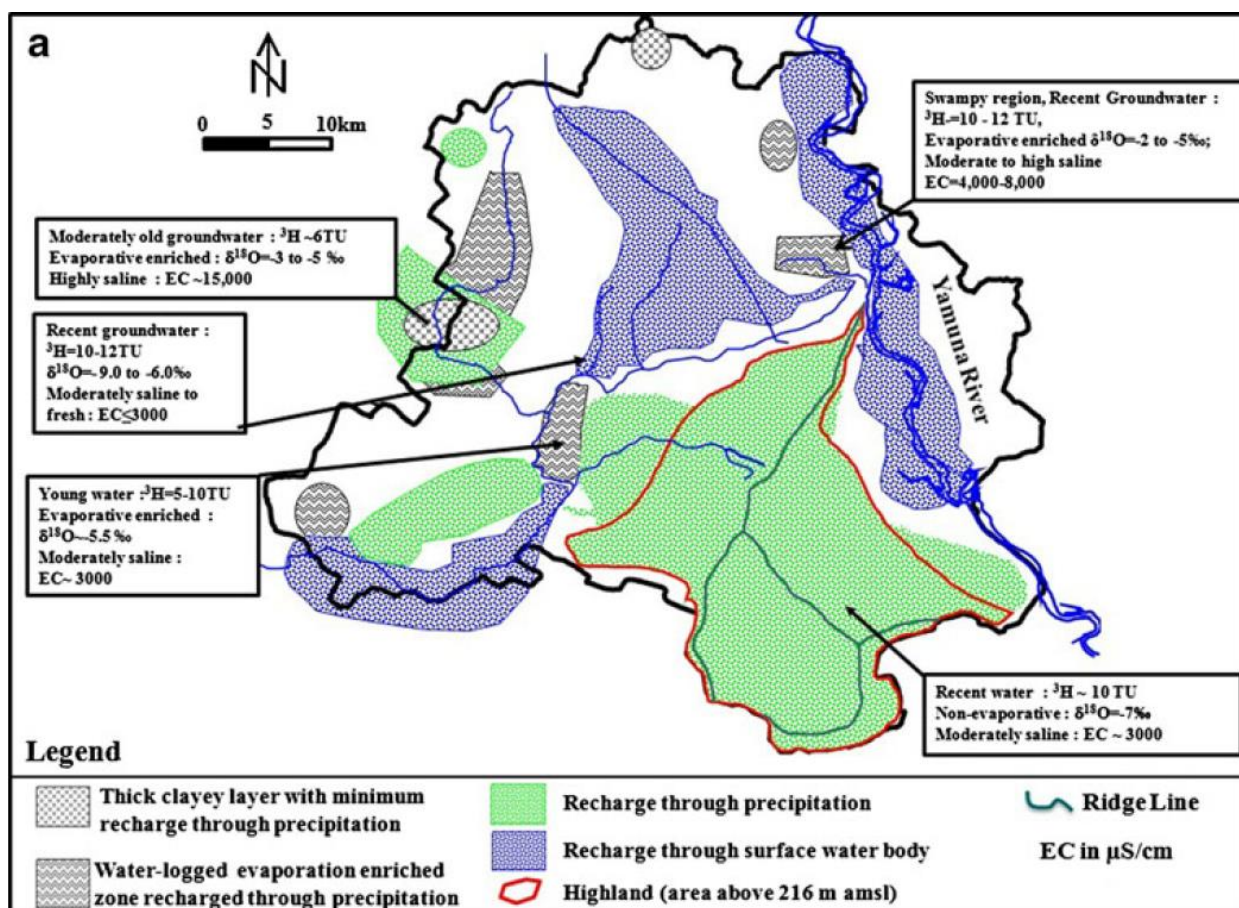


Figure 3.22: Figure displaying major sources of recharge for different areas (Kumar et al. 2011).

3.9.3 Case study 3:

Location & Background:

A study by Mekiso *et al.* (2015) was conducted on the Mohlabeti Wetland where isotope hydrology was investigated. The Wetland is in the middle part of the Limpopo basin and is part of the Oliphant's catchment area. The wetland falls within catchment B71C with the geographic coordinates 24°6'0" South and 30°6'0" East of the location of the study area and is depicted visually in [Figure 3.23](#).

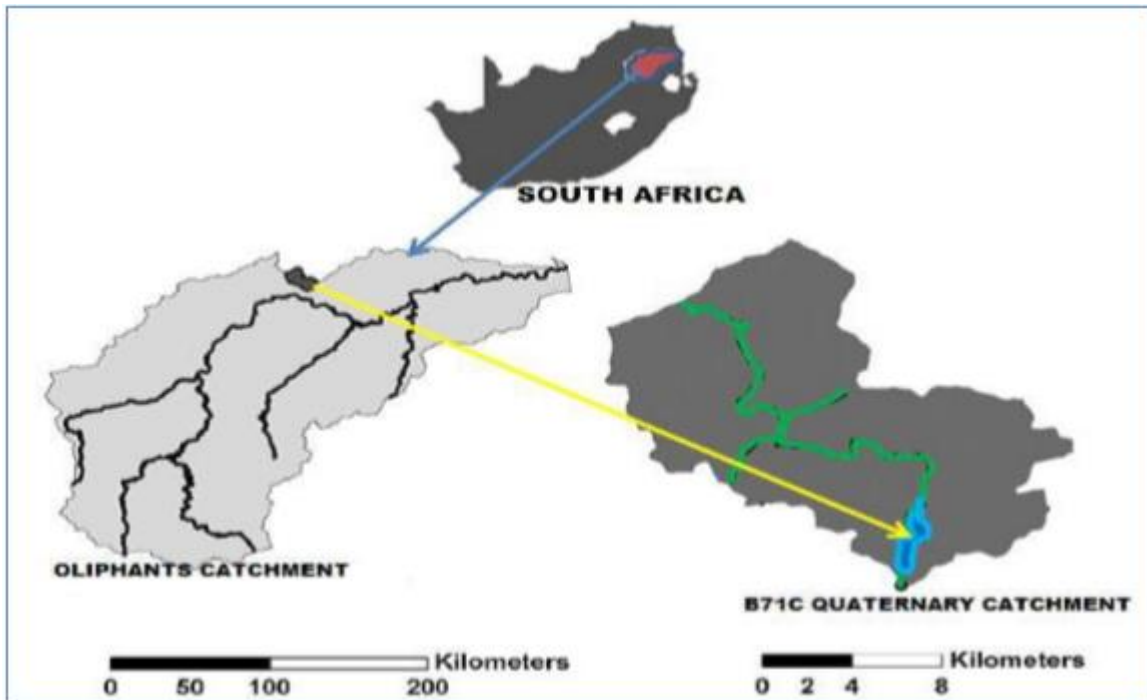


Figure 3.23: Location of the study area (Mekiso et al. 2015).

The Mohlabeti River is within the Limpopo Province and drains southwards into the Olifants River from the Wolkberg Mountains. The upper part of the Mohlabeti Catchment has a very mountainous terrain with elevations above 2050m and is covered by natural forest, where the lower part of the catchment is mainly alluvial valleys. From the location of confluence with the Olifants River, the Mohlabeti catchment has an area of 490 km² and upstream of the wetland, the area is 263 km² approximately. The valley is narrow and confined by steep hills on either side of the valley.

Methodology:

For a good analysis of isotopes, 128 samples were collected randomly from different sites of surface and groundwater such as rivers, springs, drains, piezometer wells, and boreholes. The Malmani Subgroup of the Chuniespoort Group underlies these sampling sites. Some samples were collected manually like the piezometer wells, and others like the boreholes were collected from taps. The water samples were collected in 50ml airtight plastic bottles for Oxygen -18 and Deuterium isotope analysis. The analysis of the samples was carried out by the iThemba Labs in Johannesburg, South Africa. The results from the analysis were displayed in ‰ (Per Mille) for $\delta^{18}O$ and δD relative to the VSMOW and was calculated with the following equation: $\delta\text{‰} =$

$$\frac{R_{\text{sample}} - R_{\text{vsmow}}}{R_{\text{vsmow}}} \times 1000$$

For the LMWL the Pretoria Local Meteoric Water Line (PLMWL) was used which was established from water samples taken from May 2007–November 2013 the $\delta^{18}O$ and δD were analysed and found a linear relation of: $\delta D = 7.05\delta^{18}O + 7.6$. The PLMWL was plotted against the GMWL with an equation of $\delta D = 8\delta^{18}O + 10$ and can be seen in [Figure 3.24](#).

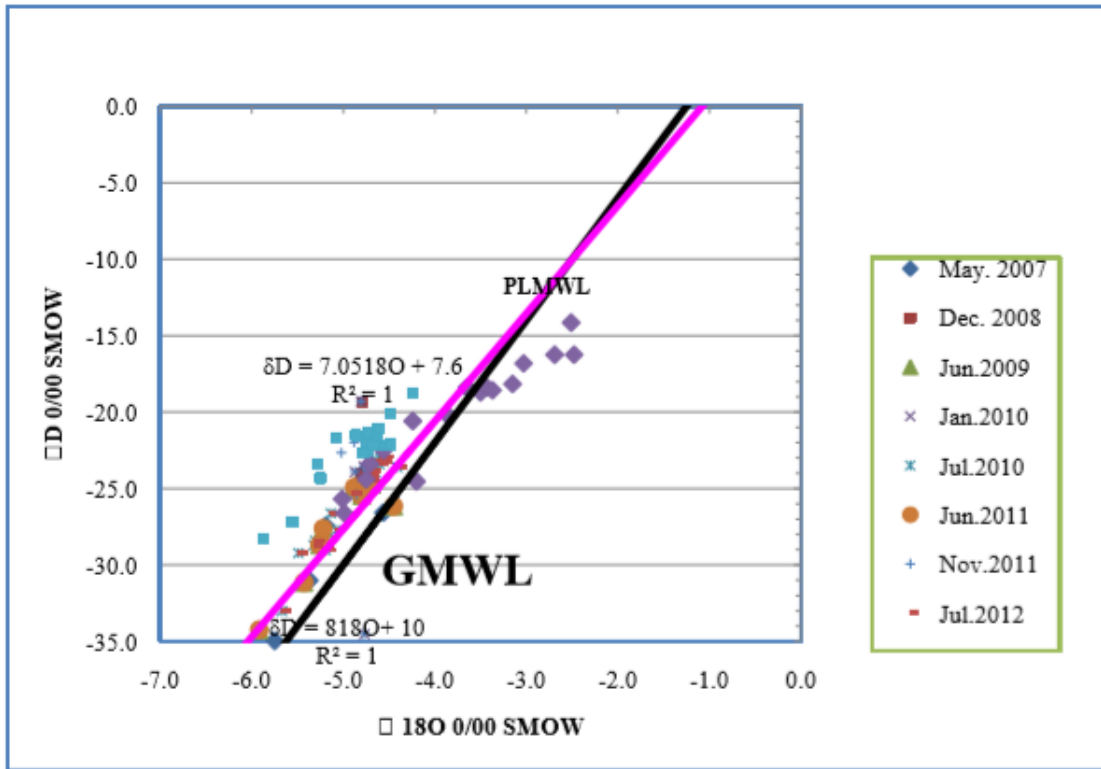


Figure 3. 24: Cross plot of Deuterium and Oxygen-18 from the samples taken (Mekiso et al. 2015).

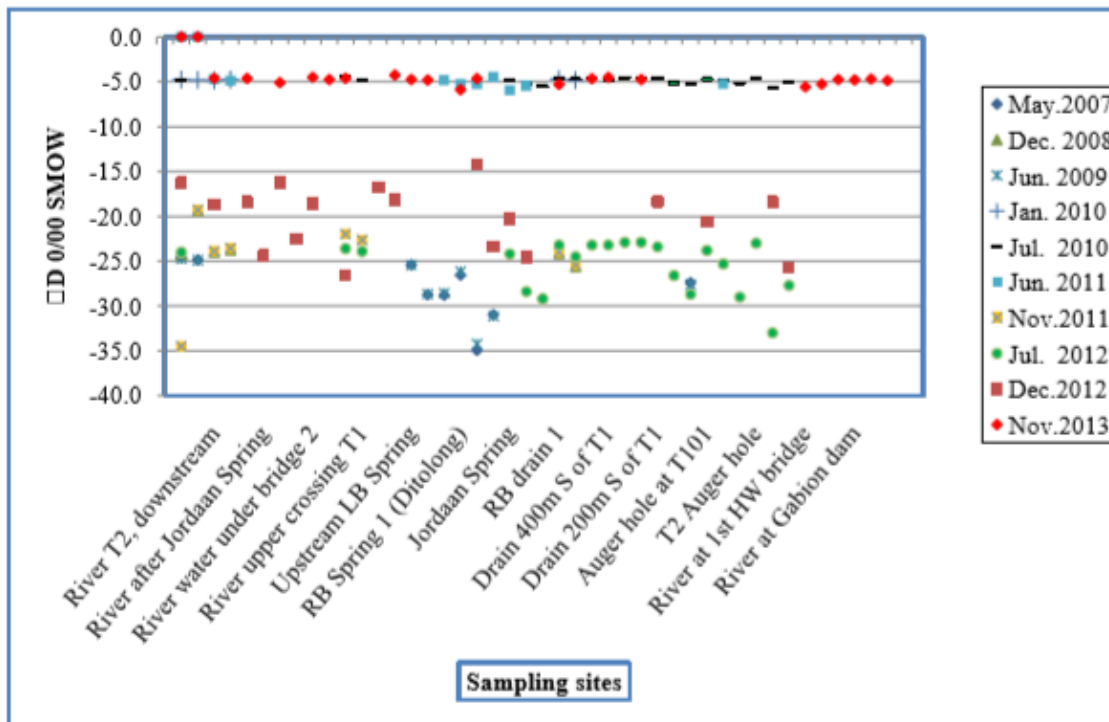


Figure 3.25: Isotopic compositions of surface and groundwater in the area (Mekiso et al. 2015).

Results & Discussion:

The results of the stable isotopic compositions from the samples showed a depletion trend, and the trend increased with the sampling year. Most of the samples taken in December 2012 showed enrichment when compared to the other years. These samples showed effects of evaporation and thus appeared to originate from any surface water, whether natural or anthropogenic. The samples from all the sampling locations showed no distinct difference, and thus indicated that they are all from the same source, and that recent water infiltrated the wetland aquifer. The similarity between the samples of the upstream and wetland aquifer confirmed that the two aquifers are hydraulically connected. As previously mentioned the samples from December 2012 plot below the GMWL and PLMWL, since they have undergone evaporation a lot that would occur with relatively heavy rainfall that causes water to collect in depressions and the evaporation enriches the water with heavy isotopes.

The enriched water then infiltrates and mixes with the groundwater or the water of the wetland aquifer. Compared to the other sample the oxygen-18 and deuterium values in all the groundwater samples revealed depletion. The standard deviation was 14.31 indicating that there was no major variation with the seasons or the years of sampling. The figures all indicate that there was no major seasonal variation, even in the low-flow and high-flow periods, [Table 1](#) also indicates this.

Table 1: Table showing statistical details of Deuterium and Oxygen-18 from the samples (Mekiso et al. 2015).

Statistical parameters	May 2007		Dec 2008		Jun 2009		Jan 2010		Jul 2010		Jun 2011		Nov 2011		Jul 2012		Dec 2012		Nov 2013	
	¹⁸ O	D	¹⁸ O	D	¹⁸ O	D	¹⁸ O	D	¹⁸ O	D	¹⁸ O	D	¹⁸ O	D	¹⁸ O	D	¹⁸ O	D	¹⁸ O	D
Maximum	-4.56	-24.6	-4.72	-19.3	-4.45	-24.7	-4.7	-19.3	-4.41	-22.9	-4.45	-22.7	-4.7	-19.3	-4.41	-22.9	-2.48	-14.2	-4.24	-18.7
Minimum	-5.75	-34.6	-4.84	-25.6	-5.92	-34.2	-4.87	-34.5	-5.67	-33	-5.92	-5.02	-5.02	-34.5	-5.67	-33	-5.01	-26.6	-5.88	-28.3
Mean	-5.07	-28.5	-4.77	-23.5	-5.1	-27.9	-4.8	-25.1	-4.87	-25.4	-5.1	-4.84	-4.84	-24.4	-4.87	-25.4	-3.76	-20.1	-4.83	-22.4

The coefficient variations from June 2011, November 2011, July 2012, December 2012, and November 2013 for δD are -0.09, -0.02, -0.07, -0.22 and 0.08 respectively thus also indicating the above that there is no seasonal variation.

Figure 3.25 shows the different isotopic concentrations of the source waters. The auger holes samples vary quite a bit from the upstream transects grouping with the drains, while the downstream transects are more like the spring samples. Indications from the springs are that the springs have highly variable isotope concentrations, and this could suggest that there are different types of springs in the area. These different types could be springs that are associated with groundwater and some that are associated with drainage of subsurface water that circulates above the regional water table. From this data, the following can be concluded. The clustering of the isotope values for samples from different locations and sources all indicate that these waters are all derived from the same source. The clustering of isotope values from drains, auger holes and river water samples, all together with the reduction of river flow between the main road and Gabion dam tends to indicate that the hydrology in the upper part of the wetland is mostly driven from upstream river inputs.

3.9.4 Case study 4:

Location & Background:

Nayak *et al.* (2016) did a study in Puri city India, where they made use of stable isotopes to determine the recharge sources. The study is in Puri city which lies between 19°44'-19° 58' northern latitudes, and 85°42'-85°54' eastern longitudes, the area is also near the Bay of Bengal and 65 km away from Bhubaneswar. The study area has a subtropical humid climate that has three main seasons, summer, winter, and rainy. Where the winter starts in November and continues until mid-February, the summer then lasts until the first week of June, and the rainy season starts in the second week of June and resumes until September which contributes to 74% of the annual rainfall. The hottest month is May and the coldest December with average maximum and minimum temperatures in summer of 37.5°C and 27°C and the winter 28.2°C and 15.2°C. The area is underlain by recent unconsolidated alluvial formations. Parallel to the shoreline, the sand dunes occur with widths from 100m to 7km, neighbouring the sand dunes are the deltaic plains with widths of 5 to 10km these plains experience extensive agriculture. Gravel and sand layers from the abundant aquifer are interconnected with dug well depths from 5 to 15m and the water level ranging from 1 to 12 mbgl. Deeper freshwater aquifers were detected at depths of 42 m and 210 m to 244 m by geographical logging. With the absence of major surface water, the groundwater is the only source of water for Puri town.

Methodology:

The water samples were selected for groundwater from dug wells and hand pumps, and for surface water samples were collected from canals, rivers, and surface water bodies. For hydrological studies, samples were collected from 21 well locations. The water samples were collected during March of 2010 with surface and ground waters being collected in different locations and sources. Samples were collected in 20ml HDPE and sealed with wax to prevent any contamination, evaporation, or exchange with the atmosphere. Samples collected from groundwater were left for sufficient time so that the samples are representative of the source of groundwater.

To analyse the samples for $\delta^{18}O$ (oxygen isotope) and δD (hydrogen 2H isotope), the sample was measured with a continuous flow isotope ratio mass spectrometer and a dual inlet isotope ratio mass spectrometer this was done at the National Institute of Hydrology (NIH), Roorkee. The error in the measurements suggested an error of $\pm 0.1\text{‰}$ for $\delta^{18}O$ and $\pm 1.0\text{‰}$ for δD . The isotopic characteristics of precipitation of the study area are expected to be represented by the local isotopic compositions that were collected at Kakinada which receives its precipitation mainly from the Bay of Bengal weather systems, and during the south-west monsoon.

Results & Discussion:

Figure 3.26 shows the best-fit lines for river water, canal water, and groundwater that were sampled within the study area together with the RMWL. The slope and intercept (D excess) are also tabulated in **Figure 3.27**. On a regional scale, the slope of the GMWL from dug wells is 4.56 and hand pumps 5.80 where both are less than the GMWL. The slope for river water is 7.82 and for canal water 7.77, this all indicates that residual water has undergone evaporation and thus plots to the right of the MWL. The effect of evaporation has affected the hand pumps less than the dug wells indicated by the GWL. The intercept of the GWL from the dug wells is -9.33 and hand pumps -5.02, both less than the RMWL, where rivers intercept at 10.22 and canal water at 6.24. This is also an indication that recharge conditions for the groundwater are relatively constant.

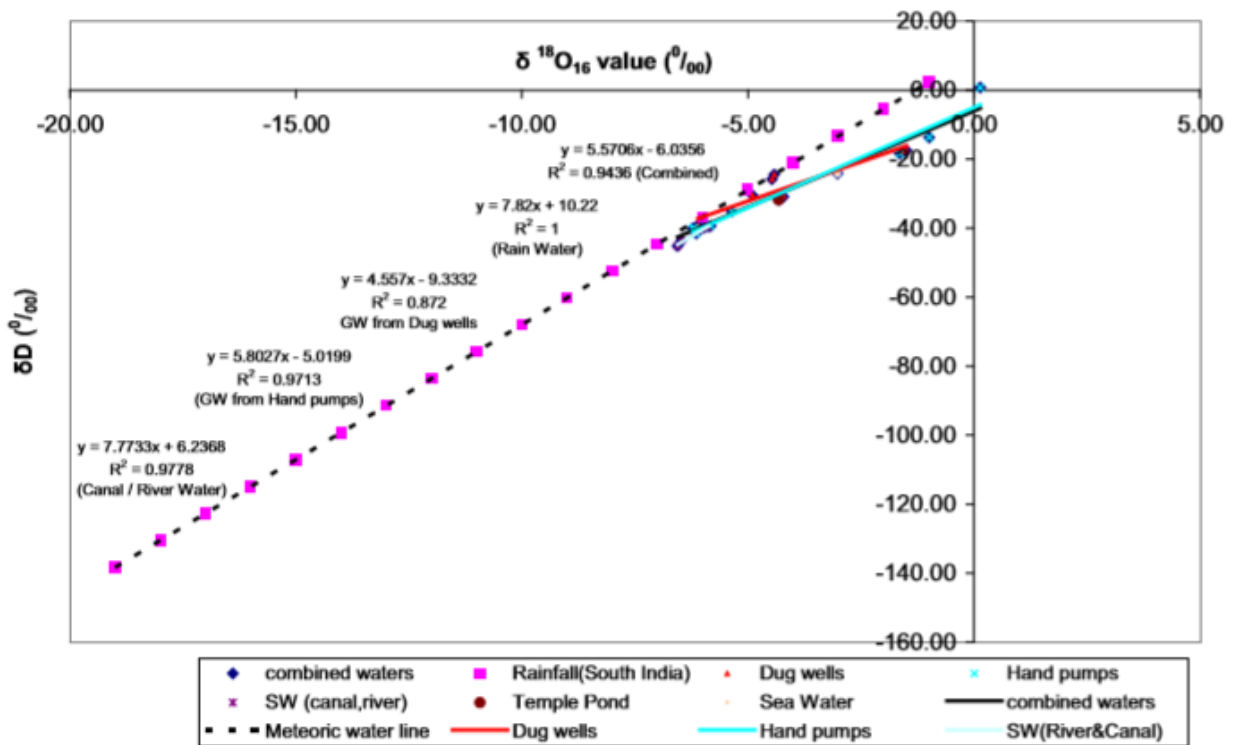


Figure 3.26: Stable isotope concentrations from different sample sites within the study area (Nayak et al. 2016).

	Combined waters	Precipitation (South India)	Groundwater dug wells	Groundwater hand pumps	River and canals
Slope	5.57	7.82	4.56	5.80	7.77
D excess or intercept	-6.04	10.22	-9.33	-5.02	6.24

Figure 3.27: Tabulated slope and intercept for best fit line for different water samples (Nayak et al. 2016).

The interaction of surface and groundwater can be studied with an isotope mass balance method, the isotope mass balance method works on the basis that rivers originate at higher altitudes, causing them to have a different stable isotopic composition than the groundwater recharged by local precipitation. The stable isotopes can thus be used to identify and understand groundwater interaction. In most of the applications, the isotopes are used to determine the contribution of river flow to groundwater. As an example, the mass balance equations of an admixture of rainwater and groundwater in a stream can be described by:

Equation 3. 20

$$mg \cdot Rg + mr \cdot Rr = Ram$$

$$mg + mr = 1$$

In the above equations, Rg and Rr represent the isotopic composition of the groundwater and river, and mg and mr are the fractions in the admixture. Ram is the isotopic composition of the admixture. And from these equations the following one can be deduced:

Equation 3. 21

$$mr = (Ram - Rg)/(Rr - Rg)$$

$$mg = (Ram - Rr)/(Rg - Rr)$$

Thus, from the above equations, it is visible that by knowing the values of Rg , Rr and Ram the fraction of river water mixed with groundwater can be evaluated. The different isotope compositions concerning oxygen are shown in [Figure 3.28](#).

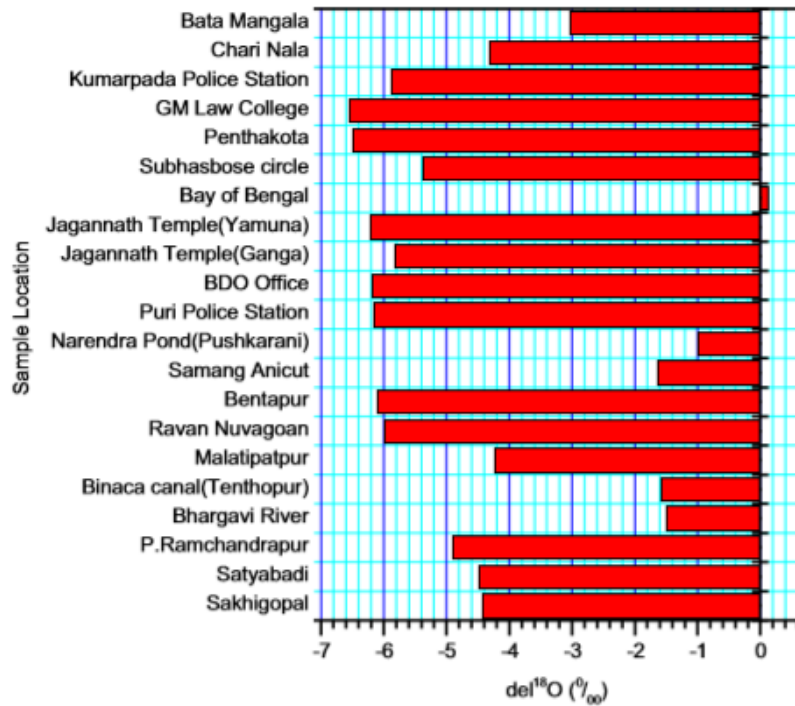


Figure 3. 28: Variation of $\delta^{18}O$ of the different sample locations (Nayak et al. 2016).

The contribution by precipitation and canal or surface water can thus be determined by using the $\delta^{18}O$ values that can be acquired from dug wells and hand pumps all through the study area. The results of the mass balance approach to understand the dominating factor of recharge is displayed in Figure 3.29.

Well location	Canal influence (%)	Precipitation influence (%)	Well location	Canal influence (%)	Precipitation influence (%)
Sakhigopal	47.3	52.7	Ganga well	22.6	77.4
Satyabadi	46.3	53.7	Yamuna well	15.2	84.8
P. Ramchandrapur	38.7	61.3	Subhasbose circle	31.2	68.8
Malatipatpur	50.9	49.1	Penthakota	10.5	89.5
Ravan Nuvagoan	19.3	80.7	GM law college	9.0	91.0
Bentapur	17.4	82.6	Kumarpada police station	21.6	78.4
Puri police station	16.6	83.4	Chari Nala	50.4	49.6
BDO office	15.9	84.1	Bata Mangala	74.5	25.5

Figure 3. 29: Contribution of Precipitation and canals to the groundwater (Nayak et al. 2016).

From the research, they found that the wells Ganga and Jamuna from the temple are primarily recharged from precipitation, and the rapid urbanization of Puri city influenced the recharge adversely by increasing pumping of groundwater, and reduction of uncovered and open recharge

areas. The recharge to the temple wells can be enhanced by regulating over exploitation of groundwater, and by diverting excess runoff from rooftops and paved areas.

3.9.5 Case study 5:

Location & Background:

Levin & Verhagen (2013) did a study in two different locations where they used isotopes and monitoring boreholes to trace pollution from waste disposal sites.

Methodology:

The first site was the Boitshepo waste disposal site located between the Tshepiso and Boipatong townships within the Emfuleni Local Municipality. Five boreholes and leachate were available for sampling that took place on the 8th of July 2010, [Figure 3.30](#) indicates the position of the sampling sites. Results from a chemical analysis proved that the boreholes BH3 and BH4 were not polluted.



Figure 3. 30: The locality of the boreholes and leachate sampling point at Boitshepo Landfill site with tritium values in TU. Arrows show inferred leachate migration (Levin & Verhagen, 2013).

Results & Discussion:

[Figure 3.31](#) Shows the stable isotope results and shows that BH4 is isotopically the least enriched but is on the GMWL and is thus representable of rainwater or shallow groundwater. The leachate, BH1 and BHB3 all plot close to each other and the GMWL. BH4A plots above the GMWL and

could be an indication of hydrogen isotope exchange within the landfill. BH3 could have possibly experienced evaporation under low moisture conditions because it plots below the GMWL.

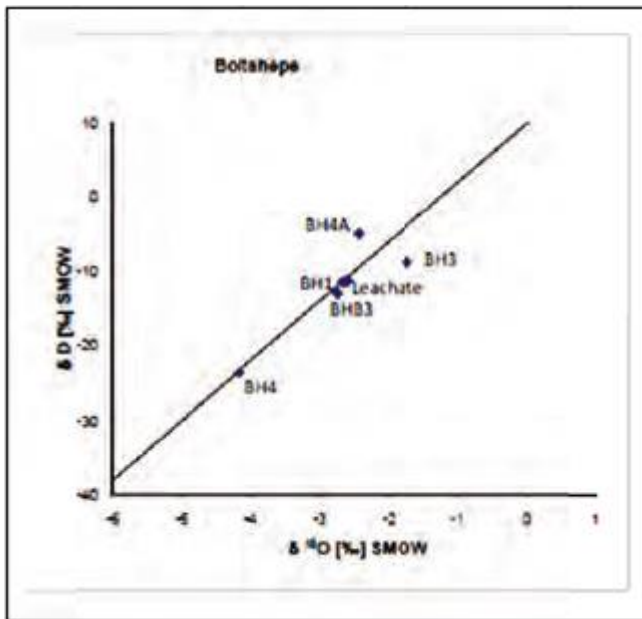


Figure 3.31 Stable isotope data of Boitshapo relative to GMWL (Levin & Verhagen, 2013).

BH3 is upstream from the landfill site and thus is not impacted or polluted. All the other boreholes except for BH4 are polluted, this is confirmed by the stable isotope results, chemical analysis, and tritium results. To establish the extent of the pollution plume a more in depth research of underlying geology should be done. Once that is completed a plan or method to mitigate the pollution can be developed.

The second site is the Rooikraal landfill site in the Ekurhuleni municipality next to Barry Marais road on the border between Boksburg and Brakpan as displayed in [Figure 3.33](#). The site was visited, and samples were collected on the 17th of January 2012 at the available boreholes and leachate, a sample of tap water was also collected at the office in Randburg for comparison.



Figure 3.32: The locality of the boreholes and leachate sampling point at the Rooikraal Landfill site (Levin & Verhagen, 2013).

The geology in the area is mainly Blackreef Quartzite, and Malmani dolomites and these are intruded by dolerite sills, and the site is underlain by a 10 to 30 m thick dolerite, with no faults or fractures in the area.

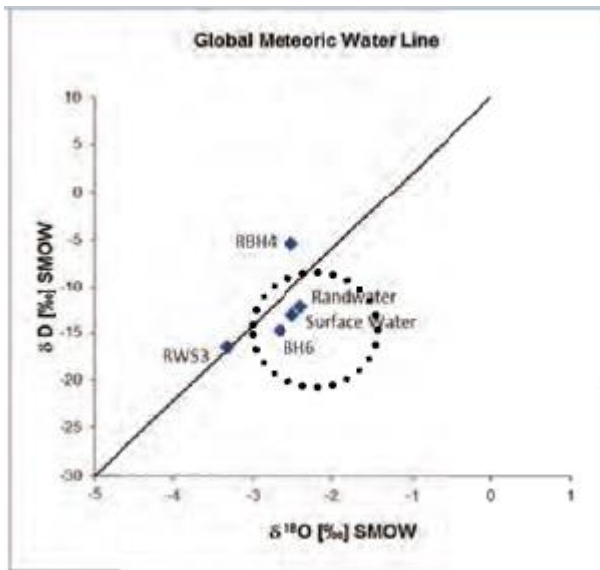


Figure 3. 33: Stable Isotope data with the GMWL (Levin & Verhagen, 2013).

The samples collected were sent for chemical and isotopic analyses. The results of the isotopic analysis are shown in **Figure 3.33**, this figure indicates that the surface water, BH6 and Randwater all plot together and the RWS3 sample plots on the GMWL as expected from groundwater. RBH4 indicates a slightly heavier isotope value than the rest. As there was no clear indication of the pollution source, the leakage was further investigated, and a leak was found in one of the Bulk Storage Reservoirs.

3.9.6 Case study 6:

Location & Background:

Harris & Diamond (2013), composed research where they used oxygen and hydrogen isotopes to do recharge studies of the Table Mountain groundwater. The base of the surrounding geology in the area is a low grade metamorphosed pelitic rock, and Cape granite. Overlying these is a sedimentary sequence and is predominantly arenaceous quartzite.

Numerous springs flow out of the sides of the mountain, and of these springs only a few were selected. These few selected springs include mainly the perennial springs and high-volume springs. Samples for rainwater was taken at two locations, one at the UCT campus where daily samples were collected, and a cumulative monthly sample was provided over 16 years and on top of Table Mountain at the upper cableway station, monthly samples were collected inconsistently over 2 years.

Methodology:

The samples collected were collected in a normal rain gauge and transferred each morning into a screw top glass container. The samples were analysed as soon as possible, using a Delta XP mass spectrometer. The results were presented in the familiar δ format:

$$\delta = \left(\frac{R_{\text{sample}} - R_{\text{standard}}}{R_{\text{standard}}} \right) \times 1000, \text{ and } R = {}^{18}\text{O}/{}^{16}\text{O} \text{ \& \& D/H.}$$

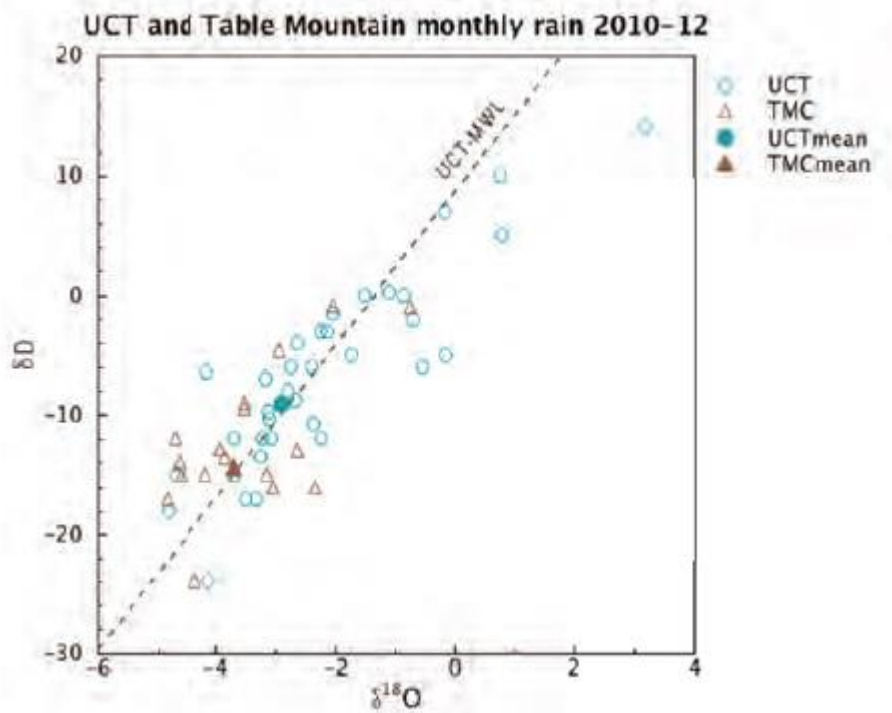


Figure 3.34: Cumulative isotopic rainfall values from the two rain stations from 2010 till 2012 (Harris & Diamond, 2013).

Fifteen springs were sampled over the 2010 to 2012 period and an attempt was made to sample each spring twice a year with 6 months apart from the sampling dates.

Results & Discussion:

The weighted mean annual rainwater isotopes vary from year to year. From [Figure 3.35](#) the shift from year to year is visible, and it is visible that the same shift occurs for the spring water as for the rainwater, and this suggests that the springs discharge is very recent rainwater. Some of the springs have a very steady discharge rate over the years, and thus they need a substantial aquifer that dampens the effects of seasonal rainfall. A model to describe this with the findings is a possible layered aquifer, where the recent rainwater flows on top of the older water in the aquifer and is thus the discharged water.

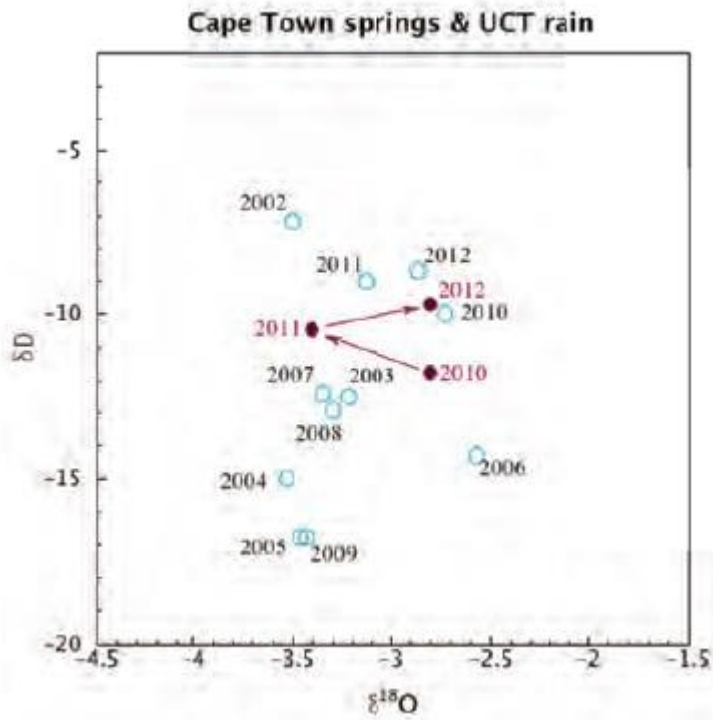


Figure 3.35: Weighted annual means for rainfall samples at the UCT site, and the springs (Harris & Diamond, 2013).

3.9.7 Case study 7:

Location & Background:

Abiye (2013) did a study where the interaction between the surface water and the groundwater was studied making use of stable isotopes, and chemical analysis. The research was carried out in the upper Crocodile River basin and made use of the isotopes, and hydrogeochemical analysis to identify the impact of acid mine decant and drainage into the different water groups in the area. Most of the groundwater discharge that occurs in the Upper Crocodile River basin is through fractures, baseflow to streams, springs, and overflow of decanting shafts. Identifying the interaction of surface water and groundwater is very important concerning Acid Mine Drainage (AMD) because if polluted groundwater interacts with surface water, the surface water, and the later the dolomitic groundwater will be polluted. The factors that influence the degree of interaction are topography, underlying geology, local groundwater flow, subsurface hydraulic properties, and temporal variation in precipitation.

The study area has a characteristic dendritic drainage pattern, and the impermeable crystalline rocks in the area cause the streams to respond very quickly, within an hour from when a rain event started the stream flow increases significantly. The streams that flow over dolomitic areas are however in constant interaction with the groundwater through cracks, fissures, and sinkholes.

The study area is underlain by crystalline basement rock such as granitic gneisses, which are meta-sedimentary rocks of the Witwatersrand Supergroup. There are also dolomites from the Transvaal Supergroup present in the study area. Making up the hydrogeology of the area it is mainly secondary aquifers in weathered and fractured crystalline rocks (Granite, Granitic Gneiss, Tonalite and Quartzite) and then karst aquifers that occur in the dolomitic formations, and intergranular aquifers that occur in the alluvial deposits next to the river valleys. The aquifers of the weathered and fractured crystalline rocks have low groundwater productivity with a borehole yield of 0.01 l/sec to 0.98 l/sec. The karst or dolomitic aquifers however have very high groundwater productivity with groundwater yields ranging from 15 l/sec to 124 l/sec. Compartments are created within the dolomitic aquifers by intersecting impermeable and semi-impermeable syenite and dolerite dykes.

The intense gold mining operations have caused the interconnection of different groundwater basins in the shallow and deep aquifers. The rate of acid mine decant in the area ranges from 18 000 m³/d to 36 000 m³/d containing iron as high as 1200mg/l and SO₄ of 5000 mg/l.

Interaction between groundwater and surface water occurs at the riverbanks and beneath river flow in the fluvial systems. When a stream channel diffuses into a wider area through dissolution structures and surfaces or fractures, an exchange of chemical constituents would occur. When the karst structures are dominant and act as a sink point they cause a lot of interaction with surface water and deep groundwater. Seepage also causes heavy metals such as Uranium to migrate from the tailing deposits into the shallow groundwater and surface water. One of the main types of surface to groundwater interactions is recharge in semi-arid regions. Another major method of surface water to groundwater interaction is seepage from streams and surface water to the aquifers. The meta-sedimentary and plutonic rocks that make up most of the aquifer causes an extremely complex exchange between the surface water and aquifers because the streams flow on top of the bedrock. The stable isotopes of $2H$ and $18O$ occur naturally in precipitation and contain information about seasonal meteoric signals in temperate and continental systems because of their unique isotopic signatures. These variations in precipitation are used to study the source of subsurface water. The main causes of water exchange in the area are topography and water levels. The groundwater is considered to have stable flow, even temperature and stable chemical composition that is reflective of underlying aquifer geology.

Methodology:

To understand the interaction, field measurements were taken over five years at different seasons. The field investigations measured pH, EC, TDS and Eh values in the water using digital Crison and Orion instruments. During the time of July 2008 until April 2012, all accessible water points were sampled for $\delta^{18}O$ and δ^2H . To identify surface water and groundwater interaction, a detailed investigation of physico-chemical and chemical parameters could be utilized. Two areas were targeted for this analysis, Sterkfontein and Malapa in the West Rand. The different quality waters showed considerable variation. Water with high EC/TDS values and very low pH is derived from AMD. As the water flows downstream and mixes with dolomitic water or precipitation the pH increases and the EC/TDS decreases. The Ca and Mg shows a linear mixing line that suggests the same source of Ca and Mg for the mixed, and shallow water. Water with high TDS is mainly related to Ca and HCO_3 ions which generally indicate carbonate dissolution.

All springs can be classified as having Ca, Mg- HCO_3 water. Water with a uniform chemical pattern is an indication of water from the same source, like the dolomitic aquifer and no dilution or interaction with different water sources. The DWA provides groundwater chemistry data that reveals the mixing of water resources with their concentrations ranging from HCO_3 to SO_4 . The complexity of the aquifer causes the nature of the interaction to be heterogeneous. High SO_4 and

HCO₃ make up the different end members, the water high in HCO₃ is dolomitic groundwater, and high SO₄ represents AMD, and everything in between indicates mixing.

Results & Discussion:

Most of the data from the stable isotopes plot below the LMWL is an indication that the recharge took place after evaporation. The stream samples rarely plot above the LMWL because the stream water is mainly rainwater. The main source of recharge for the aquifers will however be rainfall during the summer. A mixing trend can also be identified by the stable isotopes. The end members are deep circulating water in the dolomites that's depleted with $\delta^{18}O$ and δ^2H and the other end member is relatively enriched stream water, shallow boreholes that plot in between these end members is a sign of mixing. The average for rain samples plots above the LMWL, which is an indication of low humidity in the water vapour.

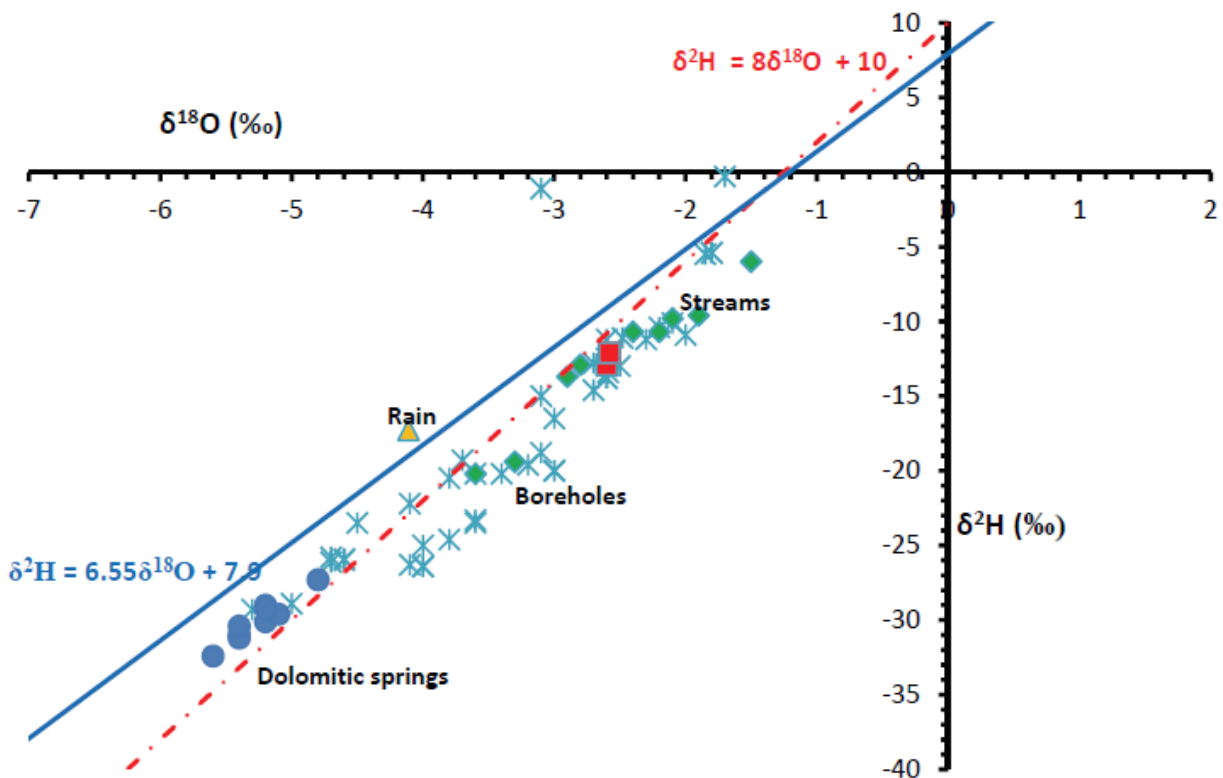


Figure 3.36: Stable isotope plot for the water samples taken in the upper Crocodile River Basin (Abiye, 2013).

Figure 3.36 indicates that the AMD correlated with the shallow groundwater, which is an indication of its source. The stable isotope data for AMD shows an average value of -5.6‰ for $\delta^{18}O$ and -22.0‰ for δ^2H . These values could be interpreted as water that is discharged from deep circulating groundwater. The fact that the perennial streams and shallow boreholes show an enrichment with respect to the heavy isotopes is an indication that evaporation happens to

those waters. The deep circulating waters and springs contain depleted water, and this could be because of recharge that takes place at a higher altitude, and a wider catchment with a wetter climate.

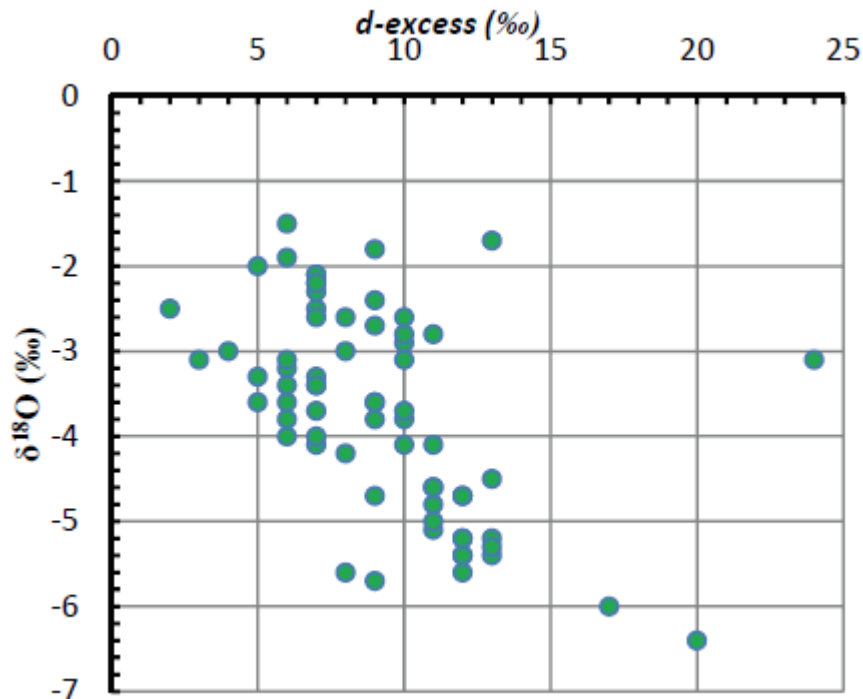


Figure 3. 37: Plot showing d-excess and $\delta^{18}O$ from the study area (Abiye, 2013).

To identify the source of precipitation the deuterium excess ($d - excess = \delta_2H - 8\delta_{18}O$) and the interpretation of that was used. **Figure 3.37** shows the plot of $\delta^{18}O$ versus d-excess the d-excess has a range from 2‰ to 24‰, which indicates circulation in the area because the influence of local and regional moisture is evident. The samples with a high d-excess is most likely an indication of very low humidity of vapour in the source area where the global average is 10‰, but humidity, wind speed and sea surface temperatures during evaporation, and a low d-excess reflects high humidity when vapour forms. The results from the stable isotope analysis also showed that the winter samples (June – Aug) in cold and dry climates are enriched with respect to $\delta^{18}O$ and δ^2H while in the hot and rainy climate of the summer (Dec – Feb) the samples are relatively depleted. This change could be due to the different evaporative rates.

It was revealed that the dominant interaction is shallow groundwater circulation within the fractured crystalline rocks and deep circulation within the dolomitic aquifer, this was revealed by the environmental isotope data. The regional groundwater circulation is defined by the compartmentalized aquifer systems, with each unique hydro geochemical and environmental

isotope result. The main factors controlling the interaction of surface and groundwater are factors such as differences in the head of streams and groundwater, local geomorphology, and groundwater flow geometry. The continuous discharge of AMD throughout the year is an indication that there is regional groundwater circulation that enables continuous base flow and spring decant & recharge. Within the groundwater, four distinct groups were identified based on the hydro geochemical analysis.

The first group is groundwater within the dolomitic aquifer that is partially affected by AMD, with high Na, Ca, Mg, HCO_3 and SO_4 . Secondly is the groundwater in the dolomitic aquifers without AMD impact, with high Ca, Mg and HCO_3 and low Na and SO_4 . The third group is water circulating within the shallow fractured crystalline aquifer with no effect of AMD and has low Na, Ca, Mg, SO_4 , HCO_3 (max \approx 150mg/L). The fourth and final group is the shallow aquifer circulating water within the quartzite and alluvial aquifers that are affected by AMD and have low Na, Ca, Mg, SO_4 and high Si. The stable isotopes $\delta^{18}\text{O}$ and $\delta^2\text{H}$ is an indication of how groundwater and precipitation vary over time and seasons and how the isotopic compositions of the sources are changed over time.

Streams will show seasonal variations more because they are representative of recent precipitation events. Groundwater and base flow will however not be so representative of seasonal changes. The isotopic compositions in the region of surface and groundwater are affected more and more by the impacts of complex mining activities and the surrounding geological setting of the area. This causes selective recharge and runoff, mixing of younger and older water from different sources that have newer rain and is affected by evaporation (Abiye, 2013:163).

CHAPTER 4: METHODOLOGY

4.1 Introduction:

To achieve the aim of this study and find the source of the GMB aquifer stable isotopes ($\delta^{18}O$ and δD) will be used as it is an accurate and effective tracing method that has been used effectively in many hydrological studies (Sharma et al. 2015:87). This chapter will discuss how the stable isotopes of water ($\delta^{18}O$ and δD) will be applied and used to answer the research question and ultimately determine the source. The stable isotope method will thus be the most cost effective single applied method that would provide quick decisive results and analysis. The Stable isotopes technique would be suitable for the study area because the stable isotopes are not affected by scale or pollutants in water. The different types of aquifers will have no adverse effects on the stable isotope composition (Gat, 2010: 134).

4.2 Sampling of Stable isotopes:

Kendall (1998b) specifies that natural water can easily be collected by using a clean, dry bottle that is capped tightly. The main aim is to protect the sample from evaporation and atmospheric vapour exchange. Filtering of water is also not required unless the water is stored under mineral oil to prevent evaporation. Sample sizes can also vary from 10 – 60 ml, and if samples are stored for later use glass bottles for storage and waxing of caps are advised. There are four methods of analysis, Gas-source mass spectrometers, Solid-source mass spectrometers, Gas and liquid scintillation counter and Accelerator mass spectrometry.

4.3 Sampling locations:

The locations chosen for sampling are crucial with stable isotopes, the reason being the isotopes from all possible sources and locations that could be the source of the GMB should be sampled. A wide variety of water bodies should thus be sampled. The amount of water that the GMB yields are an indication that water sampling should focus on the dolomites because they are the only aquifers that can produce such yields. All the samples taken will fall into one of two groups, the first is surface water which is water sampled from surface water bodies such as springs and streams. The second group is samples collected from boreholes or water pumped up from below the surface and it is the groundwater group.

Starting with the surface water group, surface water bodies were sampled in the surrounding area to give a relative idea of what the isotopic composition is for surface water bodies within the area. The samples will be collected on bodies of water relatively close to the target spring and the relevant dolomites to identify if any of them resemble the same isotopic composition. It is known from section **3.2 Factors that influence Isotope fractions**: that samples far away from the GMB would have different isotopic compositions. To identify how much change can be expected in samples from far away or different locations a sample from a distant area should be collected as well as a sample higher up in the WFS to determine if there is surface water that contributes to the GMB. According to Winde and Erasmus (2011a: 305 - 306), there is an interaction between surface waters in the WFS and groundwater in the dolomitic compartments.

18 Samples will be collected at surface water bodies, the samples are thus only collected at surface water bodies but could be representative of a groundwater source. Two of the surface samples are the GMB spring itself. Three surface water samples were taken within a 10 km radius of the GMB, two downstream and one upstream of the GMB, from the two downstream one, was taken at Boskopdam. There are four samples taken from the WFS stream and two samples taken from the Mooirvier downstream of the Klerkskraal dam. Three samples were collected from springs in the relevant areas. Five samples were collected from streams and five from dams as well. Lastly, three surface water samples were collected from canals (Mokadem *et al.* 2021). All the above-mentioned samples are displayed in [Table 2](#). with their coordinates and who sampled them, the locations are displayed geographically in [Figure 4.1](#).

Table 2: Displaying isotope samples and who sampled them.

Sample name	ID	Sample Description	Latitude	Longitude	O ¹⁸	H ²	Sampler	Elevation (mamsl)
MR01	1	Mooi River	-26.51	27.12	-2.60	-15.66	Naziha Mokadem	1395.6488
GM01	2	Grehard Minnebron	-26.48	27.15	-2.99	-16.40	Naziha Mokadem	1401.09021
WFS3	3	WFS3	-26.32	27.38	-2.85	-15.36	Naziha Mokadem	1478.15405
WPL01	4	pipeline	-26.33	27.40	-2.90	-15.58	Naziha Mokadem	1483.03516
BH1	5	BH1	-26.29	27.49	-4.13	-22.87	Naziha Mokadem	1511.44531
KKD01	6	Klerkskraal Dam	-26.25	27.16	-1.60	-10.99	Naziha Mokadem	1460
BE01	7	Bovenste eye	-26.20	27.16	-4.62	-26.91	Naziha Mokadem	1477.72546
BKD01	8	Boskop Dam	-26.56	27.12	1.20	7.38	Naziha Mokadem	1392.97778
Pot 01	9	Potchfestroom Dam	-26.67	27.09	-0.42	-2.85	Naziha Mokadem	1343.5332
JW01	10	JW01	-26.46	27.18	-2.94	-15.95	Naziha Mokadem	1481.23315
GBF01	11	Gembokfontein Spring	-26.29	27.67	-1.01	-4.39	Naziha Mokadem	1560.01904
DD01	12	Donaldson Dam	-26.28	27.68	-0.96	-4.16	Naziha Mokadem	1574.16333
WFS4	13	WFS4	-26.27	27.70	-1.27	-5.54	Naziha Mokadem	1579.59778
WFS5	14	WFS5	-26.25	27.73	-0.84	-2.98	Naziha Mokadem	1596.08411
CZ01	15	CZ01	-26.23	27.73	-3.78	-20.84	Naziha Mokadem	1612.72559
WFS2	16	WFS2	-26.44	27.15	-2.37	-13.61	Naziha Mokadem	1405.71216
CAN 01	17	Canal Mine	-26.33	27.41	-2.81	-15.01	Naziha Mokadem	1487.51563
LPV01	18	Luipaardsvlei Dam	-26.21	27.74	-0.59	-1.31	Naziha Mokadem	1618.297
GCO1	19	GCO1	-26.27	27.40	-3.73	-19.04	Naziha Mokadem	1531.64697
ABA01	20	ABA01	-26.25	27.43	-3.98	-21.91	Naziha Mokadem	1556.57544
CS01	21	CS01	-26.23	27.43	-3.96	-20.60	Naziha Mokadem	1562.51929
DP02	22	DP02	-26.23	27.45	-0.12	-3.44	Naziha Mokadem	1547.43774
CAVE1	23	CAVE1	-26.31	27.36	-2.45	-12.75	Naziha Mokadem	1480.65991
DF01	24	DF01	-26.22	27.51	-4.02	-21.26	Naziha Mokadem	1559.96729
ROD01	25	ROD01	-26.21	27.51	-3.63	-20.28	Naziha Mokadem	1558.68286
ROD02	26	ROD02	-26.23	27.50	-4.72	-25.61	Naziha Mokadem	1580.7832
EF02	27	EF02	-26.27	27.51	-1.30	-9.98	Naziha Mokadem	1582.55005
BB01	28	BB01	-26.27	27.55	-1.77	-10.57	Naziha Mokadem	1624.07837
VK02	29	VK02	-26.26	27.58	-4.27	-23.76	Naziha Mokadem	1607.38892
BB02	30	BB02	-26.28	27.55	-4.51	-24.16	Naziha Mokadem	1605.5575
VK04	31	VK04	-26.26	27.58	-4.66	-25.73	Naziha Mokadem	1606.89648
GR01	32	GR01	-26.24	27.61	-4.27	-20.01	Naziha Mokadem	1664.10071
TA02	33	TA02	-26.26	27.61	-4.32	-24.33	Naziha Mokadem	1600.59937
GR03	34	GR03	-26.24	27.63	-4.98	-27.18	Naziha Mokadem	1640.703
PV01	35	PV01	-26.26	27.67	-4.60	-25.46	Naziha Mokadem	1580.67529
GP01	36	GPO1	-26.30	27.69	-2.74	-13.73	Naziha Mokadem	1592.86694
AJS1	37	Pipeline celemanzi after treatment plant	-26.31	27.60	-3.51	-19.70	A.J. Louw	1541.10352
AJS2	38	Canal Celemanzi Shaft	-26.33	27.61	-3.55	-20.07	A.J. Louw	1580.26221
AJS3	39	Right Pipe Celemanzi Shaft	-26.34	27.61	-3.51	-20.04	A.J. Louw	1581.60181
AJS4	39	Left Pipe Celemanzi Shaft	-26.34	27.61	-3.49	-20.35	A.J. Louw	1581.60181
AJS5	40	Pipeline near Sibanye shaft 10	-26.39	27.43	-3.35	-19.49	A.J. Louw	1597.30115
AJS6	41	Canal out of pipeline Shaft4 Blyvooruitzicht shaft	-26.38	27.38	-3.36	-19.74	A.J. Louw	1543.19653
AJS7	42	GMB	-26.48	27.15	-3.21	-16.14	A.J. Louw	1400.23645

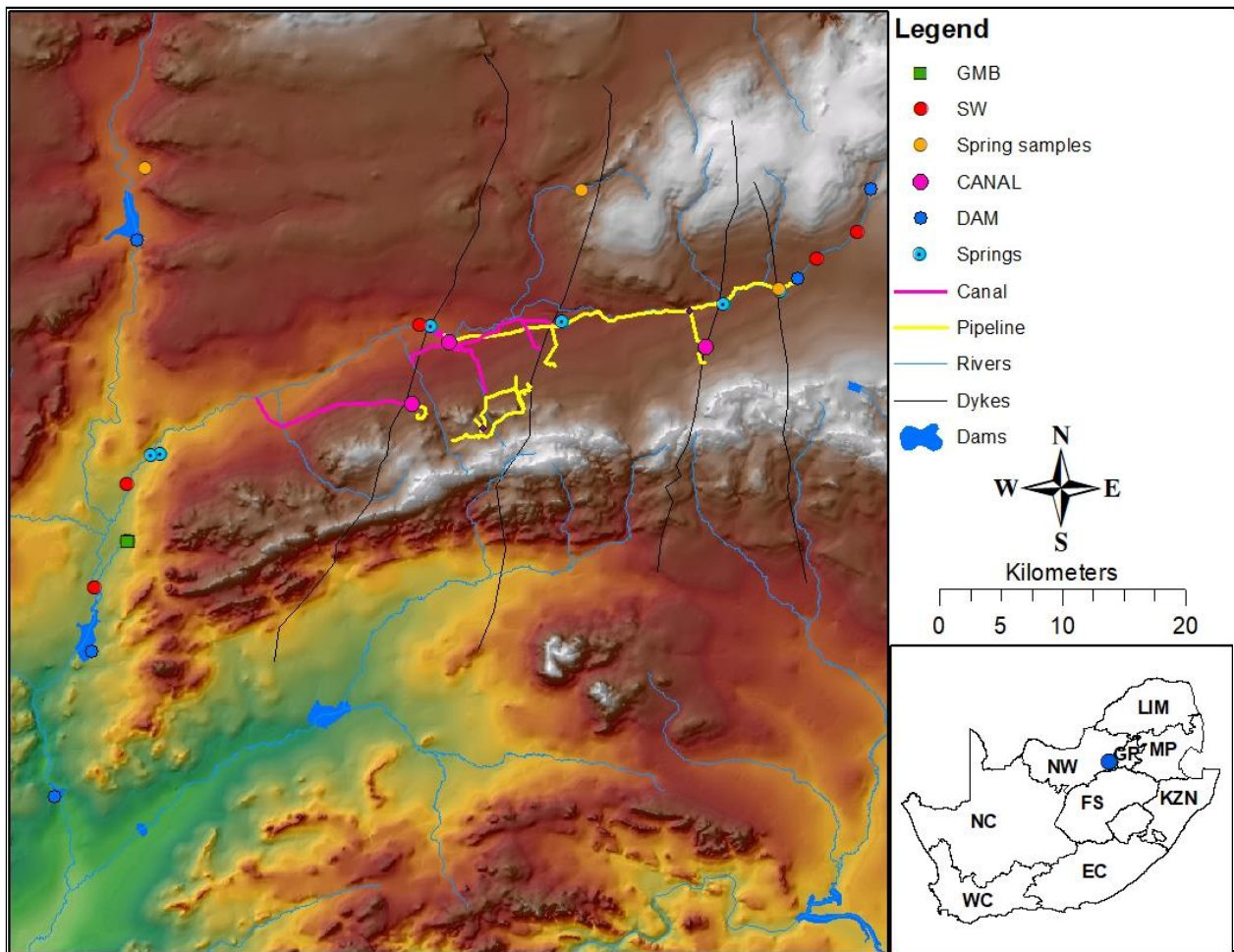


Figure 4.1: Map of the study area displaying surface water samples.

The samples close to the GMB are collected in such a manner that the isotopic composition of each stream is identified to see if they are the same or if there is a distinct change and what the composition will be if all the streams combine and determine possible mixing.

Rainwater will not be collected for this study because the variation of precipitation is too much over the study area. Stable isotopes in precipitation are also very susceptible to effects such as temperature, climate, time and length of the rainstorm. The second reason precipitation will not be sampled is because according to Bredenkamp *et al.* (2007: 24), the turnover time of the GMB aquifer is 22 years, this means that precipitation samples of 22 years ago would only be representable of samples taken now.

The last source that will be sampled is groundwater, the groundwater will be sampled at 25 different locations throughout the GMB and WFS area. The sample locations are chosen so that the samples represent different aquifers and different compartments within the dolomite

formations. The reason for this is to establish if these different aquifers interflow and where their boundaries are which will aid in the identification of the source of the GMB aquifer.

The main formation targeted by the groundwater sampling is the dolomite formations because it is assumed that the large amount of water flowing out of the GMB should be caused by a highly porous, fractured and weathered aquifer and in the surrounding geology, the dolomites are prone to providing high groundwater yields. The samples are placed in such a manner that within the dolomitic compartments to possibly reveal smaller compartments of interflow & mixing between them.

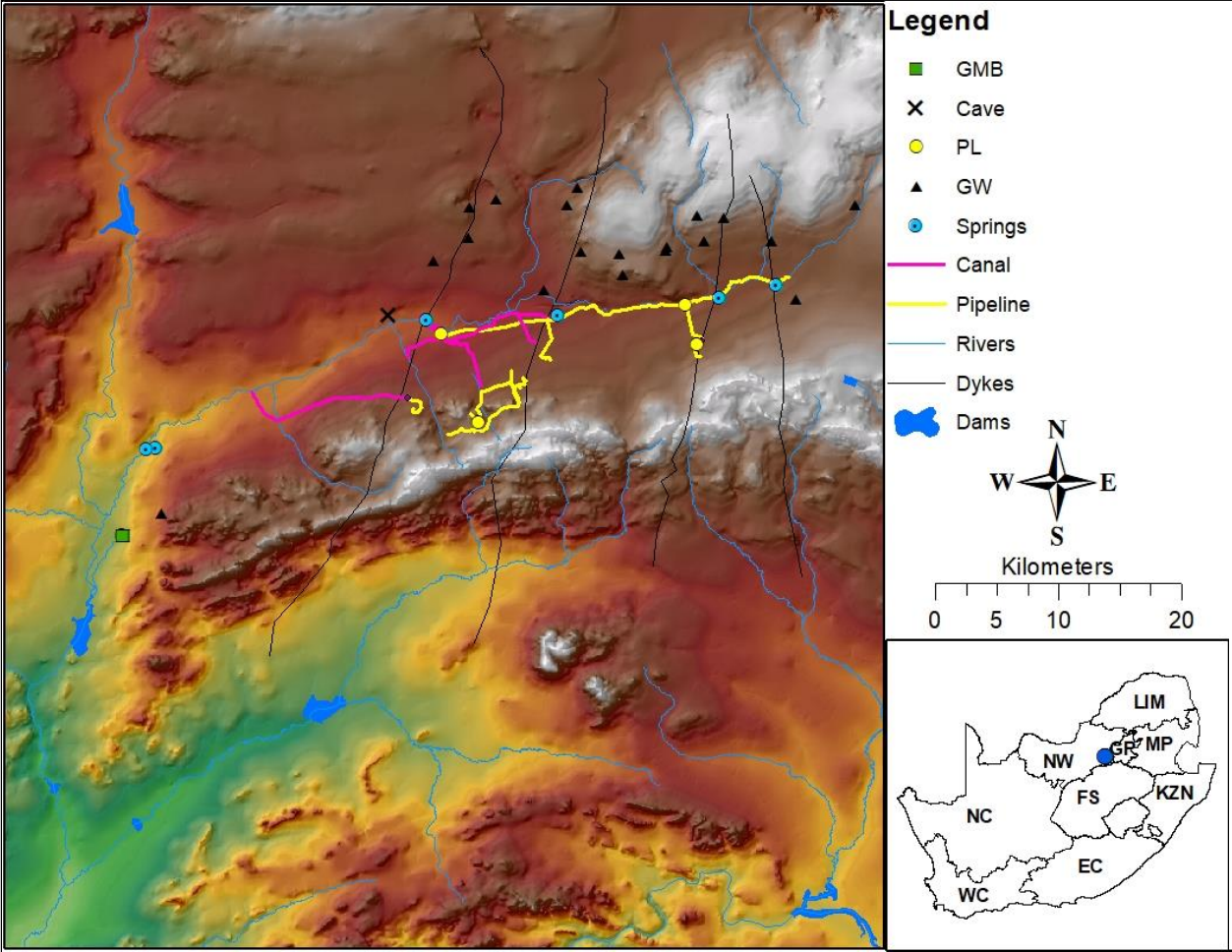


Figure 4. 2: Map of the study area showing sampling locations of Groundwater.

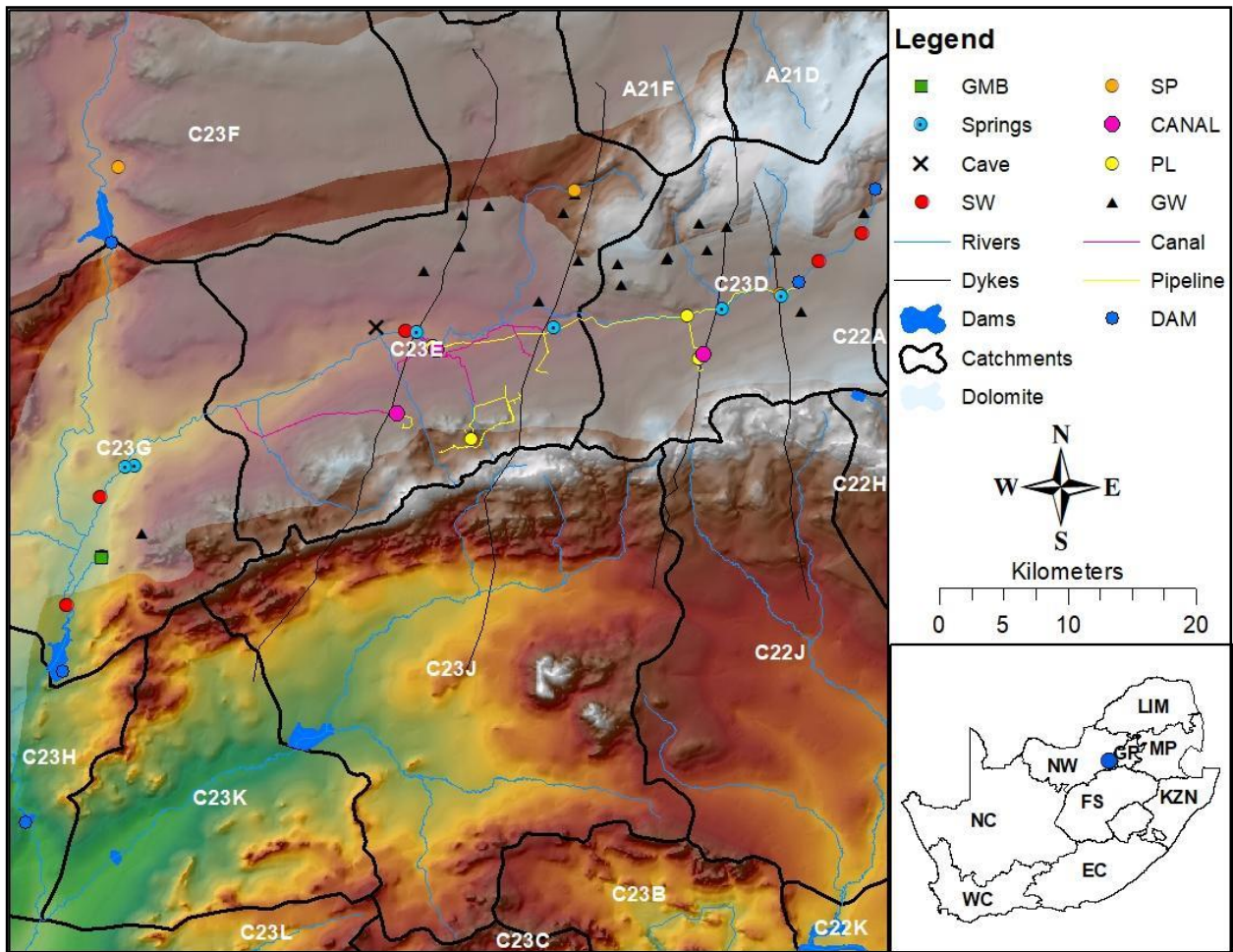


Figure 4. 3: Sampling locations with Quaternary Catchments and Dolomite.

4.4 Sampling method:

Each source type requires unique and different techniques to obtain an adequate sample. All the isotope samples will be sampled in 50ml HDPE bottles or larger with a cap and stored out of direct sunlight and heat. Studies were done by Blasch and Bryson (2007); Kendall and Caldwell (1998b); Kumar *et al.*(2011); Mekiso *et al.*(2015); Nayak *et al.*(2016), have all made use of this method and found it to be acceptable and sufficient. The amount of water required for the isotope analysis is less than 5 ml, and thus 50 ml will be more than enough and can also be stored for future analysis.



Figure 4. 4: HDPE bottles used for sample collection (Researchers personal library).

For surface water samples the sample will be collected with HDPE bottles and the samples will be taken in the middle of the water body and near the bottom of the body. This will be done to minimise the effect of evaporation and to get a respectable mixed sample as the water molecules fluctuate within a body of water. The samples will be collected with a very simple method, the sample container or bottle will just be placed underwater and rinsed once. Once the bottles have been rinsed and filled with water at the desired location they are closed and placed in a cooler box to prevent any hot temperatures, and direct sunlight. The samples were collected in bottles similar to the one displayed in *Figure 4.4*.



Figure 4. 5: Surface water example: Canal sampled (Researchers personal library).

Groundwater samples will be collected from boreholes and mine shafts primarily. The borehole that has pumps fitted will be used to collect the water. The water will also be collected at the tap that is right at the borehole and not water from a dam or reservoir because these samples will be affected by evaporation. Boreholes where there's no pump installed; a bailer will be used to collect samples. Water that is pumped out of the mine shafts will be collected at the pipelines either where they discharge or at leakages.



Figure 4. 6: Groundwater sample: Ruptured extraction pipeline from a shaft (Researchers personal library).

4.5 Analyser operation and components:

The Picarro L2130i consists of one main component, the CRDS. The CRDS component does the spectroscopy analysis and has a built-in computer to display the results and run programs. The one peripheral is the vaporizer, this component additional has the Micro-Combustion Module (MCM). The vaporizer is used to vaporize the injected sample of water into air molecules so that it can be analysed by the CRDS. The MCM is there to oxidize organic compounds and eliminate any spectral interferences. The Analyser also has two external vacuum pumps, one for the Vaporizer, and one for the CRDS. The analyser is also fitted with an autosampler that enables automatic sampling and analysis so that the machine can operate on its own and complete the samples without any human supervision or operation (Picarro, 2021).

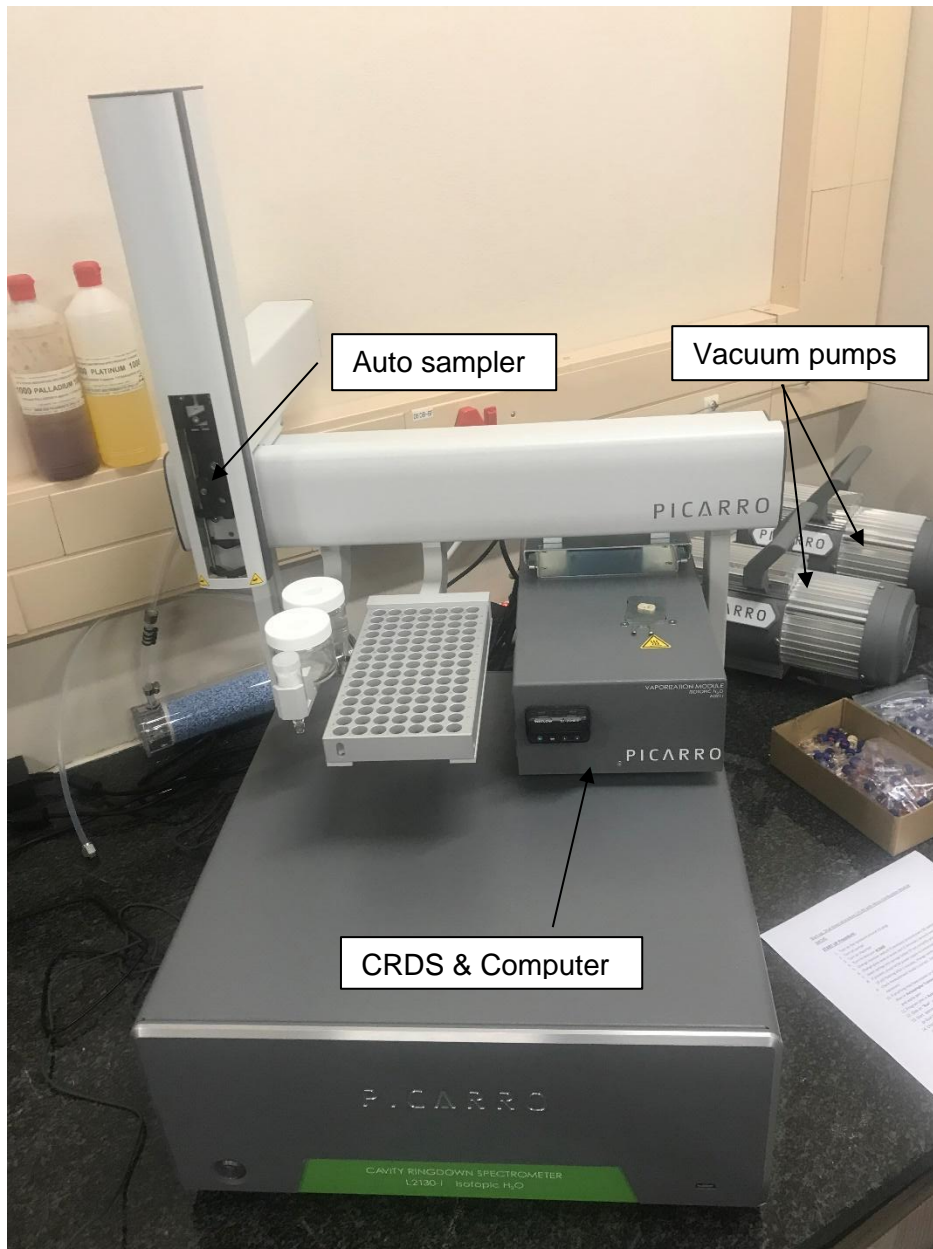


Figure 4. 7: Picarro L2130i and components (Researchers personal library).

4.5.1 Analyser:

The analysis of the samples for determining the $\delta^{18}O$ and $\delta D(\delta^2H)$ will be carried out with a Picarro L2130-i Isotope and Gas Concentration Analyser. The analyser consists of different parts, each of these parts or components have a very important use.

The analyser will determine the $\delta^{18}O$ and $\delta D(\delta^2H)$ by making use of a CRDS method. CRDS or Cavity Ring Down Spectroscopy works based on absorption spectroscopy, the method adjusts light rays to the unique molecular fingerprints of a sample species. The measurement of how long it takes the light to fade the “ring-down” time, an accurate molecular count is done in a few

milliseconds. The time the light decays thus provides an exact and rapid detection method of very small amounts of contaminants.

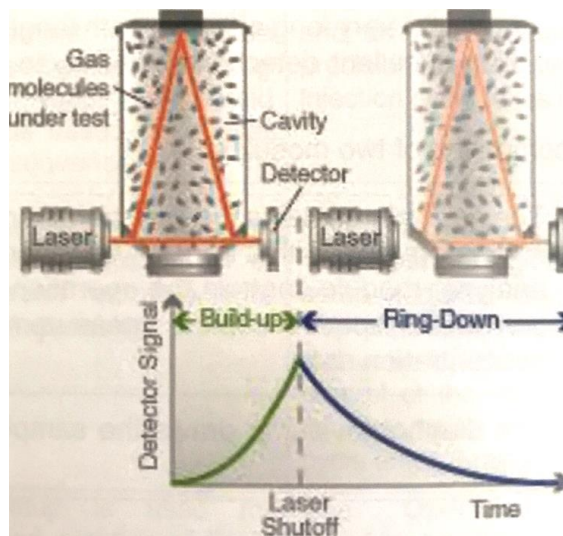


Figure 4. 8: Schematic of CRDS and ring down measurement (Piccaro, 2015).

The method works as follows and the method is shown in **Figure 4.8:**

- A diode laser emits a continuous wave beam of light energy through a highly reflective mirror into a cavity or the absorption cell.
- The light is then reflected multiple times between the two highly reflective mirrors, creating a total path length of 100 kilometres.
- The photodiode detector will cause the light source to shutter or divert from the cavity once it detects a pre-set level of light energy.
- With each succeeding pass, a small amount of light or ring-down signal is being emitted through the second mirror onto a photodetector, that produces a signal directly proportional to the light intensity within the cavity.
- When the light “rings down” the detector has achieved a point of zero light energy in milliseconds.

The time it takes to “ring down” can thus be used to identify the concentration of heavier isotopes ratio with the lighter or common isotopes in the sample.

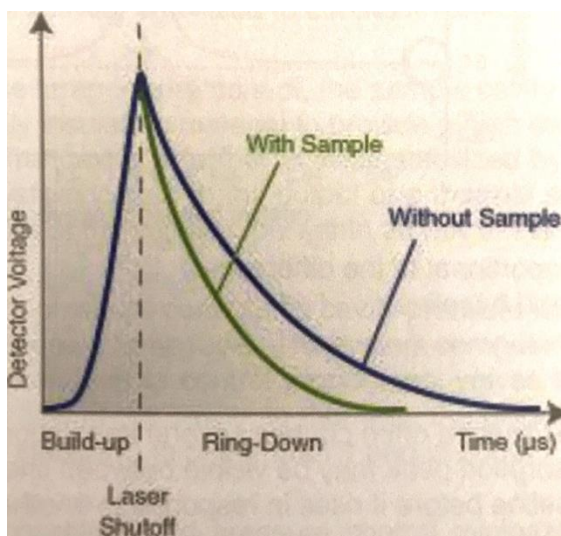


Figure 4.9: Light intensity in CRDS, and how optical loss is rendered into time measurement (Picarro, 2015).

Next is how the ring-down time can be related to absorption intensity. The ring-down time is inversely related to the optical loss (or absorption) within the cavity. Decreasing by a given percentage within the cavity is solely determined by the reflectivity of the mirrors. Once there is a gas present in the cavity the ring-down time will be shorter as displayed in [Figure 4.9](#), this reason for this being gas molecules of the sample that absorb the light intensity. To determine the absorption intensity at a specific wavelength, the ring down time of an empty cavity must be compared to a cavity that contains a gas. The CRDS in the Picarro automatically does the comparisons, and thus provides the final concentrations of the target gas or isotopes by converting the absorption intensities to concentration.

4.5.2 Application:

The Picarro L2130-i analyser may consist of very complex and intelligent components, but the operation of the analyser is quite straightforward and simple.

Before any of the operations could take place, the samples had to be prepared correctly. The sample preparation started by transferring and filtering the samples and standards into the correct Picarro analyser bottles ([Figure 4.10](#)) with a 5 ml pipette and rinsing the pipette between each transfer with Milli-Q water. The arrangement of the standards is displayed in ([Figure 4.11](#)).



Figure 4. 10: Picarro analyser bottles (Researchers personal library).

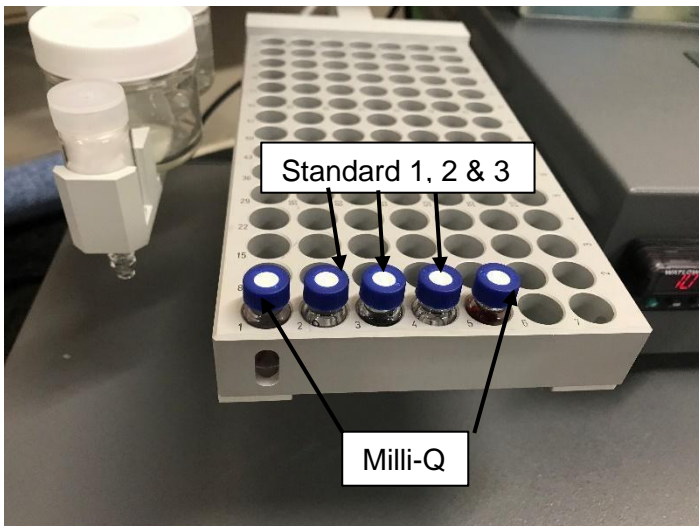


Figure 4. 11: Picarro sample tray with standards, and sample spots (Researchers personal library).



Figure 4. 12: Picarro standard (Researchers personal library).

Samples were analysed according to the manufacturer's instructions. Samples were injected via an auto-sampler into the vaporiser and micro combustion module (MCM), where vaporisation and measuring occurred. All instrument operations and data collection was controlled by PICARRO's CRDS software while CemCorrect software was used for data processing.

CHAPTER 5: RESULTS & DISCUSSION

5.1 Stable Isotope data

5.1.1 Basic Overview of data:

Overall, 43 samples were collected during the study, they all fall within 7 categories of samples based on their collection. Namely Groundwater, Springwater, Stream water, Pipeline water, Dam water, Canal water and Cave water. In [Figure 5.1](#) all the samples can be seen with the GMWL determined in Craig (1961) and the LMWL determined in Mokadem *et al.* (2021). In [Figure 5.1](#) there is also an arrow indicating the effect of evaporation from the LMWL. All the samples below the LMWL indicate that they have experienced evaporation since being introduced to the system as precipitation. All the samples will be discussed in detail in their relevant sectors. In [Figure 5.2](#) the ID number of each sample is displayed and can be cross referenced with the sample chemical plots for each source type.

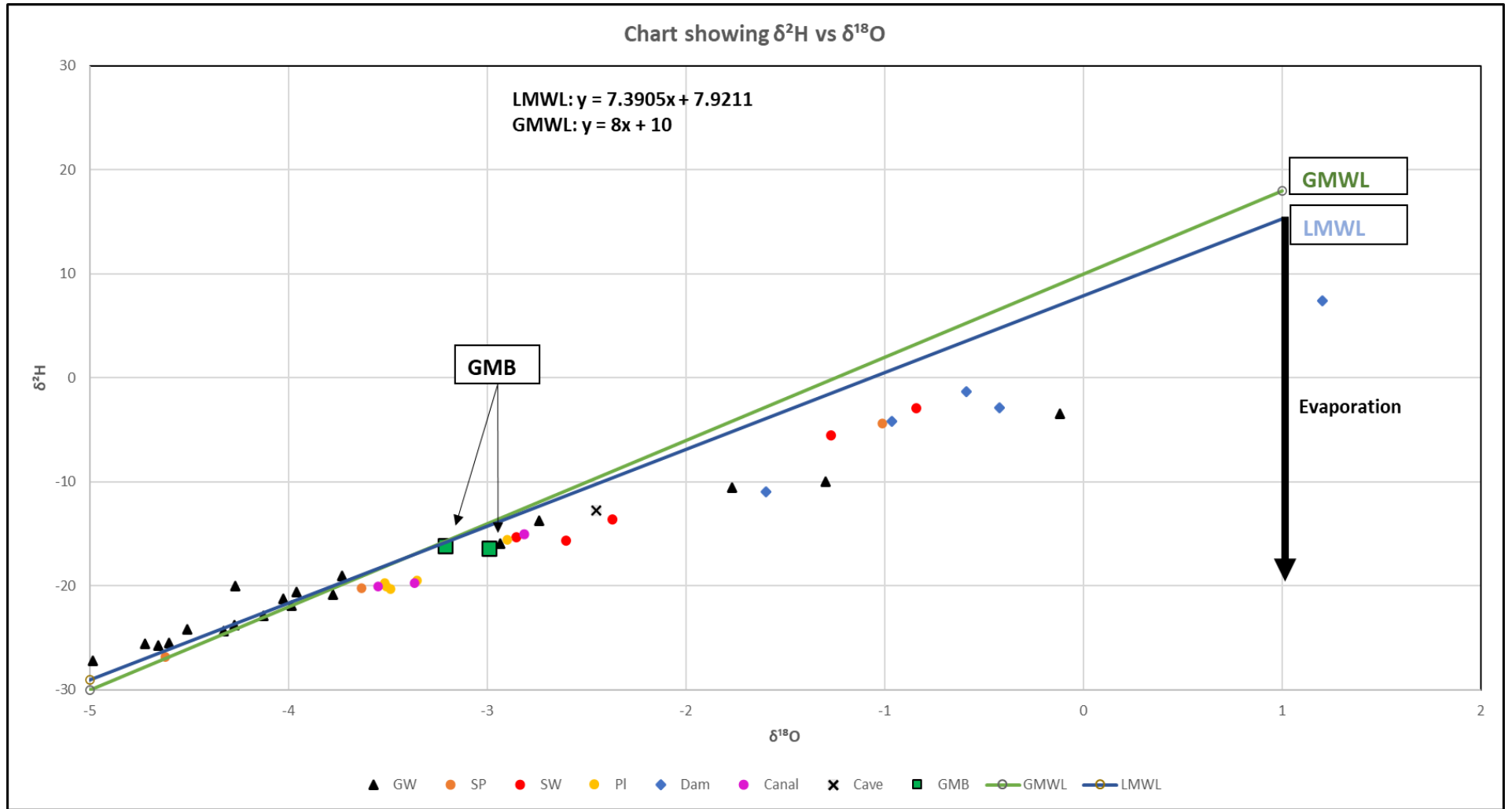


Figure 5. 1: Graph showing all the isotope data collected GMWL from (Craig 1961), LMWL from (Mokadem et al 2021).

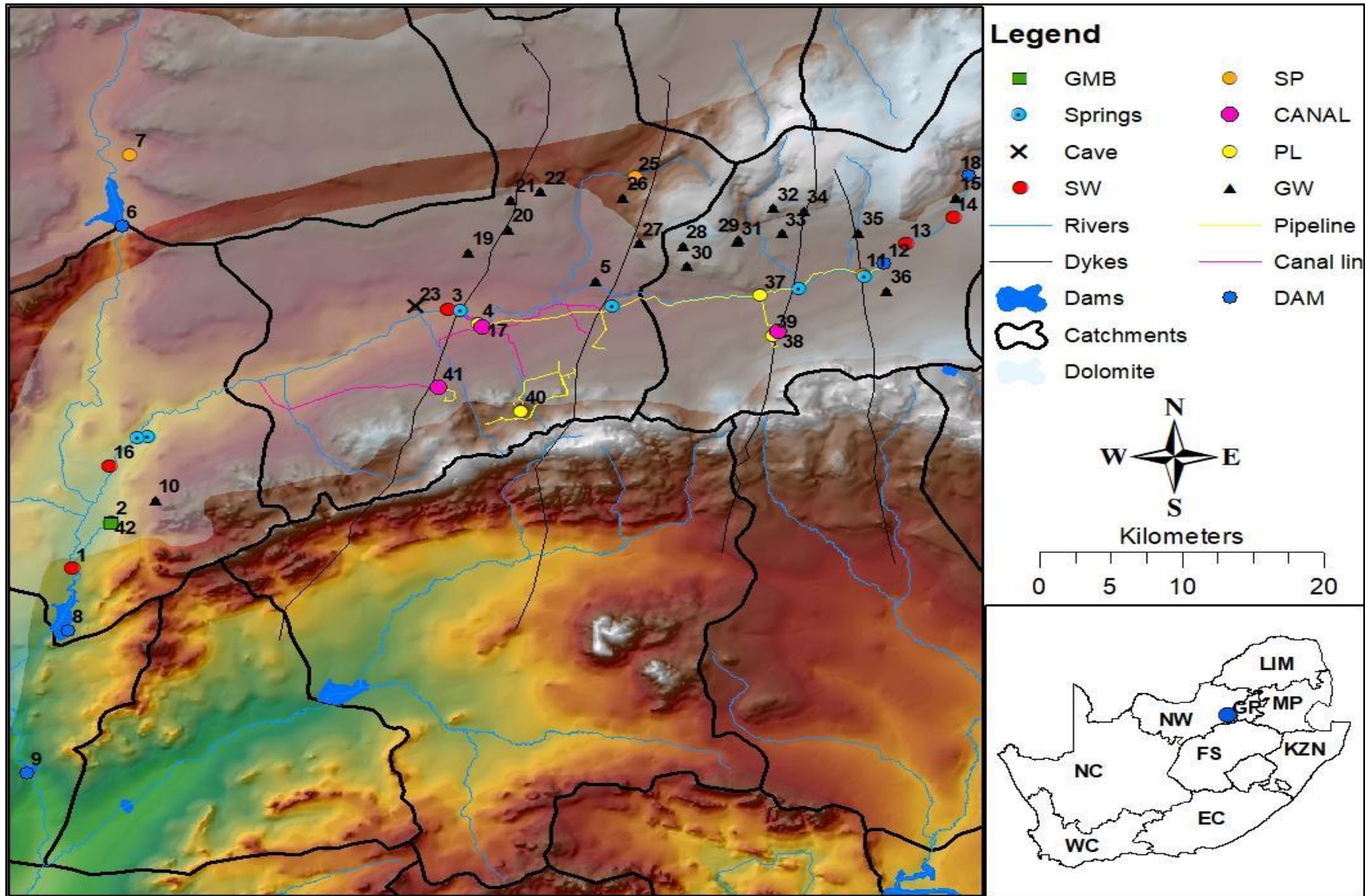


Figure 5. 2: Map indicating sample locations with sample ID's

5.1.2 Groundwater data:

In **Figure 5.3** all 19 of the groundwater samples can be seen. Most of the groundwater data plots on the LMWL, or very close to it. All the groundwater data that plots below $-3 \delta^{18}O$ plots on the LMWL or above it is indicating that recharge of the groundwater occurred prior to evaporation. The samples higher than $-3 \delta^{18}O$ all plots below the LMWL indicating that evaporation took place before recharge to the aquifer occurred.

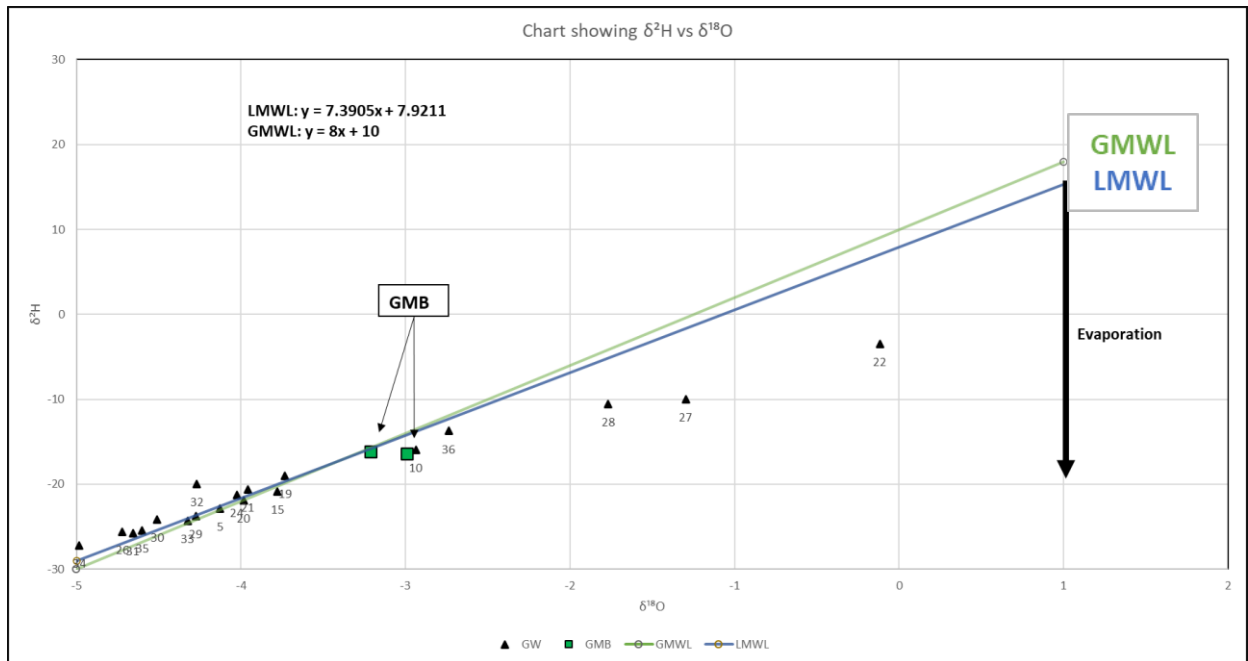


Figure 5. 3: Graph showing all the groundwater data.

5.1.3 Spring water data:

In **Figure 5.4** the spring water samples are displayed, two of which is the Gerhard Minnebron, so there are only four different springs that were sampled. The GMB samples plot on the LMWL or very close to it and two of the other spring samples also plot on the line thus indicating that only the Gemsbokfontein Spring (ID:11) sample at $-1 \delta^{18}\text{O}$ has experienced evaporation. The other four samples are indicating that the water flowing out of the springs hasn't changed that much since being added to the system as precipitation.

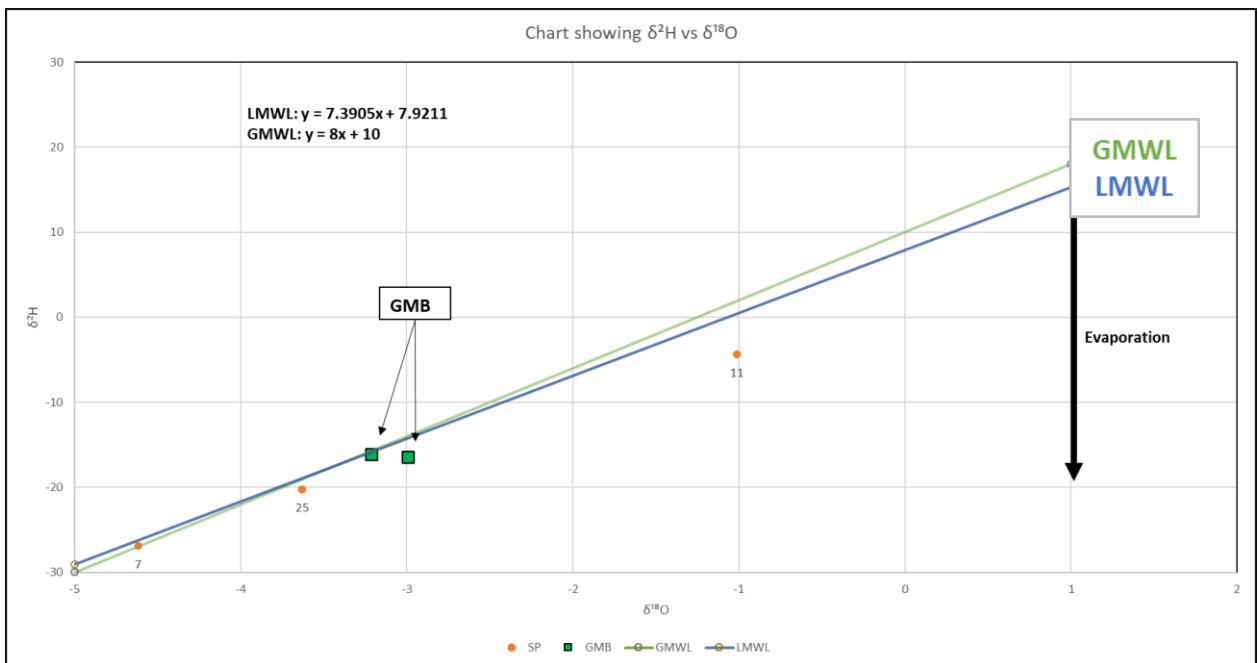


Figure 5. 4: Graph showing all the spring water collected.

5.1.4 Stream water data:

All 5 stream water samples are displayed in **Figure 5.5**. The data plots below the LMWL, as expected because all surface water would experience some form of isotope enrichment, primarily evaporation. The evaporation causes rainfall to become enriched with the heavier stable isotopes, and then the stream water samples will plot below the LMWL.

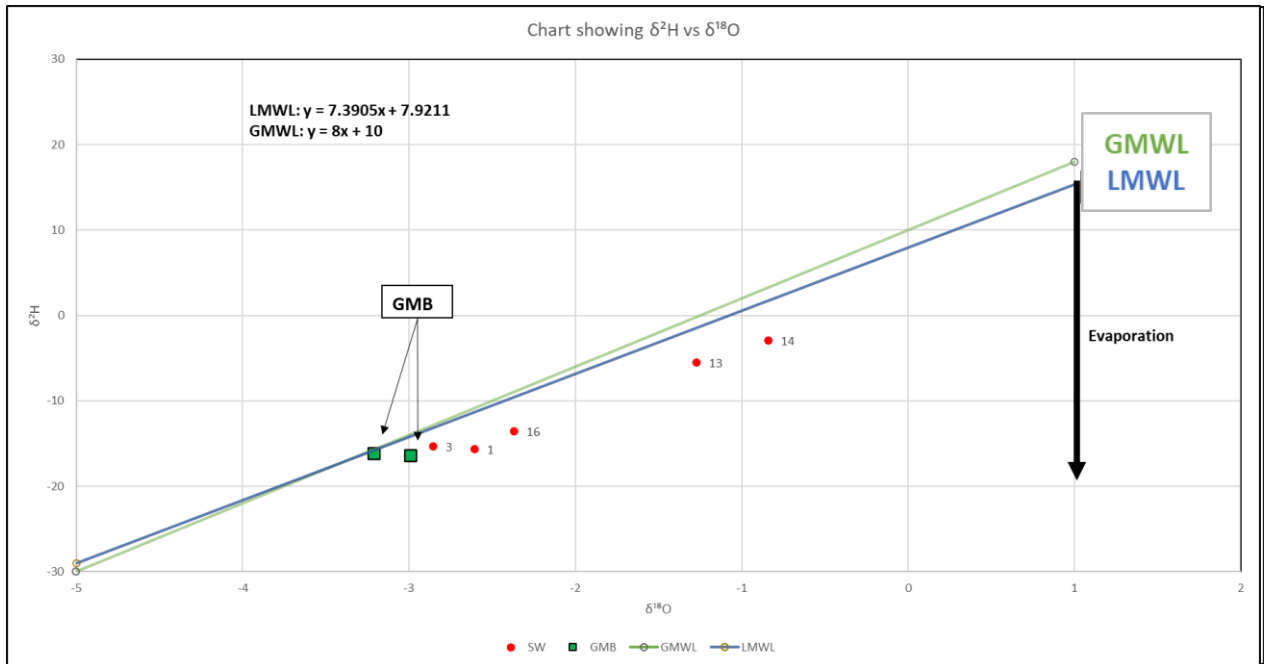


Figure 5. 5: Graph showing all the surface water data.

5.1.5 Pipeline data:

The pipeline data is a very complex set of data because the pipeline is a connected system. The pipeline samples are mainly mine discharge water, so it is better to collect the samples as close to the mine shafts themselves eliminating any other pipeline connections. The pipeline data all show slight variation of the same amount from the LMWL. This is an indication that the groundwater that's being pumped out of the shafts has experienced some form of evaporation.

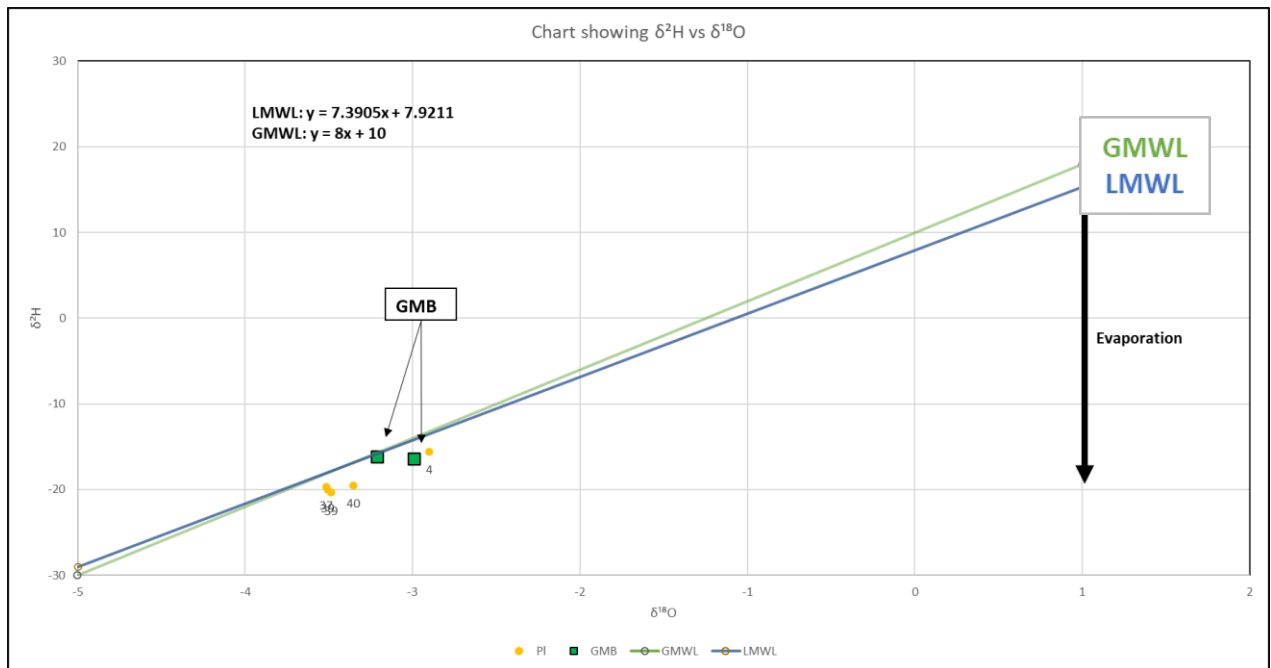


Figure 5. 6: Graph showing all the pipeline water.

5.1.6 Dam water data:

The data collected at dams displayed in **Figure 5.7** is plotting exactly as expected. The samples plot well below the LMWL indicating a large degree of evaporation which is expected from open surface water bodies like a dam.

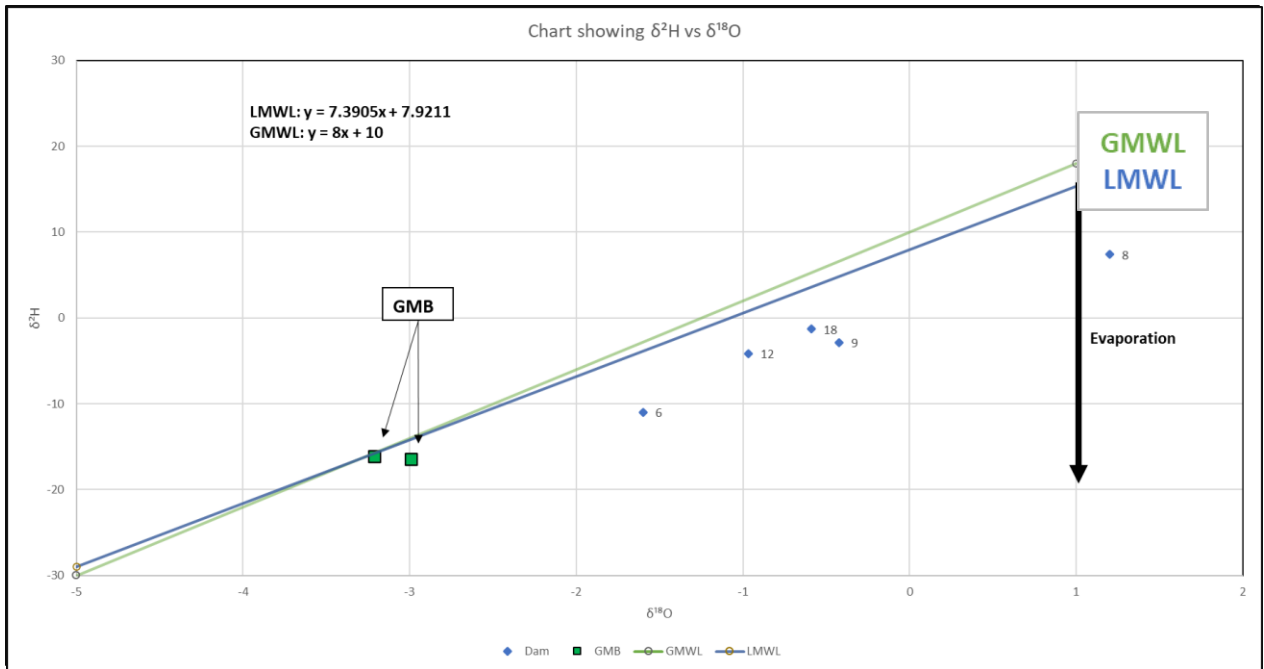


Figure 5. 7: Graph showing all the dam water data

5.1.7 Canal water data:

The canal water data displayed in **Figure 5.8** plots slightly below the LMWL. The canal water does not correlate with the other surface water samples. The reason for this anomaly is caused by the limited evaporation canal water experiences when compared to other surface waters. The less evaporation causes less enrichment of stable isotopes and in return, the canal samples plot close to the LMWL.

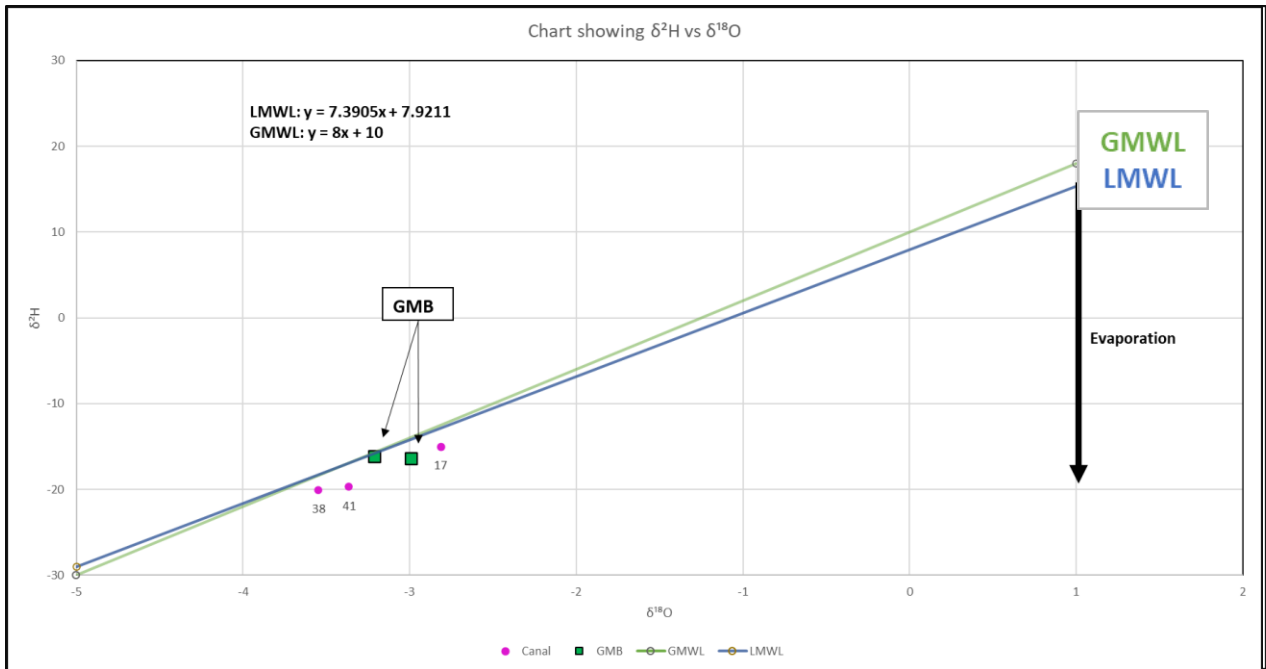


Figure 5. 8: Graph showing all the canal water data.

5.1.8 Cave water data:

The cave water data plots slightly below the LMWL in [Figure 5.9](#). The cave data plots as expected, resembling the same isotopic composition as the groundwater samples. The data plots slightly below the LMWL indicating that some but not a lot of evaporation have taken place.

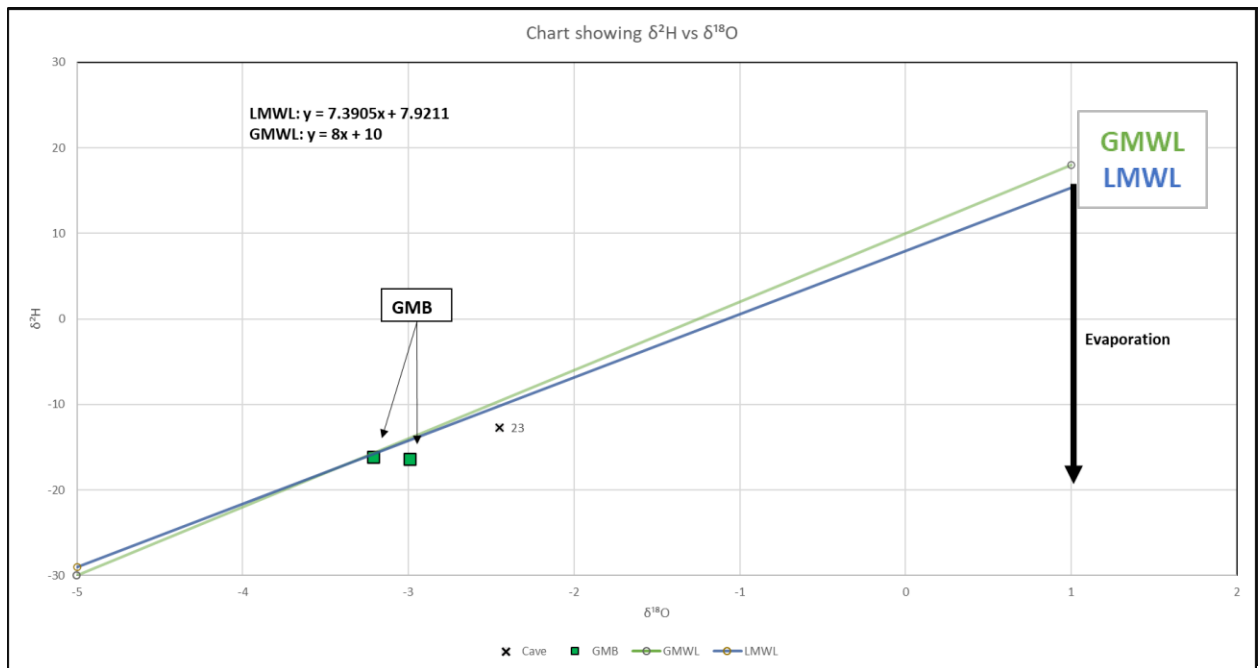


Figure 5.9: Graph showing the cave data.

5.1.9 Discussion of isotope data:

[Figure 5.10](#) displays all the isotope data. All the samples can be placed in three groups based on where they plot on the Isotope chart. The three groups are Group 1, Group 2 and Group 3.

Group 1 has the lowest $\delta^2\text{H}$ & $\delta^{18}\text{O}$ values and are predominantly groundwater data that plots on or slightly above or below the LMWL.

Group 2 includes the GMB, this group does not consist of just one source of water, but rather a mixture of surface and groundwater samples. This group's data all plot slightly below the LMWL indicating some form of heavy isotope enrichment has taken place, like evaporation.

The final group is Group 3, group 3 plots the furthest below the LMWL and although it's a mixture of different sources it's predominantly surface water samples such as streams and dams. These samples have experienced the heaviest isotope enrichment through processes like evaporation.

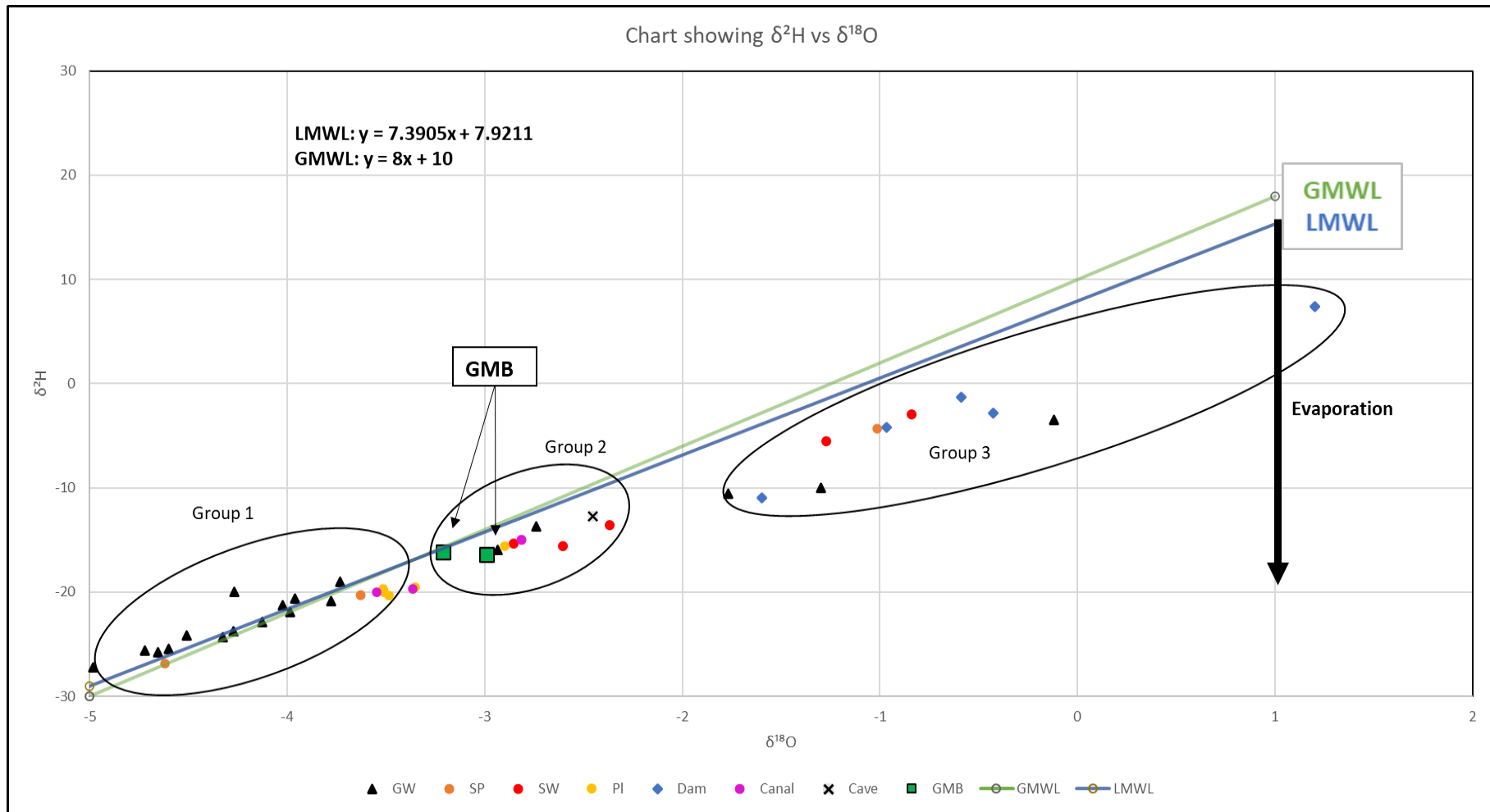


Figure 5. 10: Graph showing all data plots

By plotting the Deuterium isotopes of the samples as in [Figure 5.11](#), new correlations could be seen. There is a trend amongst the samples that the groundwater samples plot below the two GMB samples. The surface water samples plot above the GMB samples. The two GMB sample plots at -16.1 and -16.4, thus the samples below 16 are mainly groundwater samples, and above 16 there are mainly surface water samples. The GMB samples have experienced some form of evaporation or isotope enrichment compared to the samples whose origin is groundwater.

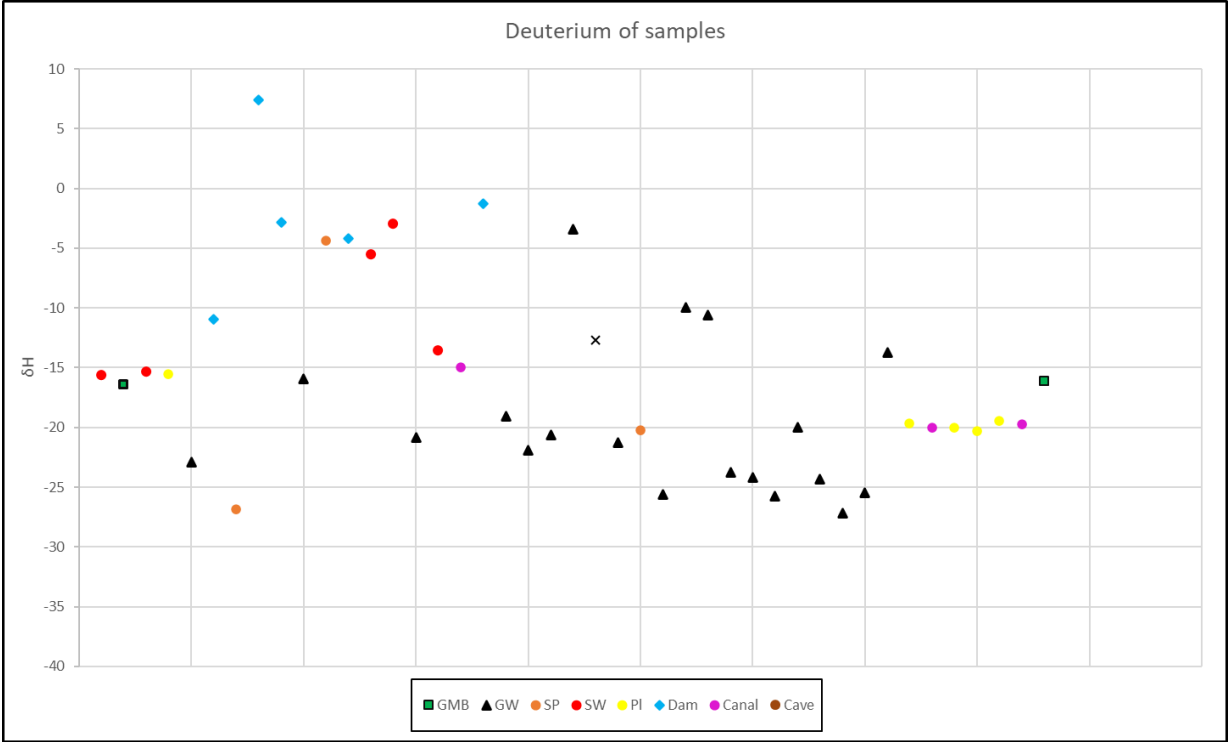


Figure 5. 11: Deuterium of samples.

[Figure 5.10](#) and [Figure 5.11](#) both indicate that the GMB has a connection to the samples that originate from dewatered mine water or mix with mine water. These samples include canal, pipeline, cave, some groundwater and some surface water samples. This is indicative that the origin of the GMB’s water and the water pumped out of the mines are connected.

The stable isotope results yielded three distinct groups based on the δ Deuterium and δ Oxygen -18 results as indicated by [Figure 5.10](#). The first group is dominated by groundwater samples and is samples that show no sign of isotope enrichment, meaning that it is just recharged water and hasn’t experienced a process causing isotope enrichment. The second group is the group that has both GMB samples in it. This group shows some signs of isotope enrichment in comparison to the first group. The second group is a mixture of stream water, groundwater,

pipeline, cave water, and canal water samples. All the samples that fall within group two have experienced some form of isotope enrichment but still less enrichment than group three. The samples in the third group are predominantly samples with a lot of evaporation exposure, such as dam and stream water samples.

In [Figure 5.12](#) below, the three identified stable isotope groups are displayed and their locations on the map. Some of the samples from group 2 are located within a different dolomitic compartment than the GMB but the isotopic compositions display a correlation. This is indicative that the dykes creating the dolomitic compartments does not restrict groundwater flow within only compartments. There is thus some connection between the compartments causing groundwater flow the connection could be the one proposed by (Winde & Erasmus, 2011a).

All the samples that show correlation with the GMB are samples that are directly linked to mine dewatering, such as canal, pipeline and decanting surface waters. The groundwater samples that correlate with the GMB samples are spatially different from the other groundwater samples. They are located south of the WFS, where all the others are north of the stream. The cave sample is located near the WFS, indicating that there is a hydrogeological connection between the dolomitic cave and surface water near it.

The Samples with correlation are samples that originated from dolomites to the south of the WFS, the pipeline and canal water samples are dewatered dolomitic mine water. The samples to the north of the WFS from within the dolomites does not show a distinct correlation. Aligning with the idea presented by (Winde & Erasmus, 2011a) that there are sub compartments. The sub-compartments are caused by the different degree of karstification in the chert-rich and chert-poor dolomites. The isotopic data reveals that the area is hydrogeologically very complex. The large dykes creating the compartments are inferred to not be impermeable based on the data, but indicates of potential sub-compartments within the larger compartments that are hydrogeologically linked with sub compartments in adjacent larger compartments.

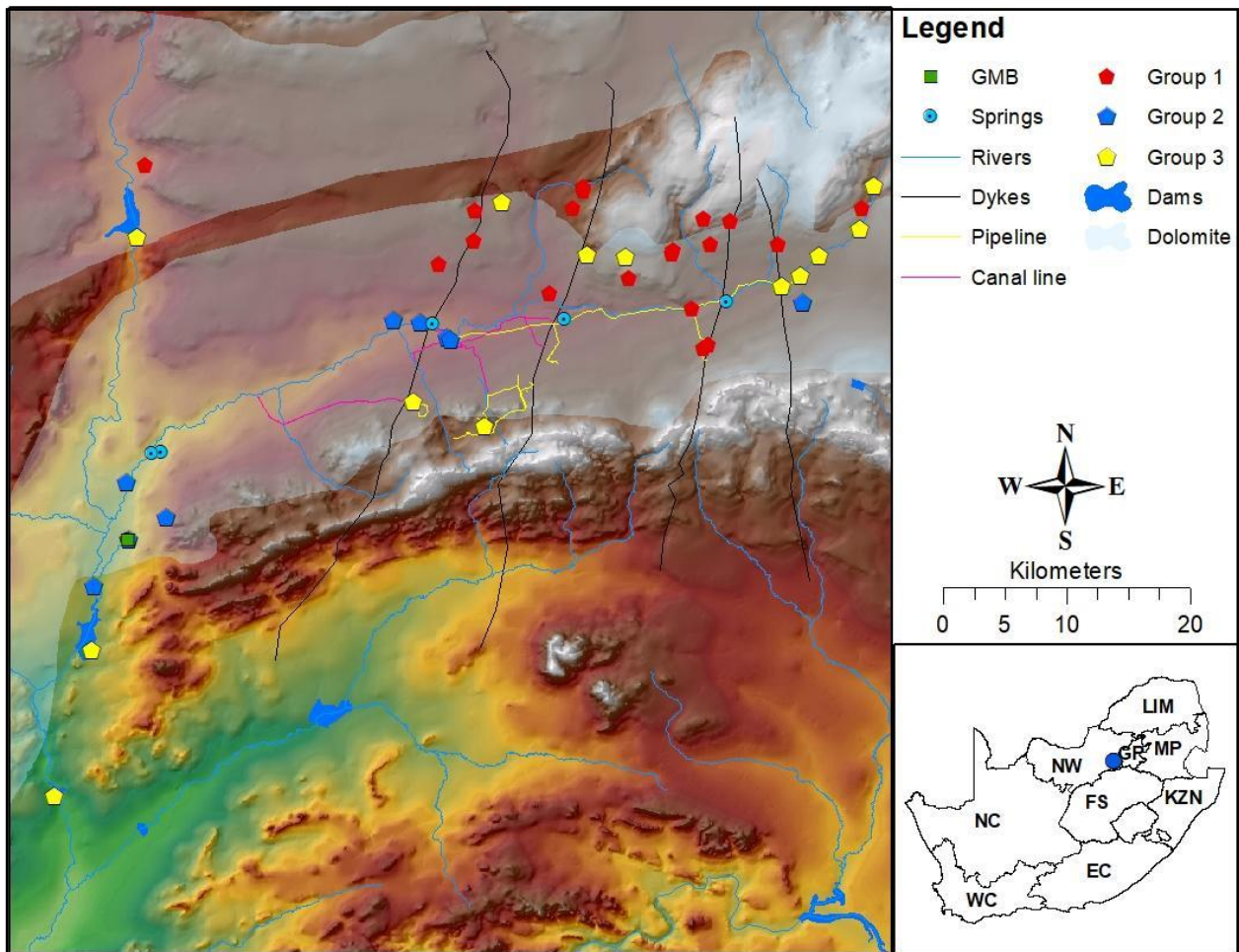


Figure 5. 12: Map indicating stable isotope groups.

Another possibility could be by taking into consideration that Group 1 samples will correlate with the GMB if they experience some form of isotope enrichment such as evaporation, which takes place at the GMB. It is possible that the source of the GMB is not just the samples that show correlation namely Group 2, but the samples in Group 1 as well or a mixture of Group 1 with Group 2. Considering the above mentioned it's very difficult to precisely identify the source of the Gerhard Minnebron to a specific location. The reason is that based on the data and studies by Frank Winde the area is hydrogeologically very complex.

The most probable explanation would be that the dolomites are all interconnected, as speculated in previous studies by (Winde & Erasmus, 2011a). The interconnection is however very complex leading to different water samples from within the same compartments also justifying the idea of

sub-compartments, connected through the previous thought aquifer boundaries. The reason for this would be because it is common knowledge that interconnections of dolomites kilometres apart have been found and are still being discovered.

The second explanation could also be possible but would be less possible because the GMB would display isotopically as a mixture between the sources from mine dewatering and the other groundwater samples. But there is still a possibility, as the aquifers and interactions are very complex, to determine the interconnections would be very difficult and would require very large amounts of research and data.

5.2 Chemical Data

The chemical samples were collected by Naziha Mokadem, as indicated by [Table 2](#). The sample locations of the chemical data are the same as the isotope samples collected by Naziha Mokadem in [Table 2](#). The samples for chemical analysis were collected in 500ml water bottles. The pH of the samples was measured with a pH meter 510. A Metrohm ion chromatography, 761 compact IC model was used to analyse the anions components (Cl^- , SO_4^{2-} , Alk , NO_3^-). The cation components (Na^+ , K^+ , Ca^{2+} , Mg^{2+}) were analysed on an Agilent 7500CE ICP-MS. All the samples were filtered before being analysed at the Centre for Water Sciences and Management of the North–West University of Potchefstroom (Mokadem *et al.* 2021:5). The results of the samples are displayed in [Table 3](#)

Table 3 Chemical and isotopic concentrations used for data analyst

ID	Identification	name	Type	Y	X	pH	EC um/cm	HCO3	Na	Mg	Ca	Cl	NO ₃	SO ₄	K	O18	H2	D
1	Mooi River	SW	MR01	-26.515	27.125	7.6	0.78	255	27.1	42.8	71.6	38.1	4.1	138.7	1.8	-2.6	-15.7	5.2
2	Grehard Minnebron	SP	GM01	-26.479	27.152	7.1	0.84	225	30.5	43.4	74.0	49.3	10.7	182.2	1.6	-3.0	-16.4	7.5
3	WFS3	SW	WFS3	-26.316	27.383	7.7	0.86	210	52.8	38.7	64.3	47.4	7.1	239.9	4.8	-2.9	-15.4	7.5
4	pipeline	PL	WPL01	-26.327	27.404	7.2	0.83	205	54.4	33.1	60.0	43.8	8.5	214.3	5.0	-2.9	-15.6	7.6
5	BH1	GW	BH1	-26.294	27.485	6.0	0.25	55	8.4	11.0	13.5	10.9	63.4	8.7	2.7	-4.1	-22.9	10.1
6	Klerkskraal Dam	DAM	KKD01	-26.253	27.159	7.6	0.37	225	3.4	29.5	22.9	2.9	0.1	3.5	1.3	-1.6	-11.0	1.8
7	Bovenste eye	SP	BE01	-26.198	27.165	7.1	0.44	265	3.1	26.3	44.6	2.7	6.1	3.5	1.3	-4.6	-26.9	10.0
8	Boskop Dam	DAM	BKD01	-26.562	27.123	7.4	0.80	300	27.3	49.1	53.5	45.6	0.6	126.8	9.6	1.2	7.4	-2.2
9	Potchfestroom Dam	DAM	Pot 01	-26.672	27.094	7.7	0.72	230	29.0	45.7	45.6	43.5	0.3	142.1	2.0	-0.4	-2.9	0.5
10	JW01	GW	JW01	-26.462	27.182	7.2	0.80	270	29.1	41.6	69.3	43.1	8.9	154.5	1.6	-2.9	-16.0	7.5
11	Gembokfontein Spring	SP	GBF01	-26.289	27.669	7.9	1.10	210	99.7	25.4	92.2	52.6	3.6	299.7	11.6	-1.0	-4.4	3.7
12	Donaldson Dam	DAM	DD01	-26.281	27.684	8.3	1.10	223	98.6	25.2	92.2	53.0	2.1	298.2	11.5	-1.0	-4.2	3.6
13	WFS4	SW	WFS4	-26.266	27.699	7.4	0.78	245	100.8	25.9	93.3	65.8	12.0	381.7	10.4	-1.3	-5.5	4.6
14	WFS5	SW	WFS5	-26.246	27.731	7.4	1.13	265	72.7	11.7	50.9	36.6	12.4	76.6	11.8	-0.8	-3.0	3.7
15	CZ01	GW	CZ01	-26.230	27.733	6.7	0.47	120	11.9	23.7	35.2	21.0	13.4	117.5	0.8	-3.8	-20.8	9.4
16	WFS2	SW	WFS2	-26.436	27.150	7.6	0.84	285	37.8	40.5	73.7	43.3	4.4	169.7	2.4	-2.4	-13.6	5.3
17	Canal Mine	CANAL	CAN 01	-26.329	27.407	7.9	0.87	285	44.8	46.2	52.6	52.2	1.2	293.6	2.9	-2.8	-15.0	7.5

18	Luipaardsvlei Dam	DAM	LPV01	-26.214	27.742	7.5	0.84	340	70.7	10.5	47.8	43.1	2.5	92.0	12.5	-0.6	-1.3	3.4
19	GC01	GW	GC01	-26.272	27.397	7.3	0.76	415	5.4	45.9	80.8	8.4	47.6	5.0	0.9	-3.7	-19.0	10.8
20	ABA01	GW	ABA01	-26.255	27.425	7.4	0.51	280	3.4	28.9	50.7	5.0	26.0	2.2	2.1	-4.0	-21.9	10.0
21	CS01	GW	CS01	-26.232	27.427	6.4	0.19	85	15.2	4.7	9.1	16.1	24.0	10.8	2.5	-4.0	-20.6	11.1
22	DP02	GW	DP02	-26.226	27.447	8.6	0.31	110	18.2	8.7	17.1	47.7	35.9	4.0	8.2	-0.1	-3.4	-2.5
23	CAVE1	CV	CAVE1	-26.315	27.361	7.1	0.94	195	62.9	39.2	62.3	76.7	7.7	243.6	5.8	-2.5	-12.7	6.9
24	DF01	GW	DF01	-26.217	27.512	5.9	0.12	40	9.8	3.7	3.4	7.9	20.7	1.3	2.5	-4.0	-21.3	10.9
25	ROD01	SP	ROD01	-26.215	27.512	5.4	0.10	23	3.8	5.9	3.0	2.6	3.1	2.4	0.8	-3.6	-20.3	8.8
26	ROD02	GW	ROD02	-26.231	27.504	6.1	0.08	45	2.6	4.9	2.3	1.7	3.0	1.4	0.4	-4.7	-25.6	12.2
27	EF02	GW	EF02	-26.265	27.515	6.7	0.11	65	5.8	5.1	5.9	1.4	1.3	1.7	0.6	-1.3	-10.0	0.4
28	BB01	GW	BB01	-26.267	27.545	7.1	0.04	55	2.0	1.0	2.3	1.1	1.1	0.8	0.7	-1.8	-10.6	3.6
29	VK02	GW	VK02	-26.262	27.584	5.8	0.06	13	0.9	2.5	3.9	0.5	1.6	1.0	0.3	-4.3	-23.8	10.4
30	BB02	GW	BB02	-26.283	27.548	6.2	0.19	50	5.3	8.8	10.4	15.0	26.3	2.2	1.7	-4.5	-24.2	11.9
31	VK04	GW	VK04	-26.264	27.583	6.5	0.07	43	1.0	2.7	5.9	0.7	0.3	1.0	0.4	-4.7	-25.7	11.5
32	GR01	GW	GR01	-26.238	27.607	5.9	0.05	23	1.7	1.3	0.8	2.3	8.7	0.4	0.3	-4.3	-20.0	14.1
33	TA02	GW	TA02	-26.258	27.613	6.3	0.06	23	1.1	2.6	3.2	0.6	2.1	0.6	0.6	-4.3	-24.3	10.3
34	GR03	GW	GR03	-26.240	27.628	6.3	0.04	20	2.4	1.5	1.4	0.9	2.2	1.2	0.4	-5.0	-27.2	12.7
35	PV01	GW	PV01	-26.257	27.666	6.8	0.19	108	1.3	10.5	14.5	1.2	5.5	1.4	0.3	-4.6	-25.5	11.3
36	GPO1	GW	GP01	-26.301	27.685	7.1	0.82	190	46.1	31.9	71.4	39.4	22.0	219.6	3.7	-2.7	-13.7	8.2
	Pipeline Celemanzi after treatment	PL	AJS1	-26.305	27.599											-3.5	-19.7	

The chemical data is displayed in [Table 3](#) and represented in a piper diagram ([Figure 5.13](#)) to give an overview of the samples ([Figure 5.2](#)). The samples are placed in groups based on their source when sampled and then the GMB for reference. The groups are made up of the same samples as the ones specified in [Table 2](#) taken by Naziha Mokadem.

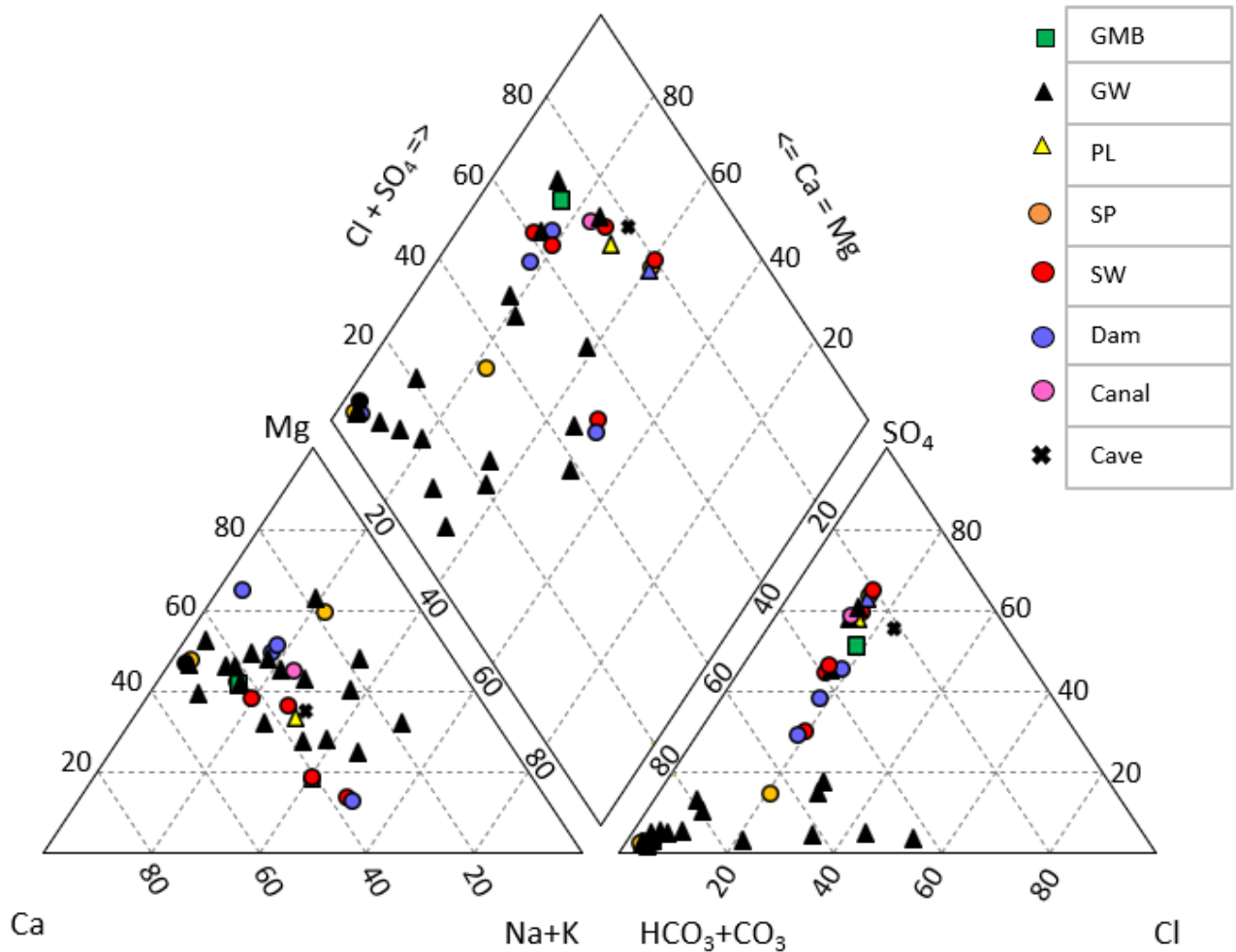


Figure 5. 13: Piper plot of data.

5.2.1 Groundwater:

Most of the groundwater samples plot with high anions concentration of CO_3^{2-} and HCO_3^- placing them in the Bicarbonate dominant type, with a few samples displaying higher Cl concentrations. Three samples displayed elevated concentrations of SO_4 . The cation concentrations of the samples fall within the non-dominant group with equal concentrations of $\text{Na}^+\text{+K}^+$, Ca^{2+} , Mg^{2+} . A couple of the samples were higher in Ca^{2+} & Mg^{2+} and resulted in a few Mg^{2+} and Ca^{2+} dominant samples. Overall the sample concentrations were dominantly Magnesium Bicarbonate type which indicates that the groundwater samples are representative of dolomite aquifers. Most of the samples plot where freshly recharged water and dolomitic waters plots with some samples

displaying mixing. The samples with high concentrations of SO_4 are all located to the south of the WFS, and the samples with low SO_4 concentrations are all to the north of the WFS.

5.2.2 Spring water:

The spring water samples plot very varying, two samples including the Bovenste eye sample plots with the anions in the bicarbonate dominant type, the GMB and Gemsbokfontein sample plots in the sulphate dominant type. The cations are all mainly in the non-dominant type. Overall, the GMB and Gemsbokfontein samples plot with high concentrations of Cl^- and SO_4^{2-} and lower concentrations of CO_3^{2-} and HCO_3^- when compared to the other spring samples and groundwater.

5.2.3 Surface water:

The surface water displays moderate to equal concentrations of the Mg^{2+} , Ca^{2+} , and $\text{Na}^+\text{+K}^+$ cations with surface water displaying no dominant cations concentrations. The anions display very high concentrations of SO_4^{2-} in all the samples and moderate amounts of $\text{HCO}_3^- + \text{CO}_3^{2-}$ and lower concentrations of Cl^- . Overall, the surface water samples plot more towards the $\text{Cl}^- + \text{SO}_4^{2-}$ and $\text{Mg}^{2+} + \text{Ca}^{2+}$ end.

5.2.4 Pipeline:

The one pipeline sample there is displays relative equal concentrations of the cations ranging from between 20 and 40 percent for each of the three cation groups. In the anions group, the sample displays high concentrations of SO_4^{2-} when compared to the other anions and medium amounts of $\text{HCO}_3^- + \text{CO}_3^{2-}$. Overall, the pipeline sample plots more towards the $\text{Cl}^- + \text{SO}_4^{2-}$ and $\text{Mg}^{2+} + \text{Ca}^{2+}$ end because of the increased concentration of SO_4^{2-} . The pipeline sample indicates that the water within the pipeline is of mine origin with the elevated SO_4^{2-} concentrations.

5.2.5 Dam water:

The Dam water samples display the same percentage of high Mg^{2+} and low percentages of Ca^{2+} , but varying amounts of $\text{Na}^+\text{+K}^+$ in the Cation group. The Anion group displays the percentages

SO_4^{2-} and low percentages of Cl^- , but varying amounts of $\text{HCO}_3^- + \text{CO}_3^{2-}$. Overall, the dam sample tends to display towards the $\text{Cl}^- + \text{SO}_4^{2-}$ and $\text{Mg}^{2+} + \text{Ca}^{2+}$ except for one sample, Luipaardsvlei dam (ID:18). This sample displays overall equal percentages of all measured constituents. This sample as indicated by [Figure 5.2](#) is located upstream and further away from any active or old mining activities than the other dam water samples.

5.2.6 Canal water:

The canal water samples display higher concentrations of Mg^{2+} and SO_4^{2-} than the other constituents. Thus, plots in the $\text{Cl}^- + \text{SO}_4^{2-}$ and $\text{Mg}^{2+} + \text{Ca}^{2+}$ end of the overall data this is caused by the elevated Mg^{2+} and SO_4^{2-} . The elevated SO_4^{2-} is also an indication that the canal water is mixed or contaminated with mine water.

5.2.7 Cave water:

The cave sample has very similar concentrations to the pipeline sample and similar trends to the GMB. The elevated SO_4^{2-} indicates that there is some influence or mixing from mine water within the cave water system. The high percentages of Mg^{2+} and Ca^{2+} is also an indication that the cave water was sampled within the Dolomites.

5.2.8 Discussion of data

Samples that display high amounts of SO_4^{2-} is inferred to be linked with mine water and possible mixing. Samples with high amounts of Mg^{2+} and Ca^{2+} can also be indicative of dolomitic contact or origin. The samples from the GMB display higher concentrations of SO_4^{2-} than some of the other samples which would explain the lower $\text{HCO}_3^- + \text{CO}_3^{2-}$ percentages than the other spring samples. The High Mg^{2+} and Ca^{2+} and relatively high $\text{HCO}_3^- + \text{CO}_3^{2-}$ are however still indicative that the GMB's water originates or passes through dolomitic aquifers.

Even though the isotopes and the chemistry don't display the same constituents, the same trend can be seen as displayed by [Figure 5.14](#). The samples from group 2 of the isotopic groups are also grouped together on the piper diagram. The high SO_4^{2-} in the GMB is also indicating that there is a link between the GMB, pipeline water, cave water, canal water, surface water and groundwater samples south of the WFS. The one thing all the above samples have in common is that mine dewatering affects them. The canal water and pipeline waters are directly linked to

dewatered mine water and the surface water samples are also connected to the dewatered mine water through the pipelines and canals. The fact that the cave water is also impacted by SO_4^{2-} is inferring that the mine water connects with the dolomitic aquifers and the surface water originating from the dewatered dolomites this causes the elevated SO_4^{2-} concentrations in the GMB.

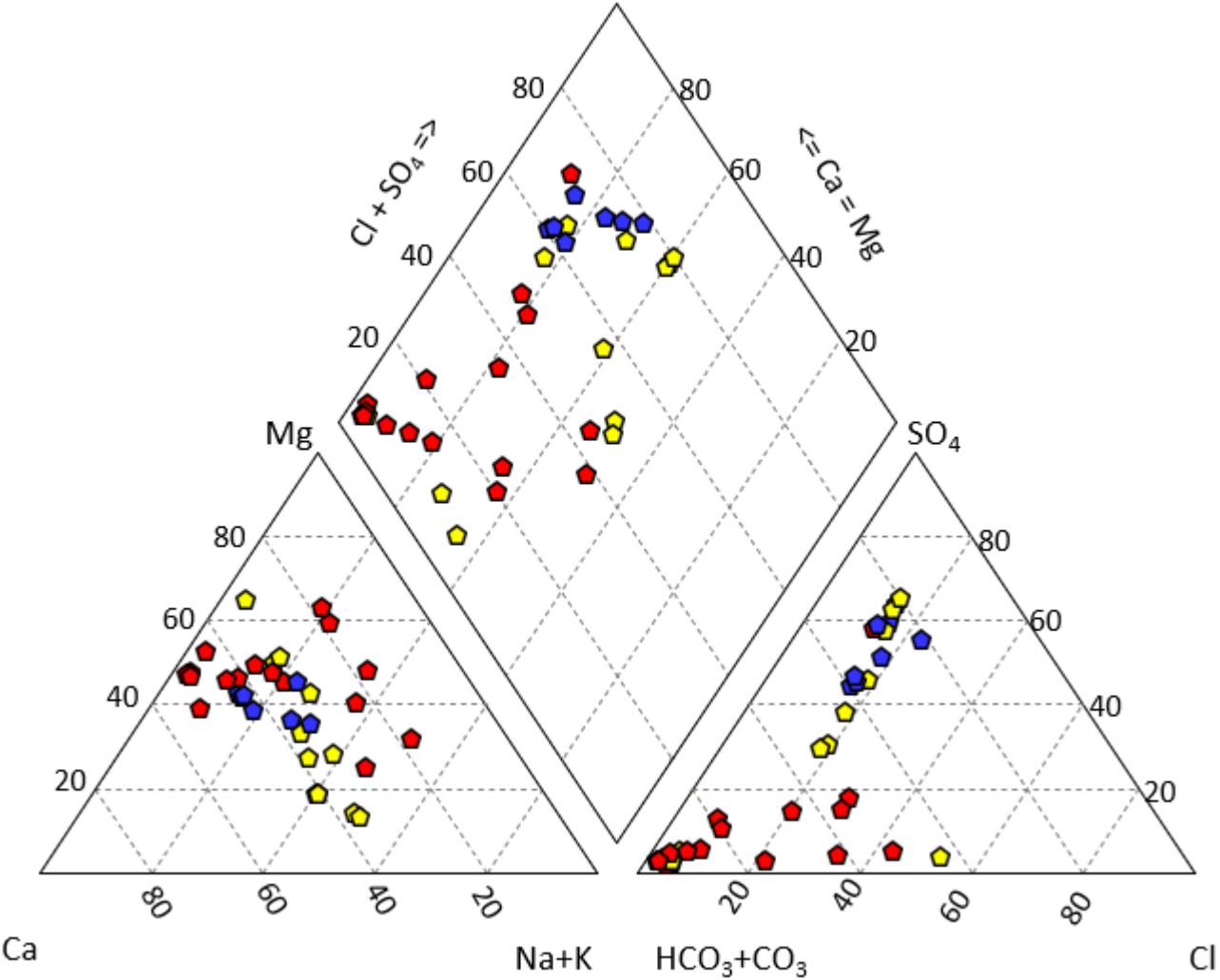


Figure 5. 14: Piper plot of data displayed as isotope groups.

The composite bar chart in [Figure 5.15](#) indicates that the chemical signature of the GMB is displayed in samples collected from pipeline water, cave water, canal water, surface water and groundwater samples south of the WFS. All the aforementioned samples that show correlation with the GMB are displayed in blue cells in [Table 2](#). These samples namely: **MR01, GM01, WFS3, WPL01, JW01, WFS2, CAN 01, CAVE1** and **GP01** are all displaying the same signatures in the isotope and chemistry results, indicating they are all from the same aquifer or interconnected aquifers. This further indicates that the GMB’s aquifer is recharged with water from varying sources and is a mix from all of the collected sources, these sources are all however influenced

or connected with the mine dewatering, and indicative that the GMB's aquifer is connected to a sub-compartment within the dolomites.

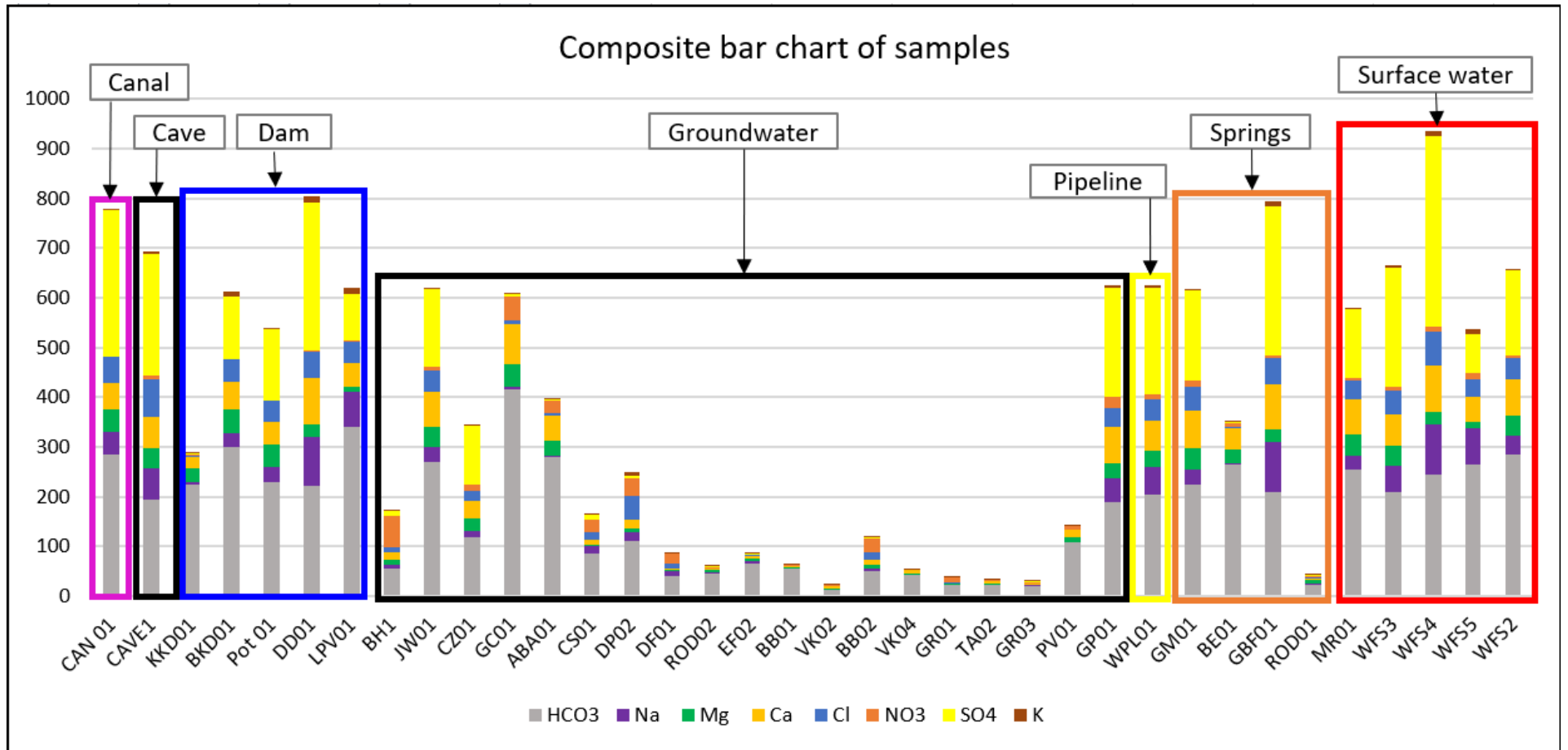


Figure 5. 15: Composite bar chart of data

CHAPTER 6: CONCLUSION & RECOMMENDATIONS

6.1 Conclusion

The focus point of this study was the Gerhard Minnebron, a critical and irreplaceable water resource of Potchefstroom and surrounding areas. The Gerhard Minnebron is a very important and large source of water to the Potchefstroom and surrounding agricultural community. In an age where freshwater is becoming a dwindling resource the value of the Gerhard Minnebron is unmeasurable.

This study aimed to determine the origins of Gerhard Minnebron's water. Stable isotopes, namely the Deuterium(^2H) and Oxygen-18(^{18}O) were used as the tools specified in **Chapter 3**. The stable isotopes were utilised as tracers with water samples being collected at various locations of interest from varying sources. The water samples were analysed with a spectrometer to give the isotope ratios that were used to formulate the results.

Utilizing stable isotopes as tracers to determine the source of the GMB was successful. They revealed that the water that flows out of the GMB spring originates higher up in the WFS and is found within the dolomites to the North-East, specifically dolomites south of the WFS. This proves the notion that was expected that the dolomites are the only geological formations near the GMB whose aquifers could produce such a high yielding spring. The isotopes revealed evidence that indicates that the water of the GMB is a mixture of water from all over the dolomites. If that is the case no specific location could be identified as the source of the Gerhard Minnebron, the source of the GMB is rather a mixture of groundwater and surface water found within the Dolomites especially dolomites to the south of the WFS.

The chemical analysis also supports the above identified trends that the water from within the GMB is a mixture of water from various sources throughout the WFS. The elevated concentrations of Mg^{2+} , Ca^{2+} and $\text{HCO}_3^- + \text{CO}_3^{2-}$ also prove the notion that the water originates within the Chuniespoort dolomitic aquifers or pass through them at some point. The elevated SO_4^{2-} concentrations prove that there is a definite link between the GMB and Mine dewatering. This link is also proof that the GMB's aquifer is located or connected to the Dolomitic compartments higher upstream of the GMB in the WFS specifically dolomites where mining occurs.

In conclusion, the Methodology developed in Chapter 4 was thus successful in reaching the desired analysis and results. The isotope and chemical data revealed that the aquifer of the GMB

is and confined aquifer with various links to the surface and surface waters. The main subsurface flow paths were identified to follow the dolomites no more accurate conclusion could be identified by the isotopes or chemistry. The stable isotopes Deuterium (2H) Oxygen -18 (^{18}H), and the chemistry data provided sufficient evidence to identify the source of the Gerhard Minnebron's aquifer. The data revealed that the source of the aquifer is the dolomites to the North-East of the GMB with inflows coming from canal, pipeline, surface water's, rainwater and groundwater from adjacent aquifers the results revealed that there is sub-compartments present within the dolomites, and that there is definite connections between the compartments as inferred by Winde & Erasmus, (2011a).

Protecting the source or dolomitic aquifers in the WFS is not impossible, but it's rather a case of minimizing the damage that has already been done to the aquifers and limiting future damage and degradation of the dolomitic aquifers. This in return would minimize the contamination and degradation of the GMB's water quality.

A valuable lesson can be learnt from the GMB and surrounding areas. What could have been an unmeasurably valuable resource for the surrounding area and province. Is now a resource that cannot be accessed at its full potential due to previous negligence and lack of knowledge resulting in contamination of water resources that impact other resources as well. Gathering more information about the GMB and the dolomites is very important and can help aid in the protection and prevention of the future and further deterioration of this valuable resource.

6.2 Recommendations

From the research done in the study, the following recommendations can be provided:

- Stable isotopes are a valuable tool, but on their own stable isotopes cannot provide a complete and accurate report on the origin of a source or subsurface flow paths. Additional tracers such as CFC's, more isotopes, chemical tracers, and physical tracers like dyes should be used together for results.
- The GMB and WFS area with the dolomites is a very complex hydrogeological area. More data on hydrogeological studies and research should be done to provide more information about the area and better understand the complexity of the area. Information regarding surface and groundwater interaction, as well as subsurface aquifer interaction, would be very important.

- More samples overall would help aid in any research, and more samples from further away and more sources would improve the research and data. Sampling data on a monthly or annual basis would also improve the data and results of data giving a clearer result and more in detail data.

REFERENCE LIST

Abiye, T. 2013. Surface water and groundwater interaction in the upper Crocodile river basin. In: T Abiye (editor). *The use of Isotope Hydrology to characterize and assess Water Resources in southern Africa*, 141-164. Report TT 570/13, Water Research Commission, Pretoria.

Balasubramanian, A. & Nagaraju, D. 2015. *The Hydrologic Cycle*. Mysore: University of Mysore.

Barnard, S., Venter, A. & van Ginkel, C.E. 2013. Overview of the confluences of mining-related pollution on the water quality of the Mooi River system's reservoirs, using basic statistical analyses and self-organised mapping. *WaterSA* 39(5): 655-662.

Blasch, K.W., Bryson J.R. 2007. Distinguishing sources of groundwater recharge by using d2H and d18O. *Groundwater* 45(3):294–308.

Bredenkamp, D., Vogel, J., Wiegmans, F., Xu, Y. & Jansen van Rensburg, H. 2007. Use of natural isotopes and groundwater quality for improved estimation of recharge and flow in dolomitic aquifers. Pretoria, South Africa: *Water Research Commission*.

Brink, M.C., Waanders, F.B., Bisschoff, A.A. & Gay, N.C. 2000 The Foch Thrust-Potchefstroom Fault structural system, Vredefort, South Africa: a model for impact-related tectonic movement over a pre-existing barrier. *Journal of African Earth Sciences* 30(1): 99 – 117.

Buttle, J.M. 1998. Fundamentals of Small Catchment Hydrology. In: Kendall, C., McDonnell, J., ed. *Isotope tracers in catchment hydrology*. Amsterdam: Elsevier. pp. 1 – 49.

Carlson-Newberry, S.J. & Costello, R.B. eds. 1997. *Emerging Technologies for Nutrition Research*. Washington DC: National Academy Press.

Coetzee, H. & Ntsume G. 2004. Identification of contaminants and contaminated sites. In: Coetzee, H (compiler): *An assessment of sources, pathways, mechanisms and risks of current and potential future pollution of water and sediments in gold-mining areas of the Wonderfontein spruit catchment*. WRC Report No 1214/1/06, Pp. 54-67.

Coplen, T.B., Herczeg, A.L. & Barnes, C. 2000. In: Cook, P.G. & Herczeg, A.L., eds. *Environmental tracers in subsurface hydrology*. New York, NY: Springer Science+Business Media. Pp. 79 – 110.

Craig, H. 1961. Isotopic Variations in Meteoric Waters. *Science*, 133(3465): 1702-1703.

Dennis, R & Dennis, I. 2012. Climate change vulnerability index for South African aquifers. *Water SA*, 38(3):417-426.

Department of Water Affairs and Forestry. 1998. Mooi River Catchment Study: Phase 1: Situation Analysis. Pulles Howard & De Lange Incorporated.

Department of Water Affairs and Forestry. 1995. Dolomitic Groundwater Resources of the Republic of South Africa, Report Number GH 3857. D.B. Bredenkamp.

Easton, Z.M. & Bock, E. 2015. Hydrology Basics and the Hydrologic Cycle. Publication BSE-191P. Petersburg: Virginia Tech.

Encyclopaedia Britannica. 2020. Water cycle. In: Encyclopædia Britannica. <https://www.britannica.com/science/water-cycle> Date of access: 1 July 2020.

Gat, J.R. 1970. Environmental isotope balance of Lake Tiberias. *Isotope Hydrology* 255: 151–162.

Gat, J.R. 2010. Isotope Hydrology: A Study of the Water Cycle. *Series on Environmental Science and Management*, 6.

Gat, J.R. 1996. Oxygen and Hydrogen Isotopes in the Hydrological Cycle. *Earth Planet. Sci*, 24:225-262.

Gilli, É. & Fandel, C. 2015. Karstology: karsts, caves and springs; elements of fundamental and applied karstology. Crc Press: Boca Raton.

Gonfiantini, R. Fröhlich, K. Araguás – Araguás ,L. & Rozanski, K. 1998. Isotopes in Groundwater Hydrology In: Kendall, C., McDonnell, J., ed. Isotope tracers in catchment hydrology. Amsterdam: Elsevier. pp. 203 – 238.

Harris, C & Diamond, R. 2013. Oxygen and Hydrogen isotopes records of Cape Town rainfall and its application to recharge studies of Table Mountain groundwater. In: T Abiye (editor). *The use of Isotope Hydrology to characterize and assess Water Resources in southern Africa*, 24-35. Report TT 570/13, Water Research Commission, Pretoria.

IGRAC (International Groundwater Resource Assessment Centre). 2021. *What is Groundwater?* <https://www.un-igrac.org/what-groundwater> Date of access: 21Jun 2021.

Ingraham, N.L. 1998. In: Kendall, C. & McDonnell, J, eds. *Isotope tracers in catchment hydrology*. Amsterdam: Elsevier. pp. 87 – 118.

Kendall, C. & Caldwell, A.C. 1998b. Fundamentals of Isotope Geochemistry In: Kendall, C., McDonnell, J., ed. *Isotope tracers in catchment hydrology*. Amsterdam: Elsevier. pp. 51 – 86.

Kinchaid, T.R. 2003. Groundwater Tracing in the Woodville Karst Plain - Part I: *Journal of the Global Underwater Explorers*, 4(4): 31-37.

Kumar, M., Rao, M.S., Kumar, B., & Ramanathan, A. 2011. Identification of aquifer-recharge zones and sources in an urban development area (Delhi, India), by correlating isotopic tracers with hydrological features. *Hydrogeology Journal*. 19(2):463–474.

Le Roux, E. 2005. Improving the quality of raw water supply to Potchefstroom. Potchefstroom: North-West University. (Thesis- MSc).
[ps://repository.nwu.ac.za/bitstream/handle/10394/790/leroux_ebenhaezer.pdf?sequence=1&isAllowed=y](https://repository.nwu.ac.za/bitstream/handle/10394/790/leroux_ebenhaezer.pdf?sequence=1&isAllowed=y) date of access: 26 February 2020.

Leibundgut, C. & Seibert, J. 2011. Tracer Hydrology. *Treatise on Water Science*. 2:215–236.

Leibundgut, C., Maloszewski, P. & Külls, C. 2009. Tracers in Hydrology. West Sussex, UK:Wiley.

Levin, M. & Verhagen, B. Th. 2013. Application of Isotope techniques to trace pollution in monitoring boreholes of waste disposal sites. In: T Abiye (editor). *The use of Isotope Hydrology to characterize and assess Water Resources in southern Africa*, 24-35. Report TT 570/13, Water Research Commission, Pretoria.

Maduabuchi, C., Faye, S. & Maloszewski, P. 2006: Isotope evidence of palaeorecharge and palaeoclimate in the deep confined aquifers of the Chad Basin, NE Nigeria. *Science of the Total Environment*, 370(2): 467–479.

Mekiso F.A., Ochieng G.M. & Snyman J. 2015. Isotope hydrology in the middle Mohlalabetsi catchment, South Africa. *International Journal of Engineering Research and Development* 11(01):1–7.

Merlivat, L. 1918. Molecular diffusivities of H₂¹⁶O, HD¹⁶O and H₂¹⁸O in gases. *Journal of Chemical Physics*, 69(6):2864-2871.

Mokadem, N. Dennis, R. & Dennis, I. 2021. Hydrochemical and stable isotope data of water in karst aquifers during normal flow in South Africa. *Environment Earth Science*, 80, 519. <https://doi.org/10.1007/s12665-021-09845-7>.

Nayak, P.C., Vijaya Kumar, S.V., Rao, P.R.S., & Vijay, T. 2016. Recharge source identification using isotope analysis and groundwater flow modelling for Puri city in India. *Applied Water Science*. 7(7):3583–3598.

Ngcobo, T.A. 2006. The risks associated with mines in dolomitic compartments. *The Journal of The South African Institute of Mining and Metallurgy*. 106(1):251-264.

Palmer, A.N. 2010. Understanding the hydrology of karst. *Geologia Croatica*. 62(2):143-148.

Picarro. 2021. Isotopic Water Analysis Systems Brochure https://www.picarro.com/support/library/documents/isotopic_water_analysis_systems_brochure. Date of access: 12 August 2021.

Rural & Urban Exploration. 2016. Gerhard Minnebron. *Ruralexploration.co.za*. <https://ruralexploration.co.za/Gerhard%20Minnebron.html>. Date of access: 16 Sep 2020.

Schrader, A., Winde, F. & Erasmus, E. 2014a. Using impacts of deep-level mining to research karst hydrology —a Darcy-based approach to predict the future of dried-up dolomitic springs in the Far West Rand goldfield (South Africa). Part 1: a conceptual model of recharge and inter-compartmental flow. *Environment Earth Science*, 72: 3549–3565.

Sharma, B., Singh, R., Singh, P., Uniyal, D.P., Dobhal, R. 2015. Water Resource Management through Isotope Technology in Changing Climate. *American Journal of Water Resources*, 3(3):86-91.

Stevanovic, Z. 2015. Karst Environment and Phenomena. In: Stevanovic, Z., eds. *Karst Aquifers - Characterization and Engineering*. London: Springer. pp. 19-44ep 2020.

Swart, C.J.U., James, A.R., Kleywegt, R.J., Stoch, E.J. 2003a. The future of the dolomitic springs after mine closure on the Far West Rand, Gauteng, RSA. *Environmental Geology*, 44:751-770.

Swart, C.J.U., Stoch, E.J., Van Jaarsveld, C.F., Brink, A.B.A. 2003b. The Lower Wonderfonteinspruit: an expose. *Environmental Geology*, 43:635-653.

Van Veelen, M. 2009. Wonderfonteinspruit Catchment Area: Remediation Action Plan. ILISO Consulting (Pty) Ltd.

Vogt, H.J. 1976. *Isotopentrennung bei der Verdunstung von Wasser*. University of Heidelberg. Institute of Environmental Physics. (Dissertation).

White, W.M. 2013. *Geochemistry*. NY: Wiley-Blackwell.

Winde, F. 2004: Gold and uranium mining in the Wonderfonteinspruit catchment and environs. In: Coetzee, H (compiler): An assessment of sources, pathways, mechanisms and risks of current and potential future pollution of water and sediments in gold-mining areas of the Wonderfonteinspruit catchment. WRC Report No 1214/1/06, Pp. 2-4.

Winde, F. 2006a. Challenges for Sustainable Water Use in Dolomitic Mining Regions of South Africa – a Case Study of Uranium Pollution. Part 1: Sources and Pathways. *Physical Geography*. 27(4): 333-347.

Winde, F. 2010a. Uranium pollution of the Wonderfonteinspruit, 1997-2008 Part 1: Uranium toxicity, regional background and mining-related sources of uranium pollution. *Water SA*. 46(3):239 - 256.

Winde, F. 2010b. Uranium pollution of the Wonderfonteinspruit, 1997-2008 Part 2: Uranium toxicity, regional background and mining-related sources of uranium pollution. *Water SA*. 46(3):257 - 278.

Winde, F. & Erasmus, E. 2011a. Peatlands as Filters for Polluted Mine Water? —A Case Study from an Uranium-Contaminated Karst System in South Africa Part I: Hydrogeological Setting and U Fluxes. *Water*. 3:291-322.

WR2012(Water Resources 2012). 2020. Resource Centre.
<https://waterresourceswr2012.co.za/resource-centre/> Date of Access: 28 Jun 2020.

Zektser, I.S. & Everett, L.G. ed. 2004. Groundwater resources of the world and their use. *IHP-VI, Series on Groundwater No. 6*. Paris: UNESCO.